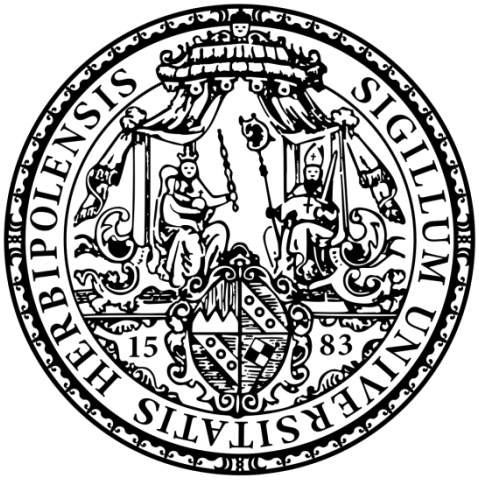

Julius-Maximilians-Universität Würzburg
Department of Neurology
University Hospital Würzburg

ALPHA SYNUCLEIN SPECIFIC T LYMPHOCYTES PROMOTE NEURODEGENERATION IN THE A53T-α-synuclein PARKINSON'S DISEASE MOUSE MODEL

ALPHA SYNUCLEIN-SPEZIFISCHE T LYMPHOCYTES VERSURSACHEN NEURODEGENERATION IM A53T-α-synuclein PARKINSON-KRANKHEITSMODELL

By

AKUA AFRIYIE KARIKARI
(From Ghana)

Dissertation
presented in partial fulfillment of the requirements
for the degree of

Doctor of Philosophy
in
Neuroscience

Julius-Maximilians-Universität Würzburg
Würzburg, Spring 2019

Members of Thesis Committee

Chairperson: Prof. Dr. Michael Sendtner
Director, Institute of Clinical Neurobiology
University of Würzburg

Primary Supervisor: PD Dr. med. Chi Wang Ip
Department Neurology
University Hospital Würzburg

Second Supervisor: Prof. Dr. Manfred Lutz
Institute of Virology and Immunobiology
University of Würzburg

Third Supervisor: Prof. Dr. med. Jens Volkmann
Director, Department of Neurology
University Hospital Würzburg

Declaration

I herewith do confirm that the dissertation entitled “Alpha synuclein specific T lymphocytes promote neurodegeneration in the A53T-α-synuclein Parkinson’s disease mouse model” is the outcome of my own research work. I did not obtain help or support from any commercial consultants. All resources and/or materials used in this study have been specified in the dissertation.

Additionally, I affirm that this dissertation has not been submitted as part of another examination process neither in an identical nor in similar form.

Eidesstattliche Erklärung

Hiermit bestätige ich die Dissertation "Alpha-Synuclein-spezifische T Lymphocytes versursachen die Neurodegeneration im A53T-α-Synuclein-Parkinson-Krankheitsmodell", das Ergebnis meiner eigenen Forschungsarbeit. Ich habe keine Hilfe oder Unterstützung von kommerziellen Beratern erhalten. Alle in dieser Studie verwendeten Ressourcen und / oder Materialien wurden in der Dissertation festgelegt.

Ich versichere außerdem, dass diese Dissertation weder in identischer noch in ähnlicher Form im Rahmen eines anderen Prüfungsverfahrens eingereicht wurde.

Place, Date	Signature

Abstract

Parkinson's disease (PD), which is the most common motor neurodegenerative disorder has attracted a tremendous amount of research advancement amid the challenges of the lack of an appropriate model that summate all the features of the human disease. Nevertheless, an aspect of the disease that is yet to be fully elucidated is the role of the immune system particularly the adaptive arm in the pathogenesis of PD. The focus of this study therefore was to characterize the contribution of lymphocytes in PD using the AAV1/2-A53T-α-synuclein mouse model of the disease that encodes for human mutated A53T-α-synuclein. This model was suitable for this research because it reflects more faithfully the molecular pathology underlying the human disease by exhibition of insoluble α-synuclein containing Lewy-like protein aggregates as compared to the more classical toxin models used in PD research. The outcome of this study showed that stereotaxic delivery of pathogenic α-synuclein via a viral vector into the substantia nigra engender the invasion of activated $CD4^+$ and $CD8^+$ T lymphocytes in the brain. The invasion of activated T cells in the brain especially in the substantia nigra then results in enhanced microglial activation and the disintegration of dopaminergic neurons. In addition, it was also discovered that $CD4^+$ T cells augmented dopaminergic cell death to a greater extent than $CD8^+$ T cells although; axonal degeneration occurred relatively independent from T cells contribution. The *ex vivo* and *in vitro*, experiments also indicated that the T cells were not only activated but they were specific to the mutated human α-synuclein antigen. As a result, they demonstrated selectivity in inducing more cell death to primary hippocampal neurons transduced with AAV1/2-A53T-α-synuclein vector than neurons with empty viral vector infection. The mechanism of T cell induced neuronal cell loss could not be attributed to the presence of cytokines neither was it mediated through MHC I and II. On the whole, this research has established that the presence of pathogenic α-synuclein in the substantia nigra has the potential to trigger immune responses that involve the transmigration of adaptive immune cells into the brain. The infiltration of the T cells consequently has a detrimental effect on the survival of dopaminergic neurons and the progression of the disease.

Zusammenfassung

Der M. Parkinson (PD) ist die am häufigsten auftretende motorische neurodegenerative Erkrankung weltweit. Trotz des Fehlens eines geeigneten Tiermodells, das alle Merkmale der menschlichen Krankheit widerspiegelt, kann die Parkinsonforschung in letzter Zeit einen enormen Fortschritt verzeichnen. Dennoch ist ein Aspekt der Krankheit, der noch nicht vollständig geklärt wurde, die Rolle von Immunzellen, insbesondere des adaptiven Arms in der Pathogenese der PD. Der Fokus dieser Studie lag daher auf der Charakterisierung des Beitrags von T-Zellen in der PD unter Verwendung des humanen mutierten AAV1/2-A53T-α-Synuclein-Mausmodells der Parkinsonkrankheit. Dieses Modell war für die vorliegende Arbeit optimal geeignet, da es die molekulare Pathologie der menschlichen Krankheit im Gegensatz zu den klassischen Toxinmodellen in der PD-Forschung besser widerspiegelt. Das Ergebnis dieser Studie zeigte, dass die stereotaktische Injektion von pathogenem α-synuclein über einen viralen Vektor in die Substantia nigra die Infiltration aktivierter $CD4^+$ - und $CD8^+$ T-Lymphozyten im Gehirn hervorruft. Die Einwanderung aktivierter T-Zellen im Gehirn, insbesondere in der Substantia nigra, führte begleitet durch eine verstärkte Mikroglia-Aktivierung zum Verlust dopaminerger Neurone. Darüber hinaus wurde beobachtet, dass $CD4^+$ T-Zellen den Untergang von dopaminergen Neuronen in einem größeren Ausmaß als $CD8^+$ T-Zellen verursachten. Interessanterweise trat die axonale Degeneration dopaminerger Fasern im Striatum relativ unabhängig von den T-Zellen auf. Durch *ex vivo* und *in vitro* Experimente konnte nachgewiesen werden, dass die T-Zellen nicht nur aktiviert waren, sondern auch antigenspezifisch gegen das mutierte humane α-Synuclein-Antigen reagierten. Als Ergebnis zeigten sie Selektivität bei der Herbeiführung eines höheren Zelltods für Dabei zeigten AAV1/2-A53T-α-Synuclein-Vektor transduzierte primäre Hippocampus-Neurone einen verstärkten Zelltod durch Inkubation mit T-Zellen aus dem Gehirn von AAV1/2-A53T- α-Synuclein-Vektor injizierten Mäusen als Neurone nach Injektion mit leerem AAV. Der Mechanismus des durch T-Zellen induzierten neuronalen Zellverlusts konnte nicht auf das Vorhandensein von Zytokinen zurückgeführt werden. Insgesamt konnte diese Arbeit zeigen, dass das Vorhandensein von pathogenem α-synuclein in der Substantia nigra in dem AAV1/2-A53T-α-synuclein Mausmodell des PD das Potenzial hat, Immunreaktionen auszulösen, welche die Transmigration adaptiver Immunzellen in das Gehirn und einen konsekutiven Verlust dopaminerger Neurone verursachen.

ACKNOWLEDGEMENTS

My heartfelt gratitude goes to the Almighty God for the wisdom, direction, strength, blessings and protection He has bestowed on me.

I am sincerely grateful and indebted to my family especially my father and mother, indeed you are the best gift I have. God bless you for all the advice, love and for being there for me.

I am particularly grateful to my advisor, PD. Dr. Chi Wang Ip, for his guidance, mentorship, patience and ideas he has provided over the years. His enthusiasm for this research greatly contributed to the success and completion of this work.

I would like to acknowledge and express my gratitude to the members of my thesis committee; Prof. Dr. med. Jens Volkmann, Prof. Dr. Manfred B. Lutz and PD. Dr. Chi Wang Ip for their various inputs and efforts to making this study a success.

I am also grateful to the Ministry of Education, Ghana and the DAAD for the sponsorship they provided for my study.

I wish to thank the members of Prof. Dr. Manfred Lutz lab especially, Eliana Ribechini and Marion Heuer for their assistance in the FACS experiments. To PD. Dr. Robert Blum and Michaela Keßler, am thankful for your support in the cell culture investigations. I wish to thank the members of Prof. Dr. Jörg Wischhusen lab particularly Valentine Bruttel and Fadhil Ahsan for their guidance in the ELISpot research. I am also grateful to Dr. med. Camelia Monoranu for her aiding in lymphocyte identification and quantification in human samples.

I am grateful to all the members of the Chi Wang Ip lab particularly to Louisa Frieß, Mohammad Badr, Heike Menzel and Susanne Knorr for all your help in the past years.

I would also like to acknowledge the members of the Graduate School of Life Sciences (GSLS) for their support in the course of my studies.

TABLE OF CONTENTS

LIST OF FIGURES AND TABLES

Chapter ONE

1.0 Introduction and Background

1.1.0 Parkinson's disease: an overview

Parkinson's disease (PD) is the most common age-related neurodegenerative motor disorder and is characterized clinically by bradykinesia, resting tremor, rigidity and postural instability (Mosley RL 2006). The prevalence of PD is estimated worldwide to be 570 per 100,000 among people aged 50 and this prevalence increases to roughly 5% by the age of 85 (Block et al 2007, Koprich et al 2017). The onset of the disease is usually at the age of 65 to 70 years. In less than 5% of PD patients in a population, disease onset can occur before the age of 40, which is mostly observed in genetic variants of the disease (Tysnes & Storstein 2017). The primary pathogenesis of PD is the progressive degeneration of the neuromelanin pigmented dopaminergic neurons that are found in the substantia nigra pars compacta (SNpc) of the brain. The loss of dopamine (DA) containing neurons in the SNpc causes an aberration in the basal ganglia circuitry which results in motor symptoms that typically describe the disease (Guatteo et al 2009). Though motor symptoms are the most apparent symptoms of PD, patients can also suffer from non-motor symptoms such as autonomic, gastrointestinal, and cognitive deficits and accumulating evidence suggests that the pathology is distributed outside the nigrostriatal pathway and occurs many years prior to overt motor symptoms (Mhyre et al 2012). Besides the loss of dopaminergic neurons in PD, the development of dystrophic/Lewy neurites and accumulation of intracellular protein aggregates, so-called Lewy bodies (Fig. 1), which are composed primarily of the protein alpha (α)- synuclein occur (Shi et al 2009). Presently, there are no curative treatments for PD available.

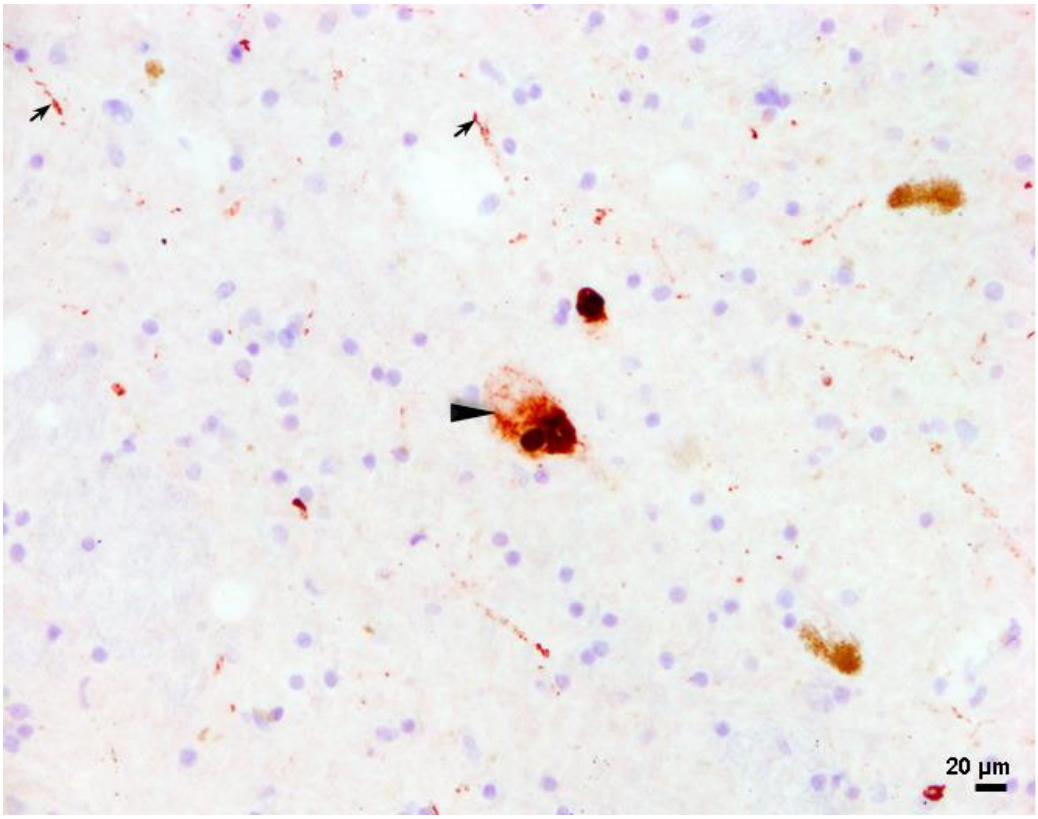

Fig. 1. An image of α-synuclein inclusions aggregated to form Lewy bodies and Lewy neurites.

Arrowhead shows aggregated α-synuclein in cell bodies (Lewy bodies) of dopaminergic neurons in the substantia nigra. Arrows indicate the strand-like Lewy neurites which are aggregates in axons and dendrites.

1.2.0 Etiology of PD

Several factors may contribute to the development of PD (Fig. 2). With the exception of the rare genetic forms, the cause of sporadic forms of PD remains unknown, which may involve a heterogeneous interplay of genetic and environmental factors. In addition, infectious agents are other risk factors that can increase the chances of developing PD (Dhawan & Chaudhuri 2007, Liu et al 2003). One of the strongest links of infections to the pathogenesis of PD is the emergence of post-encephalitic parkinsonism (PEP) (Dhawan & Chaudhuri 2007). In a research by Ogata et al. exposure of neonatal Fischer 344 (F344) rats to Japanese encephalitis virus induced the degeneration of dopaminergic neurons and gliosis in the substantia nigra (SN), with the development of movement disorders resembling human PD (Ogata et al 1997). Furthermore, administration of the highly pathogenic avian influenza virus H5N1 in C57BL/6J mice resulted in microglia activation and protein aggregation in the midbrain, which has the likelihood to initiate PD (Jang et al 2009). These findings are pointers to the fact that pathogenic organisms such as encephalitis and influenza viruses, can promote chronic inflammation in the brain that can lead to the dysfunction and vulnerability of SN neurons, increasing the likelihood of developing PD.

With regards to genetic causes, there are about five genes implicated in familial forms of PD which include mutations in α-synuclein (*SNCA),* leucine-rich repeat serine/threonine-protein kinase 2 *(LRRK2),* PTEN-induced putative kinase protein 1 *(PINK1),* parkin *(PRKN)* and DJ1 (*PARK7)* (Koprich et al 2017, Mullin & Schapira 2015). Whereas mutations in *SNCA* and *LRRK2* are responsible for autosomal dominant forms of PD, mutations in *PINK1*, *PRKN* and *PARK7* result in autosomal recessive PD.

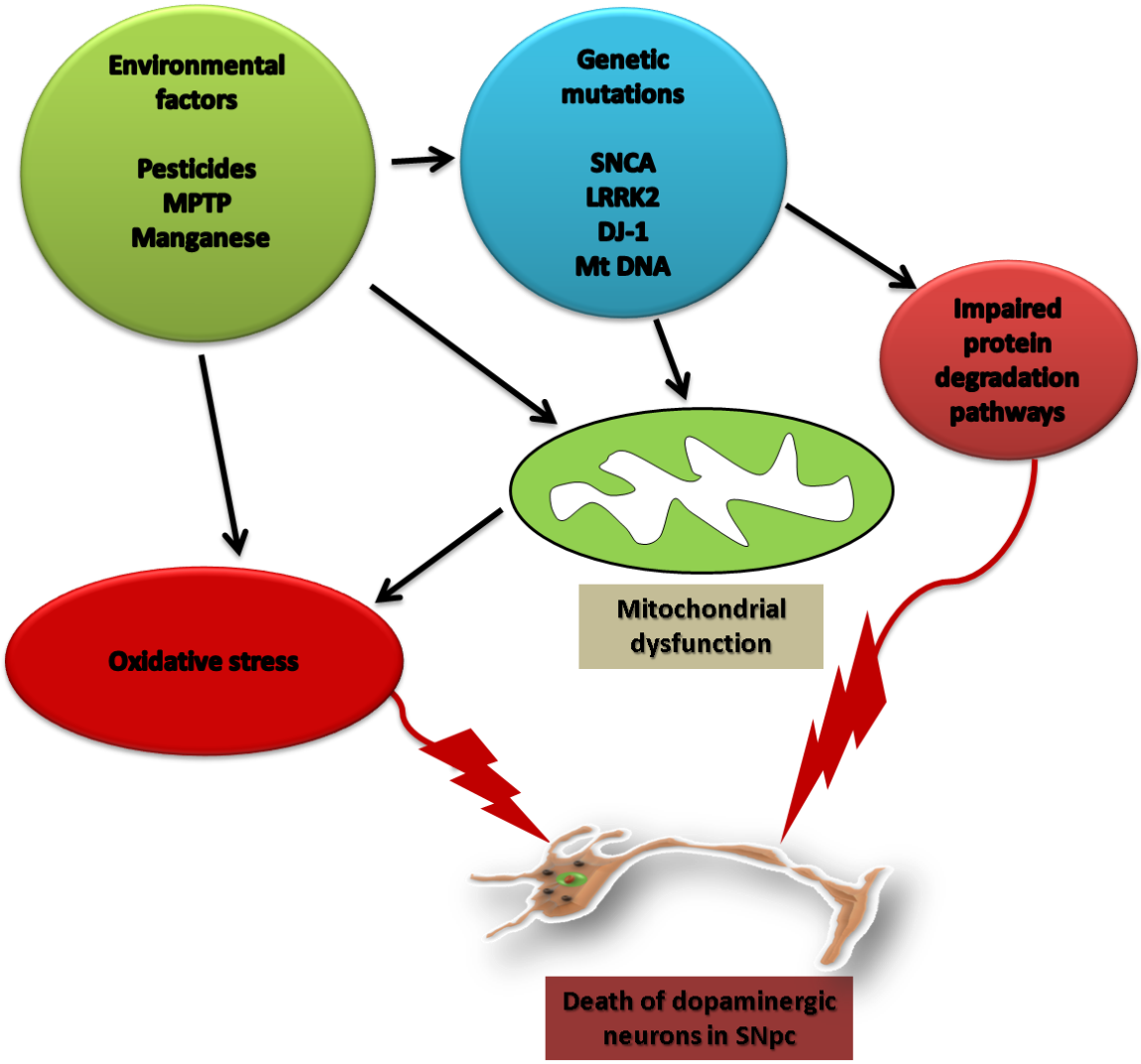

Fig. 2. A schematic illustration of the multifactorial etiology of Parkinson's disease.

1.3.0 Genetic basis of Parkinson's disease

1.3.1 Autosomal dominant genes

1.3.2 α-synuclein (PARK 1 & 4) and PD

α-synuclein is a 14 kDa (140 amino acids) protein that is encoded by the synuclein alpha (*SNCA)* gene and it's mainly associated with synaptic vesicles especially in the hippocampus, neocortex and SN (Kim et al 2004). The protein is also expressed in other cell types of the brain such as astrocytes and oligodendroglia (Mori et al 2002, Richter-Landsberg et al 2000). Within the cytosol, α-synuclein may assume an unfolded conformation without a defined structure or an α-helix structure in association with phospholipids (Bussell & Eliezer 2001, Emamzadeh 2016, Roodveldt et al 2011). This unfolded conformation makes the protein more susceptible to aggregation (Breydo et al 2012). The precise physiological function(s) of α-synuclein remains elusive; however it is known to localize at presynaptic terminals and associates with the distal reserve pool of synaptic vesicles (Lashuel et al 2013). Mice with knock out in *SNCA* show a deficit in hippocampal synaptic responses to sustained trains of high-frequency stimulation which results in the depletion of docked and reserve pool of synaptic vesicles (Abeliovich et al 2000, Cabin et al 2002). In these mice, there is also impairment in the replenishment of docked pools from reserved pools, which alludes to the fact that α-synuclein may play a role in refilling and trafficking of synaptic vesicles from reserved pools to the site of synaptic vesicle release (Abeliovich et al 2000, Lashuel et al 2013).

Missense mutations (such as the A53T mutation) and gene multiplication in the *SNCA* gene cause hereditary forms of PD (Chou & Kah-Leong 2013), thereby underlining the important role of α-synuclein in PD pathophysiology. The clinical characteristics of the A53T mutation are onset between 31 and 40 years, dysphasia, dysarthria and cognitive decline (Puschmann et al 2009). In addition to the common A53T *SNCA* mutations, A30P, E46K, G51D and H50Q missense mutations in the *SNCA* gene are also implicated in causing PD (Krüger et al 1998,

Zarranz et al 2004). Patients with the A30P variation develop clinical manifestations similar to those of sporadic PD, which includes a late onset with progressive parkinsonism (Krüger et al 1998). The E46K mutation, on the other hand, causes more critical parkinsonism with dementia, hallucinations at therapeutic doses of L-dopa and inconstancy in the level of consciousness (Zarranz et al 2004). The G51D substitution is associated with early onset of PD with autosomal dominant inheritance (Kiely et al 2013). Patients with the G51D mutations also develop neuropathological features similar to multiple system atrophy (MSA) with dementia and CA2-CA3 hippocampal and cortical neuronal loss (Kiely et al 2015). The H50Q mutation has been reported in both sporadic (Proukakis et al 2013) and familial forms of PD (Appel-Cresswell et al 2013). It is suggested that the H50Q mutation results in a shift in copper (Cu^{2+}) binding site of α-synuclein to its N-terminus excluding other sections of the protein from binding to Cu^{2+} (Proukakis et al 2013). The consequence of this is the reduced affinity of α-synuclein for Cu^{2+} and elevated levels of Cu^{2+} which may be injurious to dopaminergic neurons (Chou & Kah-Leong 2013, Proukakis et al 2013).

Lately, there have been reports on novel *SNCA* mutations reported in sporadic PD. Notable amongst them include A18T and A29S substitutions (Campelo & Silva 2017, Hoffman-Zacharska et al 2013, Kumar et al 2018). The A18T and A29S like the other aforementioned mutations in α-synuclein, results in disruption of the α-helical structure of the protein. This disruption might interfere in α-synuclein mediated interaction with membranes which may be crucial for α-synuclein dependent functioning of synaptic vesicles (Hoffman-Zacharska et al 2013).

Apart from the mutations and multiplications of α-synuclein that are pathogenic, the vulnerability of the monomeric protein to exogenous and endogenous factors can lead to its aggregation (Breydo et al 2012) hence, mimicking the outcome of α-synuclein disease-associated variants. Not surprisingly, some studies have demonstrated that various exogenous

neurotoxicants linked to PD, including pesticides, herbicides and metal ions; significantly accelerate the aggregation of α-synuclein (Han et al 2018, Yuan et al 2015). Furthermore, oxidative stress has also been shown to induce the accumulation of α-synuclein in both *in vivo* and *in vitro* studies (Esteves et al 2009, Scudamore & Ciossek 2018).

1.3.3 LRRK2 and PD

The *LRRK2* gene comprises of roughly 144 kilobases with 51 exons which encodes a 2,527 amino acid protein of 286 kDa (Dächsel & Farrer 2010). LRRK 2 protein is speculated to have both enzymatic and scaffolding functions. Though its exact physiological activity is not known, two distinct enzymatic domains namely the kinase and Ras of complex proteins (ROC)- GTPase domains characterizes LRRK2 as an enzyme (Li et al 2014). Other than its enzymatic functions, the various protein-protein interaction domains show that LRRK2 may be involved in multiprotein signaling complex (Anand & Braithwaite 2009).

There are more than 75 LRRK2 mutations identified although not all contribute to the risk of parkinsonism (Dächsel & Farrer 2010). It is important to note that variations in LRRK2 are the most common genetic cause of familial PD and contributes to sporadic PD as well (Li et al 2014). The established PD associated inherited substitutions in LRRK2 include; G2019S, R1441C/G, Y1699C, G2385R, R1628P, Y1699C, I2020T and N1437H (Anand & Braithwaite 2009, Li et al 2014). Among the established mutations, G2019S is the most redundant and is implicated in both familial and sporadic PD (Dächsel & Farrer 2010, Li et al 2014). On the other hand, the R1628P and G2385R are the most common susceptibility variants, which double the risk of developing PD (Dächsel & Farrer 2010).

1.3.4 Autosomal recessive genes implicated in PD

Autosomal recessive parkinsonism occurs when there are mutations in the same (homozygous) or different (heterozygous) in one of each gene copies. Genes associated with autosomal recessive forms of PD include *parkin*-PARK2, *PTEN-induced putative kinase 1* (*PINK-1*)-PARK6, *DJ-1*-PARK7, and *ATP13A2*-PARK9. Among these genes *parkin, PINK-1* and *DJ-1* are involved in early onset autosomal recessive parkinsonism (Bonifati 2012). Mutations in *parkin* are the most prevalent and are implicated in both familial and sporadic cases (Lücking et al 2000). Mutations in PINK-1 and DJ-1 are less frequent in causing early-onset PD (Kumazawa et al 2008). The ATP13A2 homozygous and heterogenous mutations result in atypical parkinsonism also known as the Kufor-Rakeb syndrome. This syndrome progresses rapidly at an early onset and is associated with dementia, pyramidal signs and supranuclear gaze palsy (Klein & Westenberger 2012).

1.4.0 Environmental factors and PD

Apart from protein mutations, environmental factors including exposure to pesticides, ethanol consumption and metals are also implicated in neurodegeneration in PD. The link between pesticides and PD was ignited in the 1980s when users of 1methyl-4-phenyl-1,2,3,6-tetrahydropyridine (MPTP), a potent neurotoxin precursor of 1-methyl-4-phenylpyridinium (MPP^+) developed parkinsonism (Campdelacreu 2014). The striking feature of the neurotoxin MPTP is not just its ability to induce the many characteristics of PD but also the resemblance between its toxic metabolite MPP^+ and paraquat (differing only by one methyl group), a widely used herbicide (Langston 2017). A large number independent investigations have since that time demonstrated that exposure to herbicides and pesticides particularly paraquat and rotenone lead to higher risks of developing PD, although in some instances there was no connection established (Campdelacreu 2014, Langston 2017). Nonetheless, people in agricultural occupation, especially in rural areas, have been markedly associated with PD (Greener 2013).

A study by Van Maele-Fabry demonstrated that people who worked as farmers for 10 and 20 years had the tendency of 17 and 16 % respectively to develop PD as compared to controls (Van Maele-Fabry et al 2012). The mechanism of the toxins mentioned above is mainly to block the action of mitochondrial complex I of the electron transport chain, which results in higher levels of oxidative stress (Brown et al. 2005). Abnormality in the electron transport chain of mitochondria respiration has been reported in PD brains (Rodriguez-Rocha et al 2013). Hence inhibitors of complex I activity could be pointers to dopaminergic cell death.

Pyrethroids, a class of pesticides contained in household insecticides and mosquito repellants can easily cross the blood-brain barrier (BBB) and reach appreciable concentrations in the brain (Elwan et al 2006). Interestingly, some animal studies have reported the ability of the pyrethroid pesticides; deltamethrin and permethrin to increase dopamine transporter (DAT) mediated DA uptake which indirectly induces degeneration of dopaminergic neurons (Elwan et al 2006, Nandipati & Litvan 2016). In spite of this outcome, findings from pesticide neurotoxicology in PD have been quite heterogeneous and the research field requires further studies. For instance, a recent study by Hansen et al. showed that there was no association observed between pyrethroid exposure and neuromotor performance (Hansen et al 2017). However, there was an association between high pyrethroid exposure and neurocognitive decline (Hansen et al 2017).

Parkinsonism has also been characterized in cases of high exposure to metals including manganese, iron, Cu^{2+} and lead. Investigators discovered more significant levels of manganese, iron and Cu^{2+} in the SN of PD patients as compared to controls (Campdelacreu 2014, Nandipati & Litvan 2016). Iron has been implicated in the pathophysiology of PD in some laboratory studies, though data on human exposure is scanty (Nandipati & Litvan 2016). Manganese is toxic to neurons in the basal ganglia especially those of the globus pallidum, subthalamic nucleus, striatum and SN and it is linked to parkinsonism (Ho et al 2018). Studies involving rats proved that early low-level exposure to the metal was linked to increased levels of

astrogliosis in the striatum (Nandipati & Litvan 2016). Moreover, there was a decline in motor and cognitive performance in these rats which suggests that manganese is a strong neurotoxicant (Nandipati & Litvan 2016). Howbeit, the features of manganese-induced parkinsonism are quite distinct from that of idiopathic PD with the lack of therapeutic response to levodopa, less resting tremor and more frequent dystonia (Ho et al 2018).

As compared to iron, post mortem analysis of PD brains revealed a decrease in Cu^{2+} levels (Riederer et al 1989). A reduction of Cu^{2+} levels may result in lower levels of the Cu/Zn superoxide dismutase (SOD), of which Cu^{2+} is a necessary cofactor. However, increase in the concentrations of unbound Cu^{2+} has been reported in the cerebrospinal fluid (CSF) of PD patients, which is a biomarker for the disease (Manto 2014). Copper ions can induce DNA damage in dopaminergic neurons by complementing the oxidation of DA and the intranigral application of copper results in the apoptosis of dopaminergic neurons (Manto 2014).

1.5.0 Animal models of PD

With the etiology of PD still elusive, several models have been used to mimic the pathology of the disease. To date, animal models provide the nearest to the human system in which the disease can be modeled. Modeling PD in animals particularly rodents have proven to be challenging and currently, no single model summarizes the motor deficits, clinical and pathological features of the disease entirely (Dawson et al 2010). Since the identification that insoluble α-synuclein constitutes the main component of Lewy bodies and neurites (Spillantini et al 1998), a new approach in PD research was introduced. Thus a good PD model should ideally;

(i) have an age-dependent selective, progressive and significant loss (~ 50-70%) of dopaminergic neurons (Beal 2010, Reeve et al 2018).

(ii) show motor impairments, including the pivotal symptoms of PD such as bradykinesia, rigidity and resting tremor (Beal 2010).

(iii) present the pathological hallmarks of PD including characteristic Lewy body formation (Antony et al 2011).

(iv) have a concise disease progression period to allow for expeditious and cheaper screening of therapeutic agents (Beal 2010).

Animal models used to represent PD can be grouped in into two main groups namely the neurotoxin and genetic models (Tieu 2011).

1.5.1 Toxin-mediated models of PD

Under the toxin-mediated model of PD, the more traditionally used toxins include; MPTP and 6-hydroxydopamine (6-OHDA). There are current models which make use of pesticides/herbicides such as rotenone and paraquat/maneb (Jackson-Lewis et al 2012).

The neurotoxin MPTP was discovered originally after heroin addicts incidentally self-administered a new synthetic form of the drug (Nonnekes et al 2018). This resulted in the progression of acute parkinsonism that was identical to idiopathic PD (Langston et al 1983). Since its discovery, MPTP has been the most commonly used toxin to generate a PD model. After systemic administration of the lipophilic MPTP in mice, it's taken up mainly by astrocytes and modified to its metabolite MPP^+. MPP^+ is absorbed by dopaminergic neurons, where it mediates its toxic effects. The loss of dopaminergic cells in the MPTP model is not only limited to those of the SN as there is also the loss of dopaminergic neurons in the enteric nervous system (Antony et al 2011). The main strength of this model is the specific and reproducible neurotoxic effect on the nigrostriatal system, as well as the observed motor dysfunction (Antony et al 2011, Huang et al 2017). A major drawback of the MPTP model is the lack of proteinaceous inclusions, Lewy bodies (Huang et al 2017). Although there are reports of α-synuclein positive

compositions in the chronic MPTP model, the results have not been consistent (Meredith & Rademacher 2011). Another setback of this model is the fact that not all mouse strains and rats are susceptible to MPTP toxicity (Meredith & Rademacher 2011, Sedelis et al 2000).

6-Hydroxydopamine is a structural cognate of catecholamines and induces its toxic effect on catecholaminergic neurons (Tieu 2011). It is frequently used to illustrate the degeneration of nigral neurons in both *in vitro* and *in vivo* PD models. The toxin is not only detrimental in the central nervous system (CNS) but also in the peripheral system. However, because it is hydrophilic and unsuited to cross the blood-brain barrier, it is stereotaxically injected into the CNS to achieve its neurotoxic effect. After 6-OHDA uptake into neurons, it accrues in the cytosol where it is immediately oxidized, leading to the formation of reactive oxygen species and consequently induces oxidative stress-related neurotoxicity (Blum et al 2001). 6-OHDA is typically injected into the ascending medial forebrain bundle, striatum or the SN in experimental models of PD where it damages dopaminergic neurons in the SN and depletes striatal DA levels (Blum et al 2001). An advantage of this mode of delivery is the slow gradual and partial destruction of the nigrostriatal system in a retrograde manner within 3 weeks when it is delivered to the striatum (Przedbroski et al 1995). The striatal route of administering 6-OHDA presents the following advantages:

(i) the slow and reduced extensiveness of the lesion is more applicable to PD (Tieu 2011).

(ii) the method of administration also results in non-motor symptoms of PD, including psychiatric, cognitive and gastrointestinal dysfunction (Branchi et al 2008).

(iii) moreover, injecting in the large striatum increases the rate of success especially in mice (Tieu 2011).

A unilateral injection of 6-OHDA induces nigral degeneration that produces an asymmetric and quantifiable motor deficit caused by the systemic application of either DA precursor L-

3,4-dihydroxyphenylalanine (L-dopa), receptor agonists such as apomorphine or DA releasing drugs which include amphetamine (Ungerstedt & Arbuthnott 1970). The extent of the nigrostriatal lesion correlates with the rotating motor behavior (Przedborski et al 1995). The disadvantage of the 6-OHDA model is the lack of an age-dependent progression, absence of Lewy bodies and damage to noradrenergic neurons (Jagmag et al 2015, Tieu 2011).

Rotenone, an insecticide and herbicide obtained from the roots of *Lonchocarpus* species was used as a model of PD in 1985 (Greenamyre et al 2010, Hisahara & Shimohama 2010). Rotenone is capable of crossing lipid barriers including the BBB readily without the assistance of transporters and also a potent inhibitor of mitochondrial complex I (Hisahara & Shimohama 2010). Earlier studies using rotenone reported a non-specific brain lesion with accompanying peripheral toxicity utilizing a dose of 10-18 mg/kg per day in Sprague–Dawley rats (Ferrante et al 1997). However, in 2000, Betarbet et al. identified an optimal dose (2–3 mg/kg per day) of rotenone for inducing PD pathology in Lewis rats, which produced selective nigrostriatal degeneration (Betarbet et al 2000). A prominent observation from this titrated dosage was the presence of α-synuclein positive inclusions in nigral dopaminergic neurons, similar to Lewy bodies (Greenamyre et al 2010) and the development of a behavioral phenotype including hypokinesia and rigidity (Fabio & Marie-Therese 2012). Though the rotenone rat model showed for the first time Lewy bodies in the cytoplasm of neurons in a toxin model of PD, there have been reports of substantial uncertainty in the individual animal response to the toxin in developing significant nigrostriatal lesion. This variability in response to rotenone makes it unsuited for testing therapeutic agents where reproducibility is much required (Fabio & Marie-Therese 2012). Furthermore, as rotenone is a mitochondrial toxin, it can cause systemic toxicity and mortality with increasing dosage (Greenamyre et al 2010). Thirdly, in addition to

degeneration of nigral neurons, other neuronal populations in the basal ganglia are also susceptible to the toxin and this results in characteristics which correlate with atypical parkinsonism, instead of PD (Fabio & Marie-Therese 2012).

Although there have been epidemiological reports to suggest that pesticide use could increase the possibility of developing PD, clinical proof that paraquat may cause PD is vague (Berry et al 2010). There has neither been a close association between exposure to maneb, a fungicide, and development of PD (Berry et al 2010). With regards to animal models, some reports indicate that systemic administration of either paraquat or maneb in mice induce decreased motor activity and loss of dopaminergic cells in the SN (Blesa & Przedborski 2014). The combined dosage of both paraquat and maneb, on the other hand, yielded an increased effect on the nigrostriatal dopaminergic system than using either of these chemicals alone (Blesa et al 2012). Even though these compounds are pointers to the fact that environmental factors can cause PD, the model exhibits contradictory results of variable dopaminergic cell death and loss of striatal DA levels (Blesa & Przedborski 2014). An advantage of this model, however, is the presence of Lewy bodies in the remaining dopaminergic neurons, thereby making it useful for the study of PD (Manning-Bog et al 2002).

Howbeit neurotoxins have provided useful insights into PD; there are drawbacks with these models. For instance, there is a rapid degeneration of dopaminergic neurons, the formation of Lewy bodies is absent in some models and typical motor deficit is not consistent (Blesa & Przedborski 2014).

1.5.2 Genetic models of PD

The genetic models of PD are centered on genes involved in familial forms of PD which include α-synuclein and Lrrk2 for autosomal dominant genes and *parkin* and *PINK-1* for

autosomal recessive genes. Under the genetic models, the gene of interest is knocked out, or a known human mutation of the gene is either knocked in or transgenically expressed (Gamber 2016). The genetic models have mainly been established in mice because it is relatively easier to manipulate these species genetically (Ellenbroek & Youn 2016).

Several mouse lines have been generated, that overexpress distinct human α-synuclein gene mutations (A30P / A53T) under various promoters (Crabtree & Zhang 2012, Hisahara & Shimohama 2010, Park et al 2016). Mice which contain both the A30 and the A53T mutations under the tyrosine hydroxylase (TH) promoter are reported to have a progressive decline in motor activity, loss of SN neurons and striatal DA content (Richfield et al 2002). Moreover, mice which overexpress the human wt α-synuclein under the neuron-specific platelet-derived growth factor β (PDGFβ) promoter show impaired motor performance, reduced TH immunoreactivity and DA content in the striatum (Masliah et al 2000). Similarly, under the Thy-1 promoter, mice overexpressing human wt α-synuclein demonstrate a widespread expression of the protein in cortical and subcortical neurons, as well as higher sensitivity to mitochondrial damage from low doses of MPTP (Hisahara & Shimohama 2010, Kahle et al 2002). It is evident that the phenotypic outcome of α-synuclein overexpression in mice is dependent on the promoter used to drive transgene expression. Currently, none of the α-synuclein models entirely recapitulates PD pathology in terms of progressive loss DA neurons, striatal DA loss and α-synuclein accumulation (Lim & Ng 2009).

There are mouse lines with knock out in the *LRRK2* gene which are viable and have an unimpaired nigrostriatal dopaminergic pathway at 2 years of age. Although these mice have α-synuclein accumulation and show some motor impairment, there is a lack of neuropathological hallmarks such as neurodegeneration or altered neuronal structure (Hinkle et al 2012, Tong et al 2010). Knock in mice with G2019S and R1441C LRRK2;

show no impairment in dopaminergic cell morphology, dopaminergic cell number in the SN or lower striatal dopamine levels and turnover (Blesa & Przedborski 2014, Tong et al 2010). When G2019S was overexpressed, mice had only a mild and selective loss of 20% dopaminergic cells over a period of 2 years (Blesa & Przedborski 2014). Thus, the LRRK2 model of PD has also failed to mimic the main pathological characteristics of PD.

Furthermore, there are mouse models of PD recessive genes, notable amongst them being that of *PINK-1* and *parkin*. PINK-1 knock out mice demonstrate an age-dependent slight reduction in DA levels in the striatum which is accompanied by low locomotion; nonetheless, they exhibit no impairment of dopaminergic neurons (Blesa & Przedborski 2014, Gispert et al 2009). This phenotype of PINK-1 knock out mice is very similar to that of parkin mice. Of the various parkin knock out mice, none manifest substantial DA related behavioral impairments except for the bacterial artificial chromosome (BAC) model with a C-terminal shortened human mutant parkin (Parkin-Q311X), which is driven by the DA transporter. These mice demonstrate an age-dependent degeneration of dopaminergic neurons, hypokinesia and reduction in striatal DA levels and terminals (Blesa & Przedborski 2014, Lu et al 2009). In summary, the PINK-1 and parkin models do not generate functional impairment of the nigrostriatal pathway or other PD related pathology. Therefore, their usefulness is debatable.

Thus, whereas the genetic models could have provided insight into the role of these proteins in PD pathogenesis, they have been disappointing in reproducing the cardinal characteristics of the disease. The parkinsonian phenotypes of these mice are very mild and in some models, there are no real phenotypes at all.

Owing to the disadvantages of genetic models of PD, overexpression of genes by viral vector delivery presented a useful alternative approach. Recombinant adeno-associated viruses (AAV) and lentiviruses (LV) have been explored as viral vectors to induce the

overexpression of wild type and mutant forms of genes implicated in PD in viral vector models. By using the technique of stereotaxic injection, the AAV and LV vectors are used to deliver the desired transgene commonly of α-synuclein and other implicated genes such as *LRRK2* and *parkin* into the SN or striatum of experimental animals (Low & Aebischer 2012). The vectors are efficient in transducing neurons in the brain with high efficiency, and the expression of the inserted genes can last over many years (Ulusoy et al 2010). The AAV vectors are especially effective for targeted gene delivery in the rodent brain because they have a higher tropism for dopaminergic neurons; transduction is much more potent and can be synthesized in high titers as compared to LV vectors (Low & Aebischer 2012, Ulusoy et al 2010). An advantage of the viral vector-mediated models is that they can be utilized for gene delivery in a range of animal species. In addition, the process of degeneration is progressive unlike in the toxin-mediated model, which makes it much more appropriate to study therapeutic interventions (Low & Aebischer 2012).

Inasmuch as the gene, delivery-based animal models of PD have proven better than transgenic animals in reproducing overt nigrostriatal damage, there are some limitations. For example, the period of dopaminergic cell degeneration varies from a time frame of 8 weeks in some studies to about 3-4 months in other researches (Ulusoy et al 2010). Furthermore, observable behavioral deficits are not detectable in some subset of AAV and LV treated mice (Low & Aebischer 2012, Ulusoy et al 2010). The different capsid serotypes of the AAV vectors also transduce dopaminergic neurons differently. For instance, whereas AAV serotypes 2 and 6 vectors show definite transduction for cells located in SN and ventral tegmental area, AAV serotype 5 shows un-specificity and a dispersed pattern in transducing neurons in the midbrain (Albert et al 2017, Ulusoy et al 2010).

In 2010, Koprich et al. came up with a new AAV model of PD α-synucleinopathy by using the serotype 1 and 2 of the AAV vector. The AAV vector combines the advantages of

serotype 2, which has: (i) specific neuronal tropism, (ii) capacity to produce high titers and (iii) can purify on a heparin sulfate column, with that of serotype 1 which has the exceptional ability to penetrate brain tissue (Koprich et al 2010). Thus, the serotypes 1 and 2 of the AAV vector are in a ratio of 1:1 on the viral capsid which drives the expression of mutated human A53T α-synuclein (Koprich et al 2010). For their study, they used this vector to produce a rat model of PD synucleinopathy, as α-synuclein is the main component of Lewy pathology and it's implicated in both familial and sporadic PD (Eriksen et al 2003, Shults 2006, Spillantini et al 1997).

This viral vector was used in mice to produce a mouse model of synucleinopathy by Ip et al. (Ip et al 2017). When male C57BL/6 mice were injected with AAV1/2 adenoviral vector which expresses the mutated human A53T α-synuclein (haSyn) at a concentration of 5.16 x 10^{12} genomic particles (gp)/ml, mice did not only have motor impairment but also had a significant loss of dopaminergic neurons as well as a Lewy pathology (Ip et al 2017). The AAV1/2-A53T-α-synuclein model is thus an improvement over the traditional models of PD making it more appropriate to carry out research in PD.

1.6.0 Immune System and PD

The central nervous system (CNS) was for some time described as an "immune privileged" region, where the cells of the peripheral immune system could not gain or rarely had access. This meant that the two systems had little or no interaction, a hypothesis that was backed by the observation that tissue grafts in the brain or eye persisted much longer than those in other areas of the body (Medawar 1948). Currently, there is a lot of evidence to show that there are interactions between the CNS and the immune system.

The immune system is classified into innate and adaptive immunity. Present at birth and non-specific in its response, the innate immunity is an evolutionarily ancient part of the host defense

from infection (Iwasaki & Medzhitov 2015, Janeway & Medzhitov 2002). The adaptive immune system, unlike the innate immune system, has the capacity to mount up a specific immune response against foreign antigens (Janeway & Medzhitov 2002).

An interesting question being addressed in PD research currently is the role of the immune system in the progression of the disease and whether inflammation is just a reaction to neuronal cell death or is the driving force that induces neurodegeneration. In recent times, evidence points to the fact that both innate and adaptive systems are involved in mediating inflammatory responses in PD pathogenesis.

1.6.1 The innate system

The interaction between the process of inflammation and neuronal degeneration is a complicated issue. This is because the death of neurons can trigger an inflammatory process by releasing apoptotic and cellular components that can be identified by the cells of the innate immunity (Kannarkat et al 2013). Alternatively, an inflammatory process can also result in dopaminergic cell death through the production of cytokines or as direct neuronal injury (Kannarkat et al 2013).

In the CNS, the innate immune system response is mainly mediated by the microglia and astrocytes (Subramaniam & Federoff 2017). Microglia cells are the macrophages/innate immune cells, resident in the CNS that provide defense against infectious diseases, tumors and neurodegeneration (Aloisi 2001, Kreutzberg 1996). Under physiological conditions, microglia cells have an inactive phenotype (Schmid et al 2009). With their ramified morphology and long cytoplasmic extensions, they monitor and inspect their surrounding environment and other brain cells types (Davalos et al 2005, Nimmerjahn et al 2005). Under pathological conditions as a result of pathogen invasion or tissue damage, microglia become activated and thus promote inflammatory processes (Roodveldt et al 2008). The evidence of microglia in the involvement

of inflammation in PD development came from a postmortem study over twenty years ago, which showed the presence of activated microglia in the SN of a PD patient (Su & Federoff 2014). Microglia cells densely populate the SN, and therefore could make this brain region particularly vulnerable to inflammatory stimuli (Lawson et al 1990). Microglia cells are now associated with CNS inflammation (Perry et al 2010) and it is an evidence of inflammation in PD (McGeer et al 1988, Shrestha et al 2014). The inflammatory processes further induce the recruitment of other immune cell types to the site of inflammation (Glass et al 2010). In PD, there is evidence that the release of α-synuclein aggregates can result in the activation of microglia. Indeed, some studies have proven that α-synuclein is the main trigger of microglial activation in PD (Roodveldt et al 2008) and that extracellular and nigral aggregates containing α-synuclein are encompassed by activated microglia or inflammatory mediators in PD brains (McGeer et al 1988, Yamada et al 1992). Though microglia cells can shuttle between two phenotypes; being the pro-inflammatory (M1) and anti-inflammatory states (M2), sufficient evidence in humans show a role for the chronic inflammatory state (microgliosis) of the innate immune cells in PD (Kannarkat et al 2013). There are reports of increased levels of proinflammatory cytokines including IFN-γ, IL-1β, TGF-β and IL-6 in individuals with PD as compared to healthy age-matched controls, using cerebrospinal fluid and post-mortem analyses of their nigrostriatal regions (Blum-Degen et al 1995, Mogi et al 1994, Mogi et al 1995). In studies involving mice overexpressing the AAV-human-α-synuclein, there was also the activation of microglial cells with subsequent stimulation of the adaptive immune system (Theodore et al 2008), which is indicative of the important role of these cells in the inflammatory process in PD. A significant characteristic of microglial cells is their ability to present foreign antigens via MHC II expression (Schetters et al 2018). An upregulation of MHC II is observed in almost all inflammatory and neurodegenerative conditions (Croisier et al 2005). MHC II expression on stimulated microglia can successfully engage $CD4^+$ T lymphocytes and as a result, heighten and propagate a continuous inflammatory process (Kannarkat et al 2013).

Indeed, a global loss of the MHC II molecule in a mouse model confers protection against microglial activation, neurodegeneration and T cell infiltration after the overexpression of human α-synuclein by a viral vector in the SN (Kannarkat et al 2013). Furthermore, Harms et al. also demonstrated in their study that microglial activation by α-synuclein is dependent on MHC II expression (Harms et al 2013).

Apart from microglial cells, astrocytes are the other cells of the innate immunity, which are equally crucial in immunomodulation in the CNS. Astrocytes are the most abundant glial cells in the brain (Booth et al 2017). They regulate brain homeostasis and microenvironment through the uptake of potassium ions and glutamate through the inward rectifier potassium channels and the excitatory amino acid transporter, (EAAT)-1/2 (Olsen et al 2006, Rothstein et al 1996, Simard & Nedergaard 2004). They also form a major component of the BBB and help to maintain this structure that limits the entry of blood-borne elements in the CNS (Dong & Benveniste 2001a). Astrocytes produce a variety of neurotrophic factors, including glial-derived neurotrophic factor (GDNF), which is necessary for the development and survival of dopaminergic neurons (Lin et al 1993, Scharr et al 1993). However, when astrocytes are rapidly and intensely activated, they facilitate/initiate inflammatory response, neuronal cell death and brain injury (Tani et al 1996). The activation of astrocytes is termed as astrogliosis and the cells as reactive astrocytes (Joe et al 2018). Reactive astrocytes have enhanced expression of the glial fibrillary acidic protein (GFAP), which is a marker for activated astrocytes (Brahmachari et al 2006). The expression pattern of GFAP in postmortem brains of PD patients has been quite controversial. There are reported cases of only a mild increase in reactive astrocytes with immunoreactivity for GFAP (Mirza et al 2000), whereas severe astrogliosis have been reported in some cases (Forno et al 1992). With the release and spread of α-synuclein in the brain in the course of PD (Longhena et al 2017, Recasens & Dehay 2014), astrocytes can become accumulated with the aggregated protein (Phatnani & Maniatis 2015). In one study, α-synuclein

containing astrocytes were found copiously distributed than Lewy bodies (Braak et al 2007). There is presently experimental evidence to suggest that astroglial α-synuclein pathology is caused by the direct transmission of neuronal α-synuclein aggregates, which in turn induce inflammatory responses (Lee et al 2010). Furthermore, it is speculated that astrocytes can express MHC II and costimulatory molecules such as B7 and CD4, produce cytokines which are all critical for antigen presentation and T cell activation, although these observations have been disputable (Dong & Benveniste 2001b). Ultimately, activation of the innate cells in the CNS results in the release of proinflammatory factors that mediate BBB permeability and recruitment of the adaptive immune cells (Kannarkat et al 2013).

1.6.2 Adaptive immunity in PD

Under normal physiological conditions, activated T and B cells are able to patrol the CNS, though, in low numbers, naive lymphocytes are excluded (Engelhardt & Ransohoff 2005, Togo et al 2002b). The lower infiltration of activated T lymphocytes in the CNS could be due to decreased levels of adhesion molecules on endothelial cells (Hickey 2001). However, when cytokines including tumor necrosis factor-alpha (TNF-α) and IL-1 are released by activated innate cells in the brain, or available in the circulating blood, the BBB may become more permeable through increased expression of cellular adhesion molecules such as selectins on endothelial cells (Wong et al 1999). There is *in vivo* evidence for increased BBB permeability revealed through positron emission tomography (PET) scan measurement of molecular efflux pump P-glycoprotein's ligand uptake, as well as increased albumin in the CSF of PD patients (Kortekaas et al 2005, Pisani et al 2012). Increased expression of ICAM-1 (CD54), an adhesion molecule which aids immune cell diapedesis, is also reported on blood vessels close to the SN in postmortem brain tissue from PD patients (Kannarkat et al 2013). This aid activated T and B cells to readily extravasate and migrate to the site of injury in higher numbers (McGeer & McGeer 2003). In fact, there are reported abnormalities in the BBB in PD (Farkas et al 2000),

which allows for elevated invasion of peripheral adaptive immune cells. The extravasated T cells could then be activated by inflamed microglia cells which are the primary innate immune cells of the CNS (Kannarkat et al 2013). Moreover, antigens can exit the CNS through the cranial nerves, arachnoid villi and spinal nerve root ganglia into the lymphatics (Cserr & Knopf 1992). Antigens can then be processed and presented by dendritic cells to T cells in the lymph thereby initiating and mobilizing an adaptive response to the CNS (Mosley et al 2012).

The leakiness of the BBB coupled with the presence of antigens into lymphoid organs can all contribute to the recruitment of adaptive immune cells to the brain. A study by Brochard et al. showed the presence of T lymphocytes in the SN of MPTP injected mice as well as in post mortem brains of PD patients. Other studies using the 6-OHDA model in rats (Wheeler et al 2014) and mice (Ip et al 2015) also proved the infiltration of both $CD4^+$ and $CD8^+$ T lymphocytes in the brain of injected animals. A recent study by Sulzer et al. using peripheral blood mononuclear cells (PBMC's) from PD patients demonstrated the activation of T lymphocytes in response to α-synuclein peptides, implying a probable role of autoimmune inflammation in PD pathogenesis. They also observed that the T lymphocyte responses were chiefly mediated by $CD4^+$ T lymphocytes though there were some $CD8^+$ T lymphocytes mediated responses.

In summary, the reports from the studies mentioned above point to the fact that immune responses may play a very critical role in the pathogenesis and progression of PD. Though some insights have been shed on the possible role of lymphocytes in PD, it must be stated that studies in the neurotoxic animal models reported contrasting data in the role of T lymphocytes. For instance, whereas Brochard et al. reported a detrimental role especially for $CD4^+$ T lymphocytes in the MPTP model, Ip et al. and Wheeler et al. described a protective role particularly for $CD8^+$ T lymphocytes in the 6-OHDA model of PD (Brochard et al 2009, Ip et al 2015, Wheeler et al 2014). By using WT, $Tcrb^{-/-}$, $CD8a^{-/-}$ and $CD4^{-/-}$ mice in the MPTP mouse PD model,

Brochard et al. discovered that $CD4^+$ T-cells had a detrimental effect on the survival of dopaminergic neurons. On the other hand, in the 6-OHDA model involving athymic rats ($RNU^{-/-}$, T lymphocyte-deficient) and $RNU^{-/+}$ rats (not immunodeficient) there was an increase in the number of $CD4^+$ T cells in the SN and a decline in $CD8^+$ T cells after 6-OHDA injection (Wheeler et al 2014). They also showed the absence of T lymphocytes aggravate motor behavioral deficit in this rat model of PD (Wheeler et al 2014). Ip et al. in their study using RAG-$1^{-/-}$ (which lack mature lymphocytes) and WT mice also observed a more pronounced motor behavioral impairment in the RAG-1 deficient mice as compared to WT mice corroborating the observation that lymphocytes have a beneficial effect on motor recovery in the 6-OHDA model (Ip et al 2015). However, conflicting to the findings made by Wheeler et al. there was an elevation of $CD8^+$ T cells and only a minor fraction of $CD4^+$ T lymphocytes (Ip et al 2015). Additionally, in the $RNU^{-/-}$ rats there was no significant loss of striatal TH fiber density nor SN dopaminergic cell loss as compared to controls which was contrary to the observations of Ip et al. in comparing the RAG-$1^{-/-}$ and controls after 6-OHDA injection (Ip et al 2015, Wheeler et al 2014).

With the outlined disadvantages of neurotoxic models stated earlier, it is paramount that the study of the role of immune cells be carried out in a model in which reproducibility can be guaranteed, especially after the recent findings by Sulzer et al. which suggests there might be an autoimmune component in PD pathogenesis. The AAV1/2-A53T-α-synuclein (haSyn) model of PD has given consistent results in both rats (Koprich et al 2011, Koprich et al 2010) and mouse (Ip et al 2017) models of PD with the presence of neurodegeneration, protein aggregation and behavioral deficit. Moreover, earlier studies on lymphocyte contribution in PD failed to answer some key questions such as;

(i) the precise phenotype of lymphocytes?

(ii) the cytokines involved?

(iii) which subset is most detrimental?

(iv) the specificity of lymphocytes to antigen?

It was in this regard that we studied the effect of the adaptive immune system in the pathogenesis of PD in the new haSyn mouse model of PD. In this mouse model, wild type (wt) C57BL/6 or RAG-$1^{-/-}$ mice were stereotaxically injected with haSyn viral vector in the SN, which subsequently diffuses into the striatum thereby inducing PD (Fig. 3).

1.7.0 Hypothesis and Aim

Parkinson's disease is characterized by the presence of Lewy bodies with α-synuclein being its main constituent. The haSyn mouse model is primarily a synucleinopathy model with the presence of Lewy-like pathology (Ip et al 2017). With the recent findings by Sulzer et al. (Sulzer et al 2017) where T lymphocytes were activated when exposed to α-synuclein peptides, we deduce that;

(i) the injection of haSyn vector into the SN of mice and the subsequent presence of α-synuclein will lead to higher lymphocyte recruitment into the brain as compared to control.

(ii) the presence of lymphocytes will negatively affect the nigrostriatal pathway, thereby resulting in neurodegeneration.

(iii) Neurodegeneration of the nigrostriatal tract in haSyn mice occurs in an α-synuclein-specific manner.

Therefore, the main aim of this study was to characterize and assess the impact of the adaptive immune system in the novel haSyn mouse model of PD. To achieve this, we determined the specific phenotype of T cells infiltrating the brain, which subset exacerbated neurodegeneration, the cytokines that mediated their effect and whether they exhibited specificity to haSyn antigen.

1.8.0 Declaration on participation

This study was conducted in the working group of PD. Dr. Chi Wang Ip of the Department of Neurology of the University of Würzburg. The experiments were carried out by me unless otherwise stated. Eliana Ribechini (then a postdoc at the lab of Manfred Lutz) contributed to the setup and analyses of the FACS experiments. DAT binding assay and dopamine neurochemical analysis with HPLC were conducted by the Dr. James B. Koprich lab of the Krembil Research Institute, Toronto Western Hospital, Canada. The viral vector transduced primary hippocampal neurons were provided by PD Dr. rer. nat. Robert Blum. ELISpot experiments were designed and done under the direction of Valentine Bruttel and Fadhil Ahsan of Prof. Dr. rer. nat. Jörg Wischhusen lab. Dr. med. Camelia Monoranu assisted in the identification and quantification of lymphocytes numbers in human brain autopsies. Together with Dr. Ip, Mona Gehmeyr conducted AAV injections into mice shown in Figure 8g. For the same mice, brain cuttings, stainings for $CD4^+$, $CD8^+$ and $B220^+$ lymphocytes and striatal TH were performed in collaboration with Mona Gehmeyr.

Chapter TWO

2.0 Materials

2.1.0 Chemical and reagent list

Chemical	***Company***	***Order number***
Sodium chloride (NaCl)	Sigma-Aldrich	31434-1KG-R
Sodium dihydrogen phosphate dihydrate ($NaHPO_4$ x $2H_2O$)	ROTH	T879.2
Potassium chloride (KCl)	Merck	1.049.360.500
Hydrogen chloride (HCl, 1N)	Fluka	35328-1L
Glycerol	Merck	1.040.931.000
Paraformaldehyde (PFA)	Merck	1.040.051.000
Ethanol (EtOH) (70%)	Fischar	PZN-02261207
Bovine serum albumin (BSA)	Sigma	(A4503-100G)
Optimal cutting temperature (OCT)	Sakura	4583
Triton X	Sigma	X100
Normal goat serum (NGS, 100%)	Dako	X0907
Ocular lubricant (Bepanthen)	Bayer	PZN-02182442
Isoflurane	CP Pharma	1214
Sodium hydroxide NaOH (5M)	Merck	1099130001
Rimadyl	Zoetis	141-199

D-Sucrose (>99.5%, p.a.)	ROTH	4621.1
Heparin	Ratiopharm	25000
2-Methylbutane	ROTH	3927.1
Percoll	GE Healthcare	17-0891-02
Phosphate buffered saline (Dulbecco's PBS low endotoxin)	Biochrom	L1825
Hydrogen peroxide 30% (H_2O_2)	Merck	1.072.090.250
Sodium azide (NaN_3)	Sigma	S8032-25G
Liquid blocker (Pap Pen)	Science Services	N71310
Collagenase NB4 Standard Grade	Serva	17454

Table 1. List of chemicals and reagents.

2.2.0 Solution composition and preparation

10x (0.1 M) phosphate buffered saline (PBS): 80 g NaCl, 14.2 g NaHPO4 x $2H_2O$ and 2 g KCl dissolved in distilled water. Bring pH to 6.8 with HCl. The 10x PBS was diluted to 1x (0.01 M) PBS with distilled water and pH adjusted to 7.4

PBS with heparin solution: to 150 ml of 1x PBS, 0.5 ml of heparin was added for perfusion of mice

Antifreeze cryoprotectant: consisted of 30% glycerol, 30% EtOH, 40% 0.01 M PBS

4% Paraformaldehyde (PFA): 10 g PFA was dissolved in 250 mL 0.01 M PBS. Two drops of 5 M NaOH was added and the solution constantly stirred at 60°C. When PFA was dissolved and solution cleared, it was cooled on ice and pH to was brought 7.4 with HCl. The PFA solution was subsequently filtered.

30% sucrose solution: 30 g of sucrose was dissolved in 100 ml 1x PBS

10% BSA solution: 100g of BSA dissolved in 100 ml 1x PBS and filtered

Blocking solution: 10% normal goat serum (NGS), 2% BSA 0.5% Triton X (Tx) in 0.01 M PBS

BSS (Balanced Salt Solution I, II)

BSS I: 50 g of glucose, 3 g KH_2PO_4, 11.9 g Na_2HPO_4, 0.5 g phenol red all dissolved in 5 l distilled H_2O

BSS II: 9.25 g $CaCl_2$, 20 g KCl, 320 g NaCl, 10 g $MgCl_2$, 10 g $MgSO_4$ were dissolved in 5 l distilled H_2O. Then 125 ml of BSS I was mixed with 125 ml of BSS II in 1 l of distilled water H_2O.

BSS/BSA: 0.2% BSA was added to BSS solution prepared above.

Antibody diluent for immunohistochemistry: 2% NGS, 2% BSA, 0.5% Tx in 0.01 M PBS

FACS-buffer: 1000 ml PBS with 0.1% BSA, 250 mg NaN_3

Solutions and materials for ELISpot assay

Blocking buffer: 7.5% fetal calf serum (FCS) in Iscove's modified Dulbecco's medium IMDM medium (sterile)

Dilution buffer: 0.5% BSA in PBS.

Washing buffer: 1x PBS plus 0.01% tween 20

Medium for T cells: IMDM with L-glutamine plus 10% FCS supplemented with penicillin-streptomycin.

Horseradish peroxidase (HRP)-streptavidin solution: (dilute 1:500 in dilution buffer Thermo Fisher Scientific cat # SA10001 Waltham, MA, USA)

3, 3', 5, 5'-Tetramethylbenzidine (TMB) substrate for ELISpot: (Mabtech, cat # 3651-10, Nacka Strand, Sweden)

Multiscreen-HA filter ELISpot plates: (Millipore # MAHAS4510, Burlington, MA, USA)

2.3.0 Reagent Kits

Foxp3 /Anti-Mouse/Rat staining set APC (eBioscienc-Thermo Fisher Scientific cat # 77-5775-40 Waltham, MA, USA).

LEGENDplex™ Mouse Inflammation Panel (13-plex) with Filter Plate (BioLegend, San Diego, CA, USA)

3,3-Diaminobenzidine tetrahydrochloride dihydrate (DAB) peroxidase substrate kit (Vector Labs #SK4100, Burlingame, CA, USA)

Ultra-sensitive avidin/biotin complex (ABC) peroxidase standard staining kit (1:56, Thermo Fisher Scientific cat # 32050, Waltham, MA, USA)

2.4.0 Materials for stereotaxic injection

Mouse stereotaxic frame, mouse anesthesia stereotaxic mask apparatus, motorized microinjection pump equipment were all purchased from Stoelting (Wood Dale, IL, USA), isoflurane vaporizer (Dräger AG., Lübeck, Germany), induction box (custom made) drill with handpiece (Foredom Co., Bethel, CT, USA), ocular lubricant, 70% EtOH, scalpel #10 (Feather Co., Osaka, Japan), tissue forceps, gauze, cotton swabs, suture materials (V97D9) (Ethicon Inc., Somerville, NJ, USA), 75N 5 µl microinjection syringe (Hamilton Co., Reno, NV, USA), oxygen tank, electric razor, human AAV1/2-A53T- α-synuclein or empty AAV1/2- viral vector (EV), C57BL/6N wild type mice, pain medication (rimadyl), isoflurane.

2.5.0 Materials for tissue processing

Bone scissors, heparin, 25 G needle, tissue pincers, brain matrix for mice, aluminum foil, dry ice, OCT, cryomold, methylbutane, object slides,coverslips, Aquatex (aqueous mounting media), distilled water, cryostat.

2.6.0 Antibodies for immunohistological and ELISpot assays

Rat anti-mouse CD4 (1:1000, Serotec, cat # MCA1767, Oxford UK), rat anti-mouse CD8 (1:500, Serotec, cat # MCA609G Oxford UK), rat anti-mouse CD11b (1:100, Serotec, cat # MCA74G, Oxford UK) mouse anti-human CD3 monoclonal antibody (1:50, Dako, clone F7.2.38, cat # M7254, Jena, Germany), mouse anti-human CD68 antibody (1:100, Dako, clone PG-M1, cat # M0876, Jena, Germany), mouse anti-human alpha synuclein (1:80, Novocastra, clone KM51, cat # NCL-L-ASYN, Newcastle, UK), chicken anti-mouse TH (1:500, Abcam cat # 76442, Cambridge, UK) rabbit anti-mouse TH (1:1000, Abcam cat # 112, Cambridge, UK), rabbit anti-human α-synuclein (1:30,000, Sigma cat # S3062, St. Louis, MO, USA), mouse anti-mouse microtubule-associated protein-2 (MAP2) (1/1000, clone AP20, Sigma, cat # M1406 St. Louis, MO, USA), mouse anti-βIII tubulin (TUJ1) (1:100, Neuromics, cat # MO15013, Edina, MN, USA), goat anti- anti-heat shock proteins-60 (HSP60) (1:100 Santa Cruz, cat. # sc-1052, Dallas, TX, USA), anti-mouse IFN-γ (clone AN18, Mabtech, Nacka Strand, Sweden), cleaved caspase-3 (ASP 175, 1/300, Cell Signaling Technology, MA, USA), biotinylated goat anti-rabbit (1:100, Vector Laboratories cat # BA-1000, Burlingame, CA, USA), biotinylated goat anti-mouse (1:100, Vector Laboratories cat # BA-9200, Burlingame, CA, USA), biotinylated rabbit anti-rat (1:100, Vector Laboratories cat # BA-4001, Burlingame, CA, USA) biotinylated anti-IFN-γ (clone R4.6A2 , Mabtech, Nacka Strand, Sweden) goat anti-rabbit Cy3 (1:300, Jackson ImmunoResearch Inc. cat # 111-165-003, West Grove, PA, USA), goat anti-rabbit Alexa Fluor 488 (1:300, Invitrogen cat # A-11039, Carlsbad, CA, USA), goat anti-chicken Cy3 (1:300, Alpha Diagnostics cat # 60334, San Antonio, TX, USA), goat anti-

mouse Alexa Fluor 488 (1:300, Dianova cat #115-545-166, Hamburg, Germany) goat anti-mouse FITC (1:200, ZYMED, cat# 62-6312, San Francisco, CA, USA) donkey anti-mouse Cy5 (1:500, Jackson ImmunoResearch Inc. cat # 715-175-151, West Grove, PA, USA), 4′,6-diamidino-2-phenylindole dihydrochloride (DAPI) nuclear stain (1:500, 000, Sigma cat # D8417, St. Louis, MO, USA).

2.7.0 FACS antibodies

Antibodies for FACS were all purchased from BioLegend (San Diego, CA, USA). CD4-AF647 (Alexafluor 647, clone GK1.5) CD8-PerCP-Cy5.5 (Peridin chlorophyll protein-Cyanine 5.5, clone 53-6.7), CD25-AF488 (Alexafluor 488, clone PC61), CD69-AF488 (clone H1.2F3), CD122-PE (R-phycoerythrin, clone TM-β1).

2.8.0 Software and equipment

Stereo Investigator software package (version 11.07; MicroBrightField Biosciences, Williston, VT, USA) on a BX53 microscope (Olympus Corporation, Tokyo, Japan), National Institutes of Health (NIH) ImageJ software (NIH, Bethesda, MD, USA), FlowJo software (FLOWJO LLC, Ashland, OR, USA), FACSCaliburTM (Beckton Dickinson, Franklin Lakes, NJ, USA), BD^{TM} LSR II or FACSCalibur^{TM} (Beckton Dickinson, Franklin Lakes, NJ, USA), GraphPad Prism (version 5.0; GraphPad Software, Inc., San Diego, CA, USA).

Chapter THREE

3.0 Methods

3.1.0 Ethics

Animal experiments were approved by the Regierung von Unterfranken Wuerzburg.

3.1.1 Animals

Male wt mice on C57BL/6 background (Charles River Laboratories) and RAG-$1^{-/-}$ mice were purchased from either Jackson Laboratories or obtained from the Tierhaltung Neurologie, Uniklinikum Würzburg. Wt, B6. $CD4^{-/-}$, B6. $CD8^{-/-}$ and B6. $JHD^{-/-}$ mice for bone marrow donor experiments were obtained from Charles River, Jackson Laboratories or received from Tierhaltung ZEMM, Uniklinikum Würzburg. Mice were used for experiments at 8-12 weeks old and kept in a nearly pathogen-free environment under standard conditions (21 °C, 12 h/12 h light-dark cycle).

3.1.2 Stereotaxic injection of adeno-associated vectors (AAV) 1/2 serotype injection

The AAV1/2 serotypes used in these experiments were designed as described by Koprich et al. 2010. The mice were placed in an isoflurane induction chamber with 2 L/min O_2 and 3-4% isoflurane until fully anesthetized, by ensuring there was no response to nociceptive stimuli. The isoflurane vaporizer was set between 1.5 - 2% mixed with 2 L/min of O_2. Mice were secured on a stereotaxic frame and head fastened with ear bars and mouthpiece such that there was no movement horizontally (Fig. 3). With a scalpel (#10 Feather), an incision was made in the rostrocaudal direction (to expose both Bregma and lambda) on a shaved and disinfected skull. The microinjection syringe was loaded with 2.5 µl of the haSyn or empty AAV1/2- viral vector (EV) both at a concentration of 5.16 x 10^{12} genomic particles (gp)/ml without bubbles and fastened to micro-injection apparatus (Stoelting, Kiel, Wisconsin, USA). The stereotaxic

coordinates for unilateral injection in the right SN for C57BL/6 wt and RAG-1 $^{-/-}$ mice were from Bregma: AP -3.1 mm; ML -1.4 mm; DV -4.2 mm based on Ip et al. 2017. The viral vector was injected at a rate of 0.5µl/minute, controlled by the motorized microinjection pump. Following injection, the needle was held in place for 5 min and removed gently and slowly from the brain to prevent the viral vector from being drawn out of the SN. The skin incision was closed with suture material and mice were given pain medication.

(a) (b)

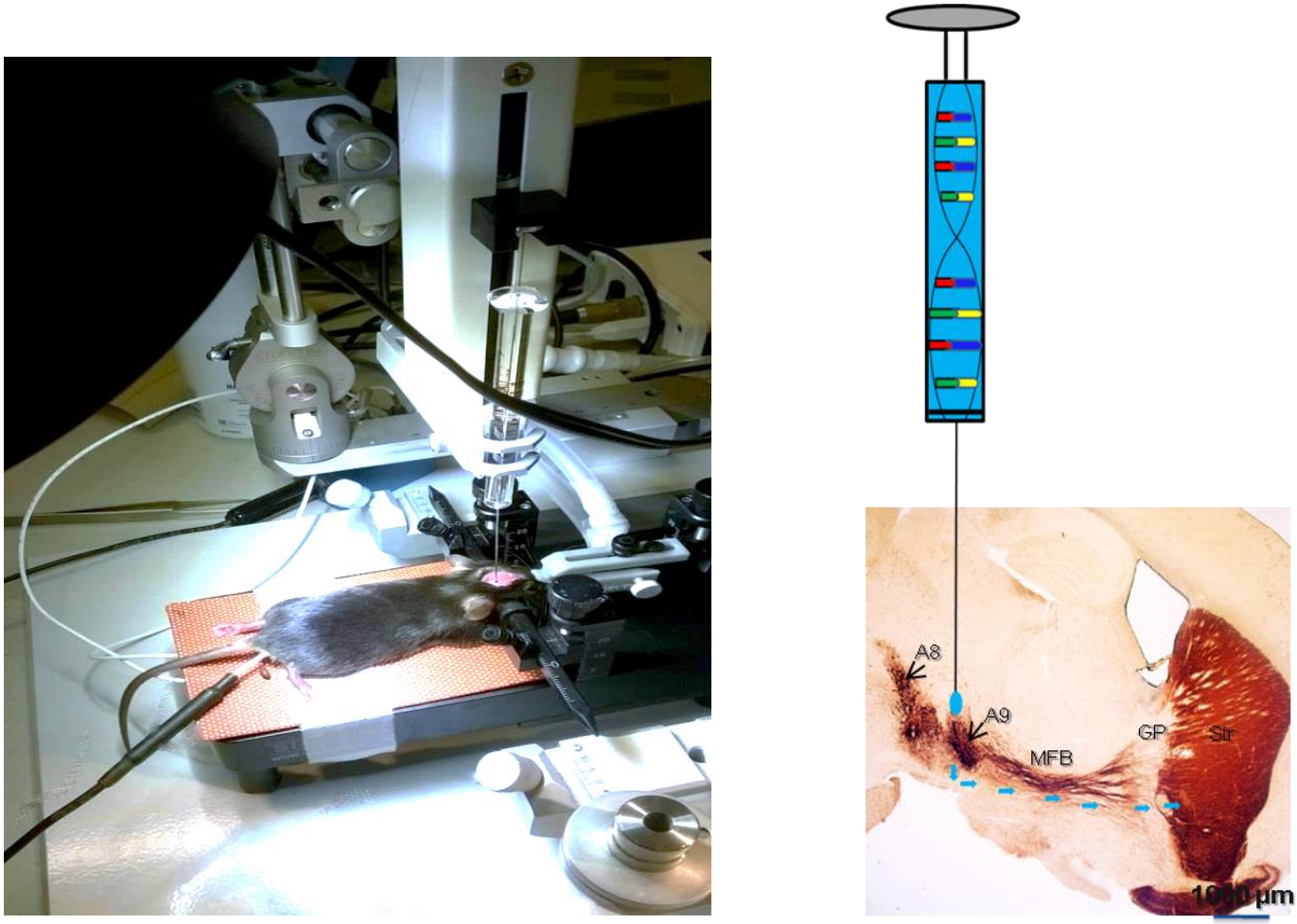

Fig. 3. An illustration of stereotaxic injection in mice and mechanism of haSyn spread.

a: Shows an image of stereotaxic injection into a mouse SN.

b: A parasagittal section depicting the proposed diffusion of haSyn viral vector from the SN to the striatum following injection. The haSyn viral vector is transported from the SN through axons of the lateral segment of the MFB into the striatum thereby inducing PD.

A8: retrorubral field, A9: substantia nigra pars compacta, MFB: medial forebrain bundle, GP: globus pallidus, Str: striatum.

3.1.3 Subcutaneous injection

Mice were secured on a stereotaxic frame and head fastened with ear bars and mouthpiece. With a 10G needle, a little opening was made subcutaneously on a shaved and disinfected skull. The microinjection syringe was loaded with either 2.0 µl of the haSyn or EV viral vectors. Injections of viral vectors were made into the openings that were made earlier with the needle. A week post-injection, mice were sacrificed and the cervical lymph nodes and spleen were harvested for FACS analysis.

3.1.4 Tissue processing and immunohistochemistry

3.1.5 Human section preparations

Human brain tissues from the SN pars compacta were collected from the Brain Bank Center Würzburg, a member of the BrainNet Europe Consortium (https://www.brainnet-europe.org). Brains were procured with the approval of the next of kin and in guidelines of the Local Ethics Committee. The mean (SD) age of the control group was 61.8 (±10.7) years and 77.1 (±12.11) in the PD group. The male/female ratio in the control group was 4/5, in the PD cohort 8/4. Tissues from twelve neuropathological characterized PD cases with different Braak stages (from 3 to 6), and nine age-matched controls were formalin-fixed and paraffin-embedded. Samples sectioned between 4-5 µm thicknesses were immunohistochemically stained for the detection of T cells, utilizing the CD3 monoclonal antibody and for microglial cells by applying the CD68 antibody.

3.1.6 Processing of mouse brain tissues

Mice were sacrificed at 1, 5 and 10 weeks following AAV1/2 injection. They were transcardially perfused with heparinized 1xPBS using a 25 G needle. The brain was carefully removed from the skull with bone scissors and tissue pincers. Next, the whole brain was either

collected in Eppendorf tubes for FACS analyses or placed in a matrix with the ventral surface (the region where optic chiasm is seen) upward and leveled. For immunohistochemistry and neurochemical examinations, the brain was dissected in the coronal plane at +0.14 mm from Bregma (Fig. 30 (Paxinos 2001)). The caudal part of the dissected brain, which includes the SN, was put in 4% PFA for 2 days at 4 °C. Brains were then transferred into 30% sucrose solution for another 2 days at 4 °C. After 2 days in sucrose solution, each brain was placed in a cryomold filled with optimal cutting temperature (OCT) compound and slowly frozen in liquid dry ice-cooled methyl butane. The rostral parts of the brain meant for HPLC and dopamine transporter (DAT) binding assay, were frozen immediately after dissection in liquid dry ice-cooled methylbutane. Tissue was quickly wrapped in aluminum foil, inserted in an Eppendorf tube and kept on dry ice until it was stored at -80°C. For striatal dopaminergic fibers, microglial and lymphocyte immunolabelling, the rostral region of brains were immediately immersed into cryomold filled with OCT compound and slowly frozen in liquid dry ice-cooled methylbutane and stored at -20°C. With free floating sections, 40 µm cryo-sections of the PFA-fixed brain were cut in the coronal plane in 4 series (sections in the same series are separated by 160 µm). The sections were collected into an anti-freeze cryoprotectant and stored at -20°C. Sections starting at -2.46 mm and ending at -4.04 mm from Bregma (Fig.s 51 to 64, (Paxinos 2001)) were taken.

Fresh frozen tissues were cryo-sectioned with a thickness of 10 µm, and mounted on object slides (3-4 sections per slide) and finally stored at a -20 freezer. Sections acquired were from

-0.10 mm to -0.58 mm from Bregma for striatum and -2.46 mm to -4.04 mm for SN sections (Fig.s 32 to 36 for striatum and 51 to 64 for SN (Paxinos 2001)).

3.1.7 Immunohistological analyses of mouse tissue

Immunohistochemical staining of mouse tissue for $CD4^+$, $CD8^+$, $CD11b^+$ was conducted using 10 µm fresh coronal cryo-sections of the SN and striatum. Sections were quickly dried at RT and encircled with liquid blocker (Pap pen). Post-fixation was done with acetone at -20 °C (for lymphocytes) or with 4% PFA for 15 mins at RT and sections washed 3 x 5 mins in 1x PBS. Blocking was carried out for 30 mins at RT with 10% NGS, 2% BSA and no Tx. Primary antibody incubation was done overnight at 4°C with rat anti-mouse CD4, rat anti-mouse CD8 and rat anti-mouse CD11b in diluent: 2% NGS, 2% BSA and no Tx. Sections were afterward washed 3 x 5 mins in 1 x PBS before applying secondary antibody (biotinylated rabbit anti-rat) for 1 hr at RT. Next, sections were incubated with avidin/biotin solution (prepared 30 mins before use) for 30 mins after washing 3 x 5 mins. The sections were washed again and incubated with DAB-Peroxidase substrate solution until staining develops. Following washing, drops of Aquatex were applied and slides were covered with slips.

3.1.8 Tyrosine hydroxylase (TH^+) staining of dopaminergic neurons in SN for stereological analysis

TH^+ staining was used to identify dopaminergic neurons in SN pars compacta and reticulata using 40 µm coronal cryo-sections. One of the 4 series of SN was chosen for TH^+ immunolabeling. The free-floating sections in anti-freeze cryoprotectant were drained into a petri dish containing distilled water and washed for 3 mins. Sections were transferred into a well containing ¾ full 1x PBS and washed in PBS 3 x for 5 mins. Blocking was done with 10% normal goat serum (NGS), 2% bovine serum albumin (BSA) 0.5% Triton X (Tx) in 1x PBS at room temperature (RT) for 1 h on a shaker. After blocking, sections were moved into a well with the primary antibody (rabbit anti-mouse TH) diluted in 2% NGS, 2% BSA, 0.5% Tx in 1x PBS, and incubated overnight at RT on shaker. Washing was done 3 x 5 mins in 1x PBS. Next, sections were incubated with secondary antibody solution of biotinylated goat anti-rabbit at RT

on shaker for 2 h. Tissues were washed 3 x 5 mins in 1x PBS and transferred into avidin/biotin reagent solution for 2 h on a shaker. Afterward, they were stained with DAB-Peroxidase solution for 10 mins (time depends on how quickly the staining develops). Washing was then performed 3 x 5 mins in 1x PBS and sections mounted on object slides with Aquatex.

3.1.9 TH^+ labeling of dopaminergic fibers in the striatum (fresh frozen sections, 10 µm)

Sections were dried encircled with Pap pen and postfixed with 4% PFA for 15 mins at RT. They were then washed 3 x 5 mins in 1x PBS and blocking carried out for 30 mins at RT. Primary antibody incubation was done overnight at 4°C with rabbit anti-mouse TH in diluent: 2% NGS, 2% BSA and no Tx. Sections were eventually washed 3 x 5 mins in 1 x PBS before applying secondary antibody (biotinylated goat anti-rabbit), for 1 hr at RT and washed 3 x 5 mins. Next, they were incubated with avidin/biotin solution for 30 mins. The sections were washed again and incubated with DAB-Peroxidase substrate solution until staining developed. Following washing, drops of Aquatex were applied and slides were covered with slips.

3.2.0 α-synuclein /TH^+ double immunofluorescence staining: fresh frozen sections

Sections were postfixed with 4% PFA for 15 mins at RT and washed 3x 5 mins in 1x PBS. Blocking was carried out for 45 mins at RT. Primary antibody (rabbit anti-human α-synuclein and chicken anti-mouse TH) was applied overnight at 4°C after which sections were washed 3 x 5 mins in 1x PBS. They were then incubated with secondary antibodies (goat anti-rabbit Alexa Fluor 488 and goat anti-chicken Cy3) solution for 1 hr at RT and after that washed in 1x PBS. Next, DAPI nuclear stain was applied for 10 mins at RT and sections washed. Slides were covered with slips using Aquapolymount.

3.2.1 Imaging and quantification of immune cells in the brain

The quantification of T cells and microglia was performed on a BH2 light microscope (Olympus). T cells and microglia from mice sections were estimated at a magnification of 200 X, with an ocular grid covering an area of 0.25 mm^2 for microglia cells. For human sections, T cells and microglia counted at 400 X magnification with an ocular grid area of 0.0625 mm^2. Images were taken with Zeiss Axiophot 2 or Zeiss Imager.M2 (Carl Zeiss) microscopes.

3.2.2 Brain sample preparation for FACS

Fluorescence activated cell sorting (FACS) analyses was done with the brain, cervical lymph nodes and spleen to assess the phenotype of immune cells. Animals were pooled (2-3 mice) for FACS because of the fewer number of lymphocytes in the brain. After brains were harvested, they were rinsed in heparinized PBS and transferred into Eppendorf tubes with 1 ml balanced salt solution with bovine serum albumin (BSS-BSA). Brains were cut into small pieces with scissors (cleaned for different treatment groups). 20 µl of collagenase NB4 (Serva Electrophoresis, stock: 100 mg/ml) and 10 µl DNase I (AppliChem stock: 10 mg/ml). The samples were thoroughly mixed with collagenase and DNase I and incubated for 30 min at 37°C in water bath with intermittent manual shaking. Afterward, tissues were homogenized through a cell 70 µm strainer with a plunger. BSS-BSA was added during and after homogenizing to rinse the strainer and plunger. Samples were centrifuged at 1500 rpm for 5 min at RT and supernatant discarded. 5 ml of 70% percoll was added to pellet (final volume ~ 6 ml). Pellet was homogenized in 70% percoll and transferred into a 15 ml conical tube. The suspension was overlaid slowly with 6 ml of 30% percoll solution. This step was done slowly to avoid the mixing of 70% and 30% layers and bubbles. The samples were then centrifuged at 2000 rpm for 30 min at RT, with no brakes. The myelin ring was carefully aspirated with vacuum or milliliter pipettes. The white buffy layer (interphase) consisting of brain infiltrating leukocytes (BILs, Fig. 4) was collected into a 15 ml tube and resuspended in medium. The suspension was

centrifuged at 1500 rpm for 5 min at RT and supernatant discarded. The pellet was then resuspended in 1 ml of BSS-BSA media.

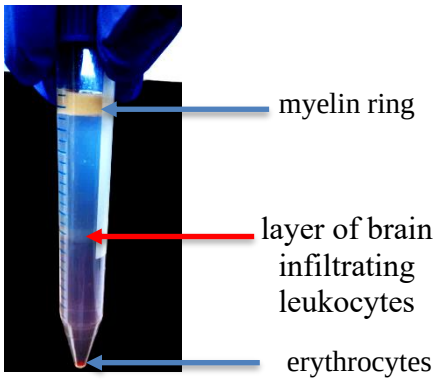

Fig. 4. An image depicting the percoll extraction gradient and location of BILs following centrifugation for 30 mins.

3.2.3 Cervical lymph nodes and spleen sample preparation

Cervical lymph nodes and spleen from pooled mice were homogenized in 1X PBS using the frosted part of microscope slides or with 70 µm cell strainer. The homogenized samples were transferred into a 15 ml conical tube and centrifuged at 1500 rpm for 5 min. The supernatant was discarded and 5 ml of red blood cell lysis solution was added to samples for 2 mins. The samples were then washed with 5 ml of BSS-BSA media at 1500 rpm for 5 mins and the supernatant discarded. Lymph node samples were resuspended in 2 ml of BSS-BSA media and 5 ml of media was added to spleen samples. The lymph node samples were subsequently filtered through 70 µm cell filter. Cells from both cervical lymph nodes and spleen were counted using a hemocytometer with trypan blue dye.

3.2.4 Flow cytometry

Cell suspensions from the brain, cervical lymph nodes and spleen (cell numbers were from minimum 200, 000 (from brain samples) and maximum 1000, 000) were overlaid with 100 µl FACS buffer and centrifuged at 1500 rpm for 5 min at RT. The supernatant was discarded and cells were incubated with 100 µl antibody (1:100) cocktail, except for Anti-FoxP3 antibody. The suspensions were quickly vortexed and incubated at 4° for 30 mins. After incubation, washing was done with 100 µl of FACS buffer at 1500 rpm for 5 min. The supernatant was discarded, 100 µl of FACS buffer was added and samples acquired on either a BD™ LSR II or FACSCalibur™.

For samples that were meant for FoxP3 intracellular staining, the cells were fixed and permeabilized by eBioscience Fix/Perm buffer for 30 mins or overnight after surface staining. Cells were then washed with 100 µl of FACS buffer at 1500 rpm for 5 min. Following washing, cells were incubated with anti-FoxP3 antibody (1:100) for 1 hour. After washing, data were acquired and analyzed using FlowJo software. The staining panel used for FACS analysis is found in Table 2.

CD4 (AF647)/CD25 (AF488)/Foxp3 (PE)/ CD8 (PerCP-Cy5.5)	**FoxP3 T cells**
CD4/CD8 staining only (control)	
CD4 (AF647)/CD69 (AF488)/CD122 (PE)/ CD8 (PerCP-Cy5.5)	**Activated and CD122 T cells**
CD4/CD8 staining only (control)	

Table 2. Staining panel for FACS analyses.

3.2.5 Cytokine Analysis

Cell suspensions from brain, cervical lymph nodes and spleen were acquired as described above and 2 x 10^5 cells from each suspension were plated in a 96-well U-bottom plate. The cells were re-stimulated with PMA (0.1 µg/ml, Sigma-Aldrich) and ionomycin (1 µg/ml, Sigma-Aldrich) for 4 hours. The supernatants were collected and stored in -20°C until further analysis. Cytokine detection was carried out using LEGENDPlex™ Multi-Analyte flow assay kit from BioLegend and data was acquired on FACSCalibur™. In total, 13 cytokines were quantified which included IFN-γ, TNF-α, IL-2, IL-4, IL-5, IL-6, IL-9, IL-10, IL-13, IL-17A, IL-17F, IL-21 and IL-22.

3.2.6 Bone marrow cell transfer into RAG-1 $^{-/-}$ mice

Bone marrow transplantation from wt, $CD4^+/CD8^-$, $CD4^-/CD8^+$ and $CD4^+/CD8^+$ (JHD $^{-/-}$) (donor) mice into RAG-$1^{-/-}$ (recipient) mice was done as described by (Ip et al 2006). Bone marrow cell preparation from one donor (~8 weeks old) mouse was used for 2 recipient (7 weeks old) mice. For the various genotypes, different bone and organ harvesting tools such as scalpels, scissors, needles, and forceps were used. The process of harvesting the bone marrow and cell suspension preparation were all done on ice. Mice were placed in a CO_2 chamber until there was no response to nociceptive stimuli. The carcass was then disinfected with 70% EtOH. Mice were pinned on a styrofoam box lid (covered with aluminum foil and disinfected with EtOH) with unused needles and such that the ventral side is on top. Next, the skin over the hip/femoral head was removed, cutting along the groin. The femoral limb was amputated from the acetabulofemoral (hip) joint ensuring that the head of the femur was not cut through or damaged. Tissue, muscles and tendons around the femur and tibia were removed with the aid of scalpel and forceps. One can also use autoclaved or sterile paper to aid in tissue removal. The fibula (the smaller lateral bone) was broken or removed. The foot was twisted or cut from the ankle joint and the bones (now femur and tibia only) were placed in a 50 ml falcon filled with

ice and covered with more ice. These steps were repeated to remove the other limb. In a similar vein, the spleen was also taken out and collected in a 15 ml falcon filled with cold, sterile 1xPBS on ice. Under the hood, the tibia and femur were held so that the patella (knee cap) was exposed. With the aid of bigger forceps, the patella was removed from the joint; tibia and femur were then separated by hand. The distal ends of the bones (head of the femur and lateral and medial malleolus) were cut open with a fine, sterile scissors. The bone was held with forceps above a 50 ml falcon tube filled with 10 ml sterile 1xPBS and a 1 ml syringe filled with sterile 1xPBS inserted at the patella (for femur) and tuberosity (for tibia). The marrow was flushed until the femur and tibia bones are pale/white using as much PBS as needed. All bone marrow from the same genotype were collected together into one 50 ml falcon tube. The suspension of bone marrow and PBS was passed through a 70 µm cell strainer and marrow homogenized with a plunger of a syringe above a 50 ml falcon. Cell strainer and plunger were rinsed with 1xPBS and centrifuged at 4000 rpm/ 10min, 4°C and supernatant was removed afterward. For each recipient mouse, a calculated volume of 500 µl of cells suspended in 1xPBS was to be injected. The bone marrow pellet was then resuspended with half of the calculated 1xPBS.

For spleen samples (1 spleen for 4 recipient mice), fat was taken out and spleen was homogenized in 70 µm cell strainer above a 50 ml falcon filled with ~ 5 ml 1xPBS. The plunger and strainer were rinsed and centrifuged at 4000 rpm/ 10min, 4°C. The resuspended bone marrow cell suspension was added to the splenocyte pellet and homogenized gently with a pipette tip. The bone marrow tube was washed with the rest of the calculated 1xPBS and added to the total cell suspension. Cells were stored at 4°C or on ice until injection. For the recipient mice (4 - 12 weeks old RAG-$1^{-/-}$), 350 µl of bone marrow/spleen suspension corresponding to 2 x 10^7 cells was injected. The tails of mice were held under warm water for ~1 min. The mice were then restrained in an injection cage and the tail was pressed at the proximal end to make the vein more visible. When the lateral tail vein was visible enough, injection was carried out

slowly and gently. Seven weeks after intravenous injection RAG-1$^{-/-}$ mice were stereotaxically injected with EV or haSyn viral vectors. Spleens from recipient mice were tested for T and B cell reconstitution by FACS analysis. All mice examined had the expression of CD4^{+}, CD8^{+} or both antigens for JHD$^{-/-}$ recipients.

3.2.7 Dopamine transporter (DAT) binding assay (fresh frozen tissues)

Striatal DAT binding autoradiography was done as described by Koprich et al. 2011. Sections were incubated in binding buffer containing 50 mM Tris, 120 mM NaCl and 5 mM KCl at RT. They were then placed in a buffer as earlier mentioned with additional 50 pM (125I) -RTI-121 (specific activity 2200 Ci/mmol) for 2 h at 25 °C. The sections were washed in ice-cold binding buffer, followed by rinsing in ice-cold distilled water and dried. The sections were juxtaposed with an autoradiographic film with (125I)- microscale standards (Amersham) and left for 2 days at 4 °C before development. Autoradiograms were assessed with MCID software (Image Research Inc.) Densitometric measurement of 3 striata slices per mouse was done with a reference curve of c.p.m. against optical density and calculated from b- emitting (^{14}C) micro-scale standards and used to quantify the intensity of signal as nCi/g. The background intensity was also subtracted from each reading and data was represented as signal intensity for the treatment groups.

3.2.8 High performance liquid chromatography (HPLC) quantification of catecholamines

Brain tissues were sonicated in 200−750 µl of 0.1 M TCA (10 - 2 M sodium acetate, 10 - 4 M EDTA, 10.5% methanol). Samples were centrifuged at 10000 g for 20 min. The supernatant was removed and pellet conserved for protein analysis. Analysis of catecholamines was done with a specific HPLC assay with an Antec Decade II (oxidation: 0.5) electrochemical detector that operated at 33 °C. The samples were injected by using a Water 717+ autosampler onto a Phenomenex Nucleosil (5u, 100A) C18 HPLC column (150 x 4.60 mm). The mobile phase for

elution was made up of 89.5% 0.1M TCA, 10 - 2 M sodium acetate, 10 - 4 M EDTA and 10.5% methanol. Solvent delivery was at a rate of 0.8 ml/min with a Waters 515 HPLC pump. Analytes were examined as follows: DA and homovanillic acid (HVA). Waters Empower software was used for data acquisition and control of HPLC. Protein concentration was determined for each sample by Peirce BCA protein assay. Data for catecholamines values were expressed as ng analyte/mg total protein.

3.2.9 Analysis of dopaminergic fibers in the striatum

TH^+ fiber density in the striatum was measured by the optical density assessment using the NIH ImageJ software. Colored images (8-bit) were transformed into 8-bit greyscale images. Using the freehand tool, both left and right striata were measured as well as the non-specifically stained corpus callosum. For each section analyzed, the values of left and right striata were subtracted from that of the corpus callosum. Striatal optical density was then represented as a percentage of the right in relation to the left striatum. For this analysis, at least 2 striatal slices per mouse were measured.

3.3.0 Unbiased stereological estimation of TH^+ neurons in SN

Unbiased estimation of dopaminergic cells in the SN was done with the optical fractionator method of the Stereo Investigator software package (version 11.07; MicroBrightField Biosciences, Williston, VT). After opening the software, Probes was selected and then the ‘Optical Fractionator’ to open a workflow window. In the pop-up window, the ‘Start a new subject’ icon was selected. Next, the investigator's name was inserted under “Name” and SN in the “Subject's name.” The thickness of the cut tissue sections was entered as 40 µm. The option ‘number of sections per series to count,’ was left blank as sections were always added in the last step. The microscope was set to low magnification of 2X and from the drop-down menu of the workflow window, 2X was also chosen. With the microscope still set at 2X, the region of interest was traced using the left mouse button. TH^+ neurons in the SN pars compacta and

reticulata were included as described by (Baquet et al 2009). In the next step, the microscope objective was set to 100X and again 100X was selected from the drop-down menu of the workflow window. In the next step, the mounted tissue thickness must be provided. For this, the mounted thickness can either be determined before or during counting by focusing to the top and bottom of the section. Section thicknesses were all automatically determined. A counting frame size of 50 x 50 μm (size of the optical dissector) was chosen as this worked better with all of our analysis. The grid size was defined as 110 x 110 μm and the guard zone was set at 2 μm. All sampling parameter settings were reviewed and when necessary, the settings were saved. To ensure that counting was done in the region of interest, the cursor was placed inside the traced region in the 'Macro view' by right clicking 'go to'. Next step, 'count objects' icon was selected to count TH^+ neurons in each grid at every counting site. A preferred marker was chosen and this was used for all sections in a series. Markers were never changed for counting within a series. After the counting was completed for one section, the 'Add New Section' button was clicked to begin the Optical Fractionator workflow for the next SN section of the same series. When the last section of a series was quantified, the 'I've Finished Counting' icon was selected. For the next step, the 'View Results' button was chosen to display the sampling data. Section interval value was entered as 4 (cutting was done in a series of 4) in this case. The Gundersen coefficient of error for m= 1 was less than or equal to 0.1 for series counted.

3.3.1 Peptides for ELISpot assay

Peptides of 8 -15mer from haSyn were predicted for their ability to bind MHC I (H-$2D^b$ and H-$2K^b$) and MHC II (I-A^b) molecules using SYFPEITHI (www.syfpeithi.de, Ver. 1.0) and netMHC software. For each allele of MHC molecules, 3 peptides with the highest predicted affinity were synthesized by Thermo Scientific in aqua basic quality. In addition, an 8mer

peptide was synthesized where P at position 128 was exchanged with L to increase the predicted binding affinity of this peptide to H-2K^{b}.

3.3.2 Measurement of specific T cell responses by IFN-γ ELISpot

Cells were extracted as described previously. The polyvinylidene fluoride (PVDF, MSIPS4510, Millipore) plate was activated 35% EtOH for 1 minute under the hood and washed 3 x with sterile PBS. Next, the plates were coated with 50 µl of capture antibody (anti-mouse IFN-γ in sterile PBS) (Fig. 5) at a concentration of 2 µg/ml and incubated overnight at 4°C. Following overnight incubation, excess capture antibody was cautiously removed without touching the membrane. A volume of 200 µl blocking buffer (7.5% FCS in IMDM medium (sterile)) was added per well, incubated for 2 hrs at 37°C and subsequently aspirated. The peptide stimulants for the assay were concurrently prepared at a concentration of 5 µg/ml, together with 1000 cells in 50 µl of IMDM supplemented with 10% FCS. In the next step, 50 µl of medium and 50 µl of peptide-cell suspension were pipetted into negative control and experimental wells respectively, followed by overnight incubation at 37°C. The supernatant was removed and washed 10 x in washing buffer ensuring that excess buffer was removed. Secondary antibody (biotinylated anti-IFN-γ) was prepared at a concentration of 2 ug/ml in dilution buffer and 50 µl of it was added to each well for 2 hours at 37°C. Wells were then washed 6 x in washing buffer being sure to remove the excess buffer. 50 µl of diluted HRP-streptavidin solution was added to wells and incubated for 1 hr at RT in the dark. Wells were then washed 3 x with washing buffer and further with 3 x sterile PBS only. For a full 96 well plate, 5 ml of TMB was used. Before use, TMB was filtered through a 0.45 µM syringe filter. TMB solution was pipetted into wells to develop blue spots stain. The reaction was then stopped by washing wells thoroughly under tap water. The plastic underdrains of the plates were removed and the bottom of wells was washed again. Plates were left to dry under the vacuum hood on paper towels

(plate, underdrain and lid were dried separated). Reading of plates was conducted with Immunopost S6 Core Analyzer Analyzer (Cellular Technology Limited).

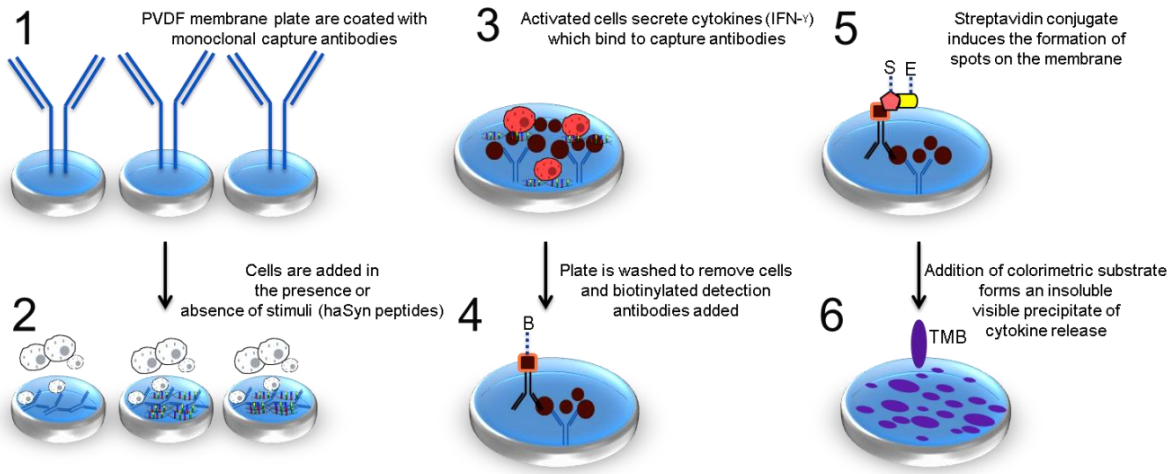

Fig. 5. An illustration of the ELISpot assay.

3.3.3 Primary hippocampal cell culture preparation

Primary hippocampal neurons were prepared from a pregnant mouse with embryonic day 18 (E18) of development. Hippocampi neurons were removed from pups and immersed in Hank's balanced salt solution (HBSS) media. Under the hood, hippocampi were transferred to 15 ml falcon tube filled with 7 ml HBSS dissection/dissociation media (supplemented with 1x Na-pyruvate, 0.1% glucose and 10 mM Hepes (pH 7.3)). The hippocampi were washed twice with dissociation medium. Afterward, the tissues were incubated with 4.5 ml dissociation media with 500 µl of 2.5% trypsin at 37°C for 20 minutes. 500 µl of DNase was then added to the suspension and incubated for 5 minutes under the hood as tissue was allowed to settle at the bottom of the conical tube. The supernatant was removed and tissue washed 2 x with 10 ml of media. In 2.5 ml of dissection medium, 200 µl of trypsin inhibitor was added to the suspension and tissue gently triturated (20 x) with a 1000 µl micropipette tip. Media was filled up to ~ 7

ml and centrifuged at 1400 rpm for 3 minutes. The supernatant was removed and again in dissection media, the pellet was triturated (10 x) using the 1000 µl micropipette tip and centrifuged at 1400 rpm for 3 minutes. The pellet was then resuspended in 3 ml maintenance media (Neurobasal medium with 1x B27, 1x glutamax and 1x penicillin/streptomycin) and gently homogenized (10 x) with 200 µl micropipette tip. The cell number was counted accordingly and 20, 000 cells were plated on coverslips or in a 96 well plate which had been coated overnight with poly-L-lysine at 4 °C, washed 5x with HBSS media.

3.3.4 Investigation of T cell-mediated toxicity in vitro

After 7 days of plating primary hippocampal neurons, cells were transduced with either 3 x 10^9 (concentration at which there was sufficient transduction and cell survival) of haSyn or 3 x 10^9 of EV viral vectors. After 4 days of transduction, T cells (200,000) were isolated from haSyn (19 weeks post-injection) mice and incubated with neurons in culture overnight (Fig. 7). For control experiments, lymph nodes from C57BL/6 mice were processed until cell suspension as described previously. In a 48-well plate, 2x10^6 cells were plated in 1 ml of R10 media and stimulated for ~ 24 hrs with soluble CD3/CD28 antibodies at a concentration of 2.5µg/ml each. Cells were collected, counted and used for experiments. The activation state of T cells ($CD69^+$) was always determined by FACS before use in experiments.

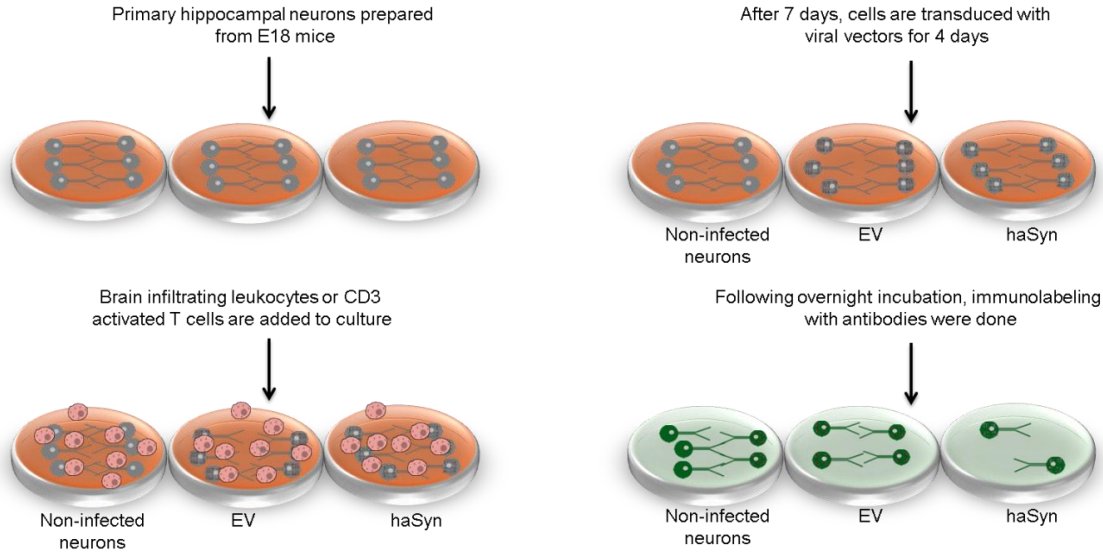

Fig. 6. A depiction of in vitro cell culture experiments.

3.3.5 Assessment of MHC molecules capacity to abrogate T cell neurotoxicity

The capacity of MHC molecules to alleviate T cell-induced cytotoxicity was assessed with Ultra-LEAF™ purified anti-mouse H-2 M1/42 MHC I (20 µg/ml, BioLegend) and anti-mouse MHC Class II M5/114 (20 µg/ml, Abcam).

3.3.6 Evaluation of cytokine toxicity

Neurons were incubated with cytokines which included: recombinant human (rh) IFN-ɣ (20 ng/ml, ImmunoTools), rh Il-4 (400 ng/ml, PeproTech) and rh TNF-α (10 ng/ml, ImmunoTools) either alone or as a combination. All concentrations used in the experiments corresponded to a biological activity of 200 units/mg.

3.3.7 Immunocytochemistry and measurement of fluorescence intensity

Neuronal cells were fixed with 4% PFA and then blocked with 5% NGS and 0.3% Tx in 1X PBS. They were labeled with anti-mouse MAP2, rabbit anti-human α-synuclein, mouse TUJ1 goat anti-HSP60 and anti-rabbit cleaved caspase-3. Secondary antibodies of goat anti-rabbit Alexa Fluor 488, goat anti-mouse FITC, goat anti-rabbit Cy3, donkey anti-mouse Cy5 were employed and cells were counterstained with DAPI nuclear stain (1:500, 000, Sigma). For experiments conducted in 96 well plate, each well was imaged randomly with the 20 X objective on a Leica DMi8 (Leica Microsystems) inverted microscope. The luminosity of MAP2 staining for every treatment condition was measured unaltered after conversion to 8-bit greyscale using ImageJ. A rectangular frame was drawn around cells to determine area and mean fluorescence. Background measurements were taken adjacent to cells and the corrected total cell fluorescence (CTCF) was calculated as integrated density – (area of selected cells × mean fluorescence of background intensity).

3.3.8 Statistical analyses

Before using any statistical test, the distribution of each data set was investigated for normal distribution using the D'Agostino & Pearson omnibus normality test or the Q-Q-plots. For normally distributed data, parametric methods were utilized and for non-normal distributed data, non-parametric methods were employed as statistical tests. The analyses of striatal TH^+ optical density, stereological estimation of SN cell numbers and measurement of corrected total fluorescence were conducted with the parametric one-way ANOVA. For the estimation of lymphocyte numbers, HPLC, DAT, FACS and cytokine analysis, non-parametric tests were utilized. The measurement of T cell-specific responses was done with two-way ANOVA with uncorrected Fisher's LSD test. *P < 0.05, **P < 0.01, ***P < 0.001 were considered as significant P-values. All statistical analyses were conducted with GraphPad Prism 5.0.

Chapter FOUR

4.0 Results

4.1.0 Introduction

Studies involving brain autopsies from patients as well as animal models of PD have pointed to the fact that there are inflammatory processes during the progression of the disease (Brochard et al 2009, Qin et al 2007). However, data from the different animal models of PD were conflicting. With the etiology of PD unknown and cure still elusive, it is necessary that there is reproducibility and consistency in data from animal models of the disease. Thus, in this study, we sought to characterize the role of the adaptive system in the new α-synucleinopathy model of PD, the haSyn mouse model. The results of this study will be focused on the nigrostriatal system (Fig. 7), which is impaired in PD and the effect of T cells on the different compartments. The specificity of T cells to haSyn antigen and in causing neuronal cell death will be demonstrated by ELISpot and cell culture experiments.

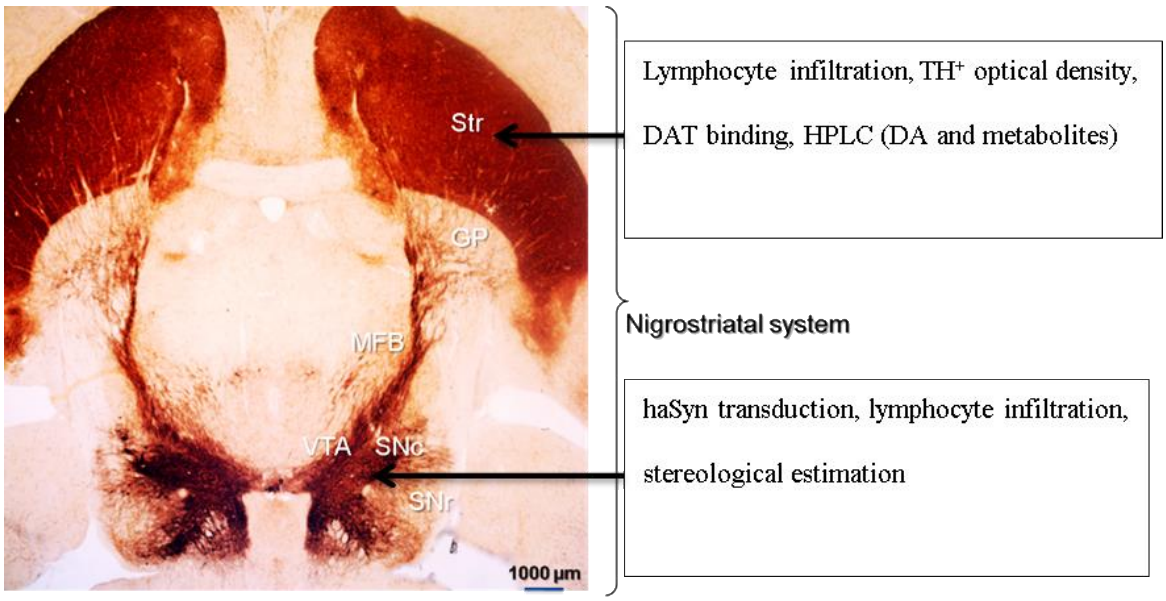

Fig. 7. An illustration of the nigrostriatal pathway.

A horizontal image of the nigrostriatal pathway showing the projection of dopaminergic neurons from SN to the striatum and the various tests conducted in the different compartments. SNc: substantia nigra pars compacta, SNr: substantia nigra pars reticulata, VTA: ventral tegmental area, MFB: medial forebrain bundle, GP: globus pallidus, Str: striatum.

4.1.1 Lymphocyte infiltration in the brain

To verify the presence of neuroinflammation as reported in previous studies, we carried out a histological analysis on human brain autopsies from non-PD controls and PD patients for activated microglia and lymphocyte infiltration. We further stereotaxically injected C57BL/6 wt mice with either EV or haSyn to assess neuroinflammation of the nigrostriatal tract in our mouse model. Histological analyses showed an increase in extravasated $CD3^+$ T lymphocytes and higher levels of $CD68^+$ microglia in PD SN samples as compared to control non-PD group (Fig. 8a-f). Though we detected the presence of B cells, their numbers were significantly low compared to T cells in both PD and control groups (Fig. 8s). A similar trend was observed in our mouse model of PD. There were higher levels $CD4^+$, $CD8^+$ lymphocytes and activated $CD11b^+$ microglia in the SN and striatum of haSyn injected mice as opposed to the EV control group, Fig.8 g-r. Again, B lymphocyte numbers were relatively low and there was no significant difference comparing haSyn and EV mice in SN.

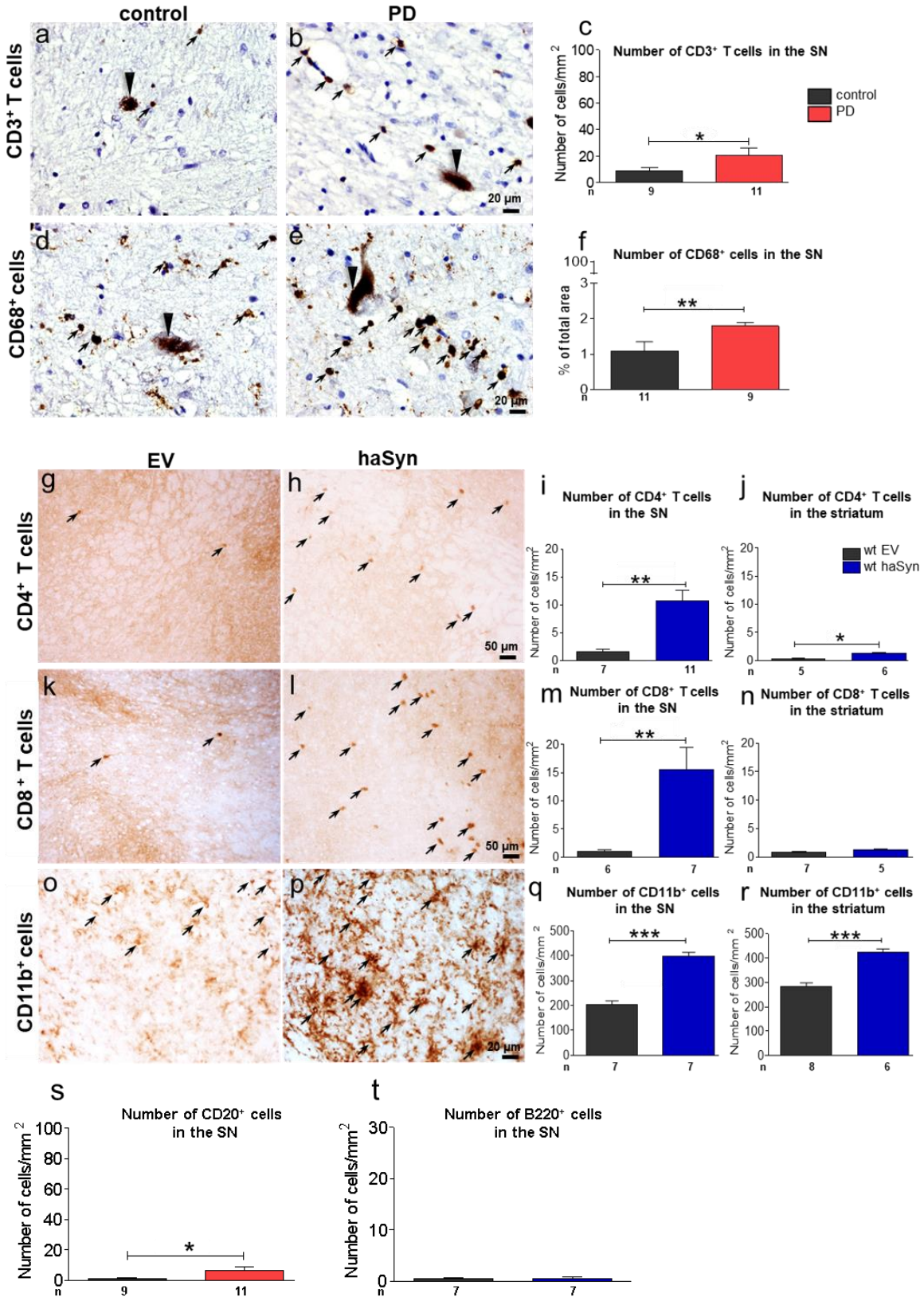

Fig. 8. Invasion of T lymphocytes and activation of microglia in brains of PD patients and haSyn injected mice.

*a-f: Depictive images of the substantia nigra of PD patients and control brain autopsies that show an elevation of CD3$^+$ T cells and C68$^+$ microglia in PD patients. g-n: haSyn injected wild type mice exhibit an increase in CD4$^+$ and CD8$^+$ T cells in the SN compared to EV control mice (g-I & k-m). In the striatum, cell numbers were higher for only CD4$^+$ but not the CD8$^+$ T cells (j&n). o-r: Quantification of microglia confirmed significantly higher cell numbers in haSyn mice than control in both SN and striatum (q,r). s-t: Quantification of B cells in the SN of human autopsies (s) and mice (t). Statistical analysis was done with the Mann-Whitney test. Mean values ± SEM are shown, n = number of independent brain samples / number of independent animals * P< 0.05, ** P< 0.01, *** P<0.001.*

4.1.2 Phenotypic characterization of immune cells

Following the determination of immune cell infiltration into the brain, the phenotype of the immune cells was examined by FACS analysis after isolating cells from the brain, lymph nodes and spleen. For the regulatory compartment, the numbers of both CD4$^+$CD25$^+$ Foxp3 and CD8$^+$CD122$^+$ regulatory T cells were relatively stable in all the experimental groups at the different time points with the exception of the cervical lymph node and spleen at week one where there was an elevated CD8$^+$CD122$^+$ T cell number in haSyn mice compared to controls. An interesting observation, however, was the increase in the levels of activated T cells in the brain,1 and 10 weeks post-injection. Employing the CD69$^+$ marker for activation, we observed an increment in CD4$^+$CD69$^+$ and a significant elevation in CD8$^+$CD69$^+$ T cells in the brains of haSyn injected mice as compared to controls at one week (Fig. 9a,d). At ten weeks post-injection, the percentage of activated T cells increased from ~26% (at one week) to ~52% for CD4$^+$ and 53% to ~74% for CD8$^+$ T cell population in the brains of haSyn mice. The control mice, on the other hand, showed only a tenuous elevation of activation state from ~13% to ~19% for CD4$^+$ and ~18-36% to ~47% for CD8$^+$ cells (Fig. 9a,d). In the peripheral lymphoid organs, haSyn injected mice did not manifest an elevation in CD4$^+$CD69$^+$ or CD8$^+$CD69$^+$ T

cells at the early stages (Fig. 9b,c,e,f). However, at ten weeks there was a substantial increase of both $CD4^+CD69^+$ and of $CD8^+CD69^+$ T cells (~41% and ~30% respectively) observed in haSyn mice, though these levels were lower compared to the activation states in the brain at the same time point (Fig. 9b,e). Contradictory to the cervical lymph nodes, there was no evident elevation in the activation states of T cells in the spleen.

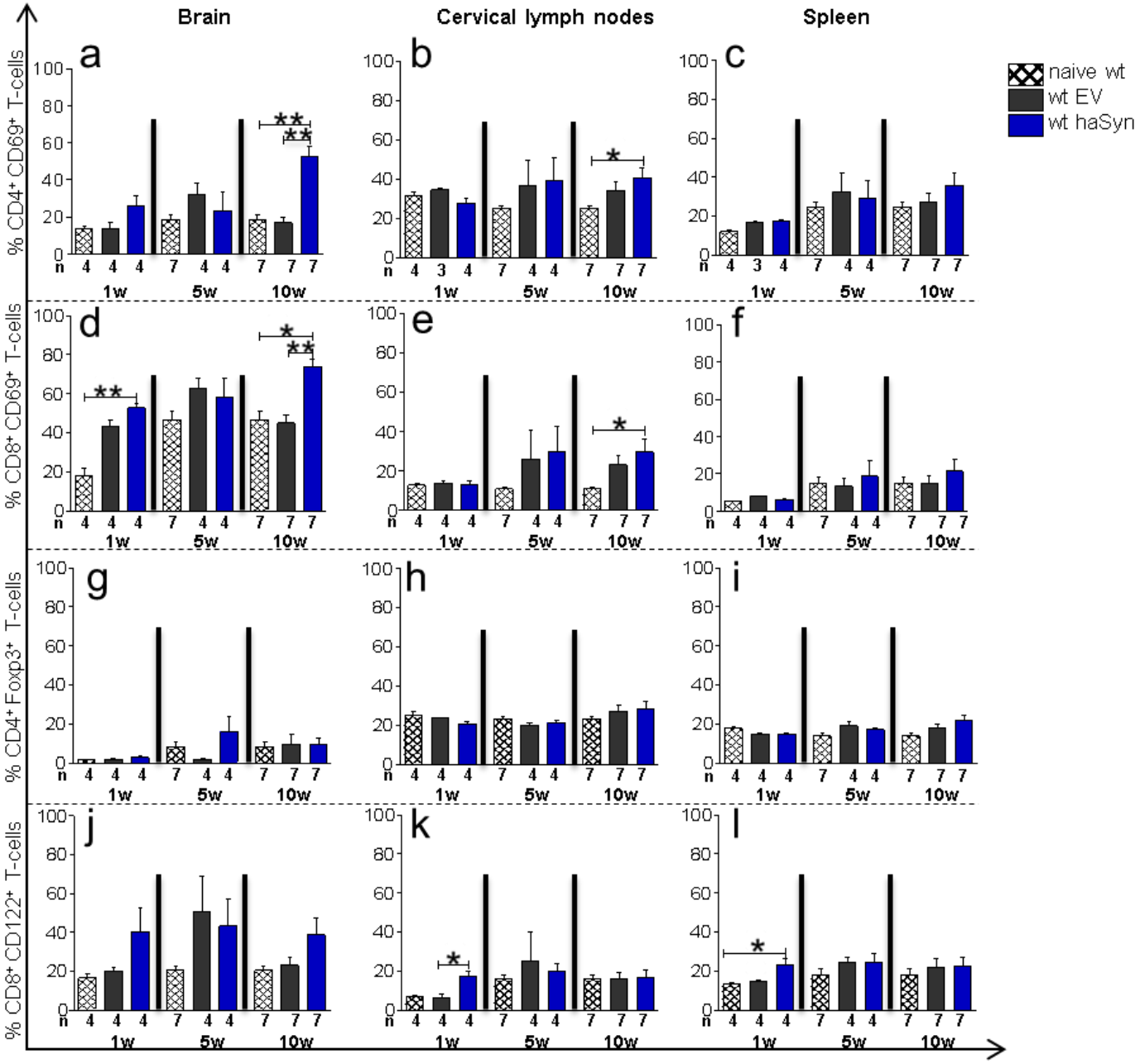

Fig. 9. Activated T cells infiltrate the brain of haSyn injected mice.

a-f : Shows an elevation in activated $CD4^+$ and $CD8^+$ in the brains of wt haSyn injected mice at 1^{st} and 10^{th} weeks of disease induction as compared to wt naïve and wt EV mice. In the lymph nodes, there was a slight increase in the activation status of T cells at 10 weeks (b&e), whereas no apparent differences were observed in the spleen (c&f). There were no significant changes in the numbers of regulatory T cells except for an increase in $CD8^+CD122^+$ T cells in the cervical lymph nodes and spleen at week 1 (k-l).

*Statistics was done with Kruskal-Wallis test followed by Dunn's multiple comparison test, n = number of independent samples, each consisting of two pooled mice. Mean values ± SEM are shown. * P<0.05, ** P<0.01*

4.1.3 Cytokine screening

Following phenotypic characterization of the immune cells, we assessed the possible cytokines that are associated with the immune response in this model of PD. Cytokines are key regulators of immune and inflammatory responses and when produced excessively or insufficiently undoubtedly contribute to the pathophysiology of a disease (Van der Meide & Schellekens 1996). The macrophage-activating cytokine IFN-γ was elevated in the spleen of haSyn mice 1 and 5 weeks post-injection as compared to EV and naïve mice, Fig.10c. At ten weeks, the IFN-γ level in haSyn mice reduced to comparable levels in EV. In the brain and cervical lymph nodes, IFN-γ levels were low in all groups of mice, Fig. 11a. IL-2, on the other hand, was elevated in the cervical lymph nodes and spleen at 1 week and these levels were lower at 5 weeks in haSyn mice though it was higher compared to controls (Fig. 10h, i). At ten weeks, the elevated levels of IL-2 levels in cervical lymph nodes and spleen in haSyn injected mice were not observed. With the exclusion of a significant increase in IL-4 in the spleen at one week in haSyn mice as compared to controls, there were no significant changes comparing the different groups at the various time points. IL-17A, on the other hand, was detected only slightly in haSyn mice at 1 week in the brain and cervical lymph nodes. Innate cytokines TNF-α and IL-6 were increased 1 week and 5 weeks (TNF-α) in the brain only in EV mice, Fig.10 d and m.

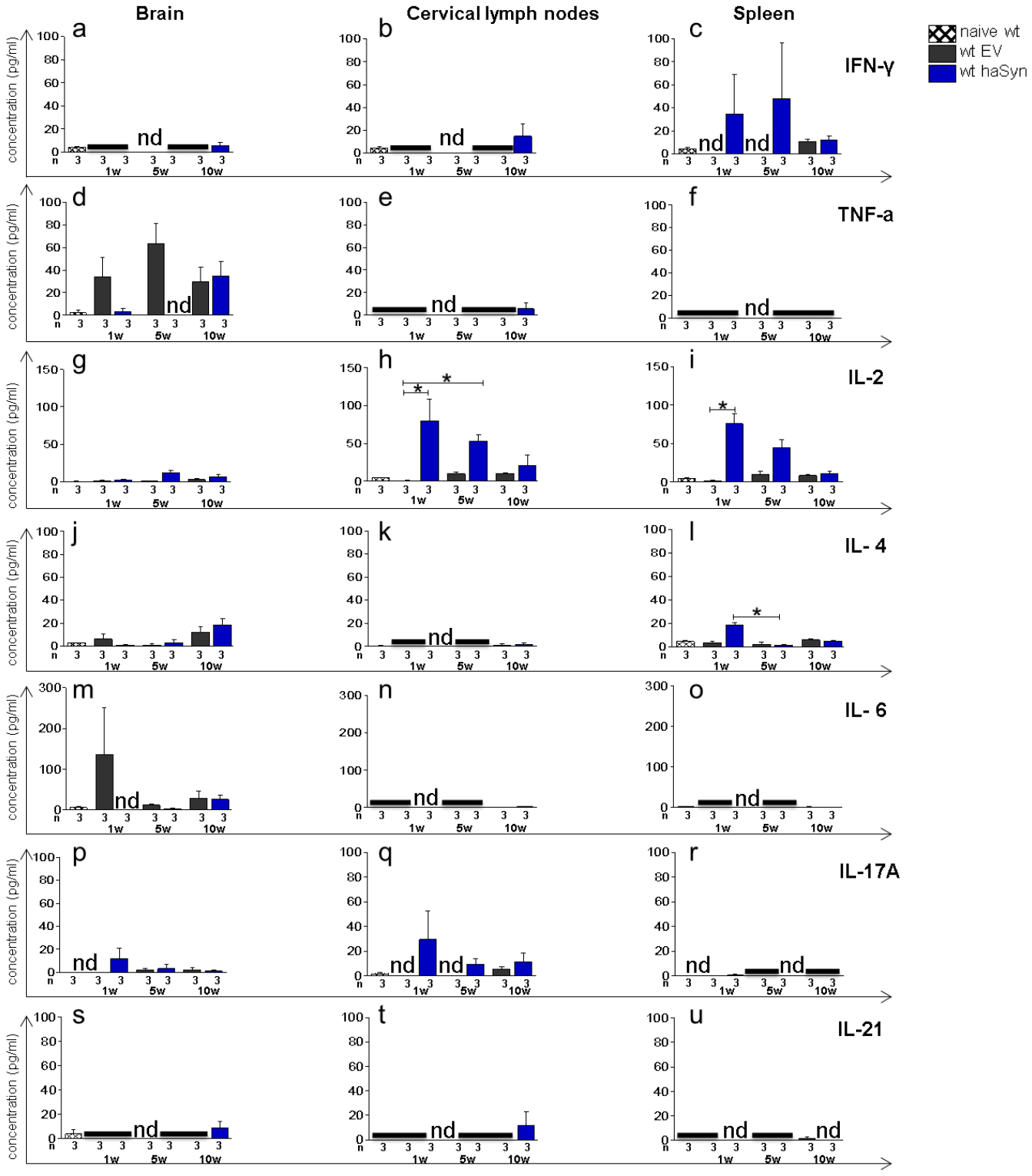

Fig. 10. Early elevation of T cell growth factor in peripheral organs.

Cytokine screening of the 3 organs revealed an early and significant increase of IL-2 in both cervical lymph nodes and spleen but not the brain (g-i) in wt haSyn mice. There was also a

*significant increase in IL-4 in the spleen at 1 week time point (l). The pro-inflammatory cytokines IFN-γ and IL-17A, were only elevated in the spleen and the cervical lymph nodes, respectively. Data is represented as mean ± s.e.m. n = number of independent samples, consisting of two pooled animals. Kruskal-Wallis test followed by Dunn's multiple comparison test was employed for statistics. * P<0.05.*

4.1.4 Peripheral immune response is not due to leakage of viral vector

The detection of a surge in IL-2 and IL-4 concentrations at week one in the spleen raised the question of whether the transcranial injection of the viral vectors caused leakage into peripheral lymphoid organs which induced the observed responses. To address this question, subcutaneous injection of haSyn and EV viral vectors at the same concentration used for intracranial injection was carried out. We also performed immunohistological staining for the presence of haSyn in the brain of haSyn containing AAV injected mice at one week, to confirm that dopaminergic neurons were indeed transduced at this period. The results as shown in Fig. 11 reveals a decreased IL-2 and non-detection of IL-4 concentration in the spleen of subcutaneously injected mice. There was also lower activation states of T lymphocytes in subcutaneously injected mice.

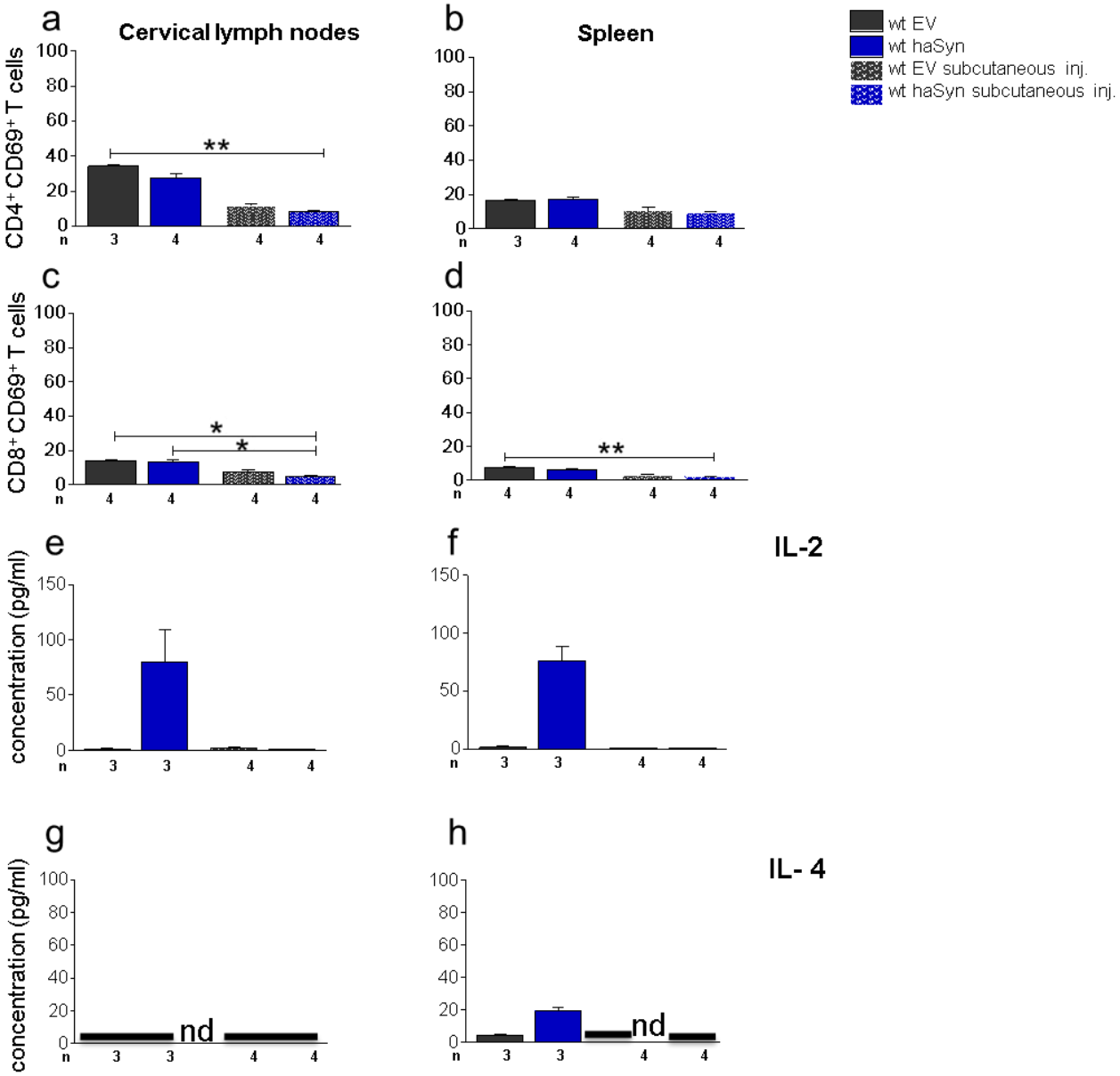

Fig. 11. Subcutaneous mice show lower activation and cytokine levels.

*FACS analyses reveal that subcutaneously injected mice have no pro-inflammatory responses after injection (a-h). n = number of independent samples, each consisting of two pooled animals. Mean values ± SEM are shown. * P<0.05, ** P<0.01.*

4.1.5 Dopaminergic neurons are haSyn transduced a week post-injection

Following the lower inflammation in subcutaneous mice, we addressed the issue of whether dopaminergic neurons were at all transduced with haSyn viral vector one week post-injection, which would account for the early pro-inflammatory responses observed in the intracranially injected mice. Immunohistological labeling of haSyn in EV and haSyn mice shows the presence of haSyn transduced dopaminergic neurons in the SN of haSyn injected mice a week after injection, which was absent in EV mice (Fig. 12). These results indicate that there was the transduction of dopaminergic neurons which was sufficient to drive the inflammatory condition.

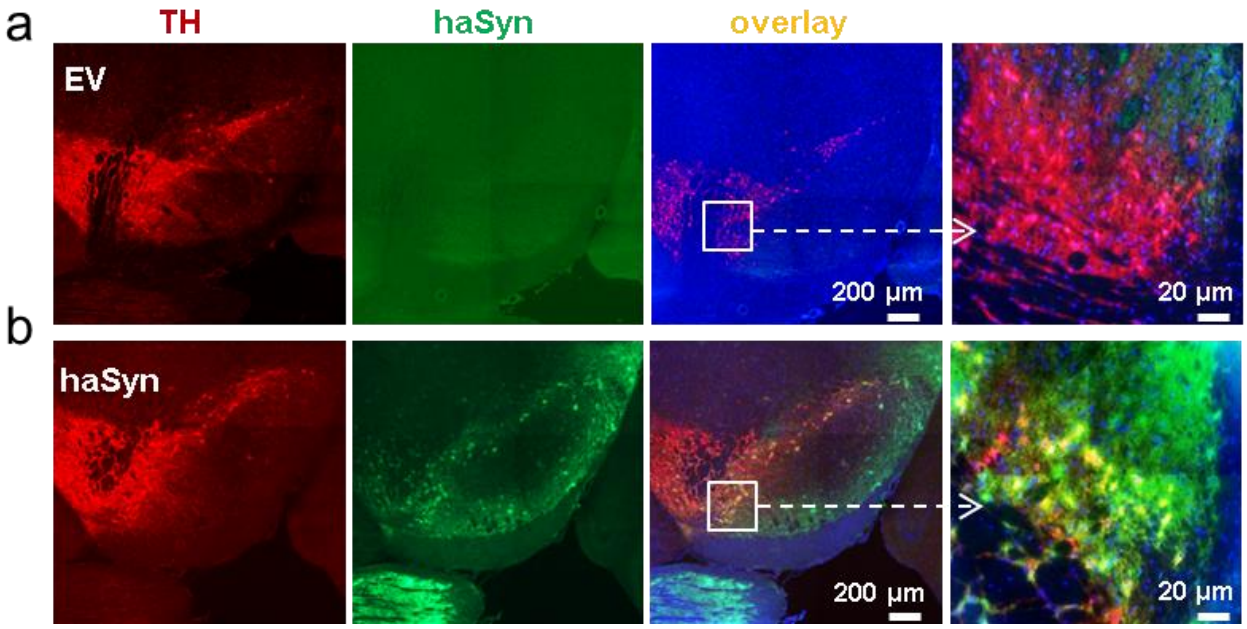

Fig.12. Presence haSyn transduced dopaminergic neurons in SN one week post intracranial injection.

a: Absence of haSyn in EV injected mice.

b: haSyn transduced dopaminergic neurons in the SN of haSyn injected mice.

4.1.6 Assessment of the role of lymphocytes in neurodegeneration; absence of T cells protects RAG-1$^{-/-}$ mice from haSyn-induced SN dopaminergic neuron loss.

From the histological and FACS analyses which proved that activated T lymphocytes infiltrate the brain in this model of PD, we further evaluated the effect of the presence these cells on neurodegeneration in the SN using RAG-1$^{-/-}$ mice. Lymphocyte reconstitution was carried out in RAG-1$^{-/-}$ mice by bone marrow cell transfer (wt BM RAG-1$^{-/-}$). The success of lymphocyte regeneration was determined by histological and FACS analyses after viral vector delivery into SN. The histology showed higher infiltration of lymphocytes in both the SN and striatum of wt BM RAG-1$^{-/-}$ haSyn as compared to EV injected wt mice (Fig. 13a-f). The FACS data likewise indicated the absence and presence of T cells in RAG-1$^{-/-}$ and wt BM RAG-1$^{-/-}$ respectively (Fig. 13g-h), which proved the success of the reconstitution process. Stereological analysis was subsequently conducted to determine the numbers of dopaminergic cells in the SN of controls namely wt EV, RAG-1$^{-/-}$ EV and haSyn injected mice which were wt haSyn, RAG-1$^{-/-}$ haSyn and wt BM RAG-1$^{-/-}$ haSyn. Representative images of the SN of these groups are shown in Fig. 8i. The images and stereological data indicate a loss of TH^{+} dopaminergic cells in the wt haSyn mice as compared to the EV (both wt and RAG-1$^{-/-}$) injected mice, 10 weeks post-injection. On the contrary, in the RAG-1$^{-/-}$ haSyn there was a rescue of TH^{+} cells, while the reconstitution of wt bone marrow into RAG-1$^{-/-}$ mice (wt BM RAG-1$^{-/-}$ haSyn) induced a significant reduction in the numbers of TH^{+} neurons in the SN.

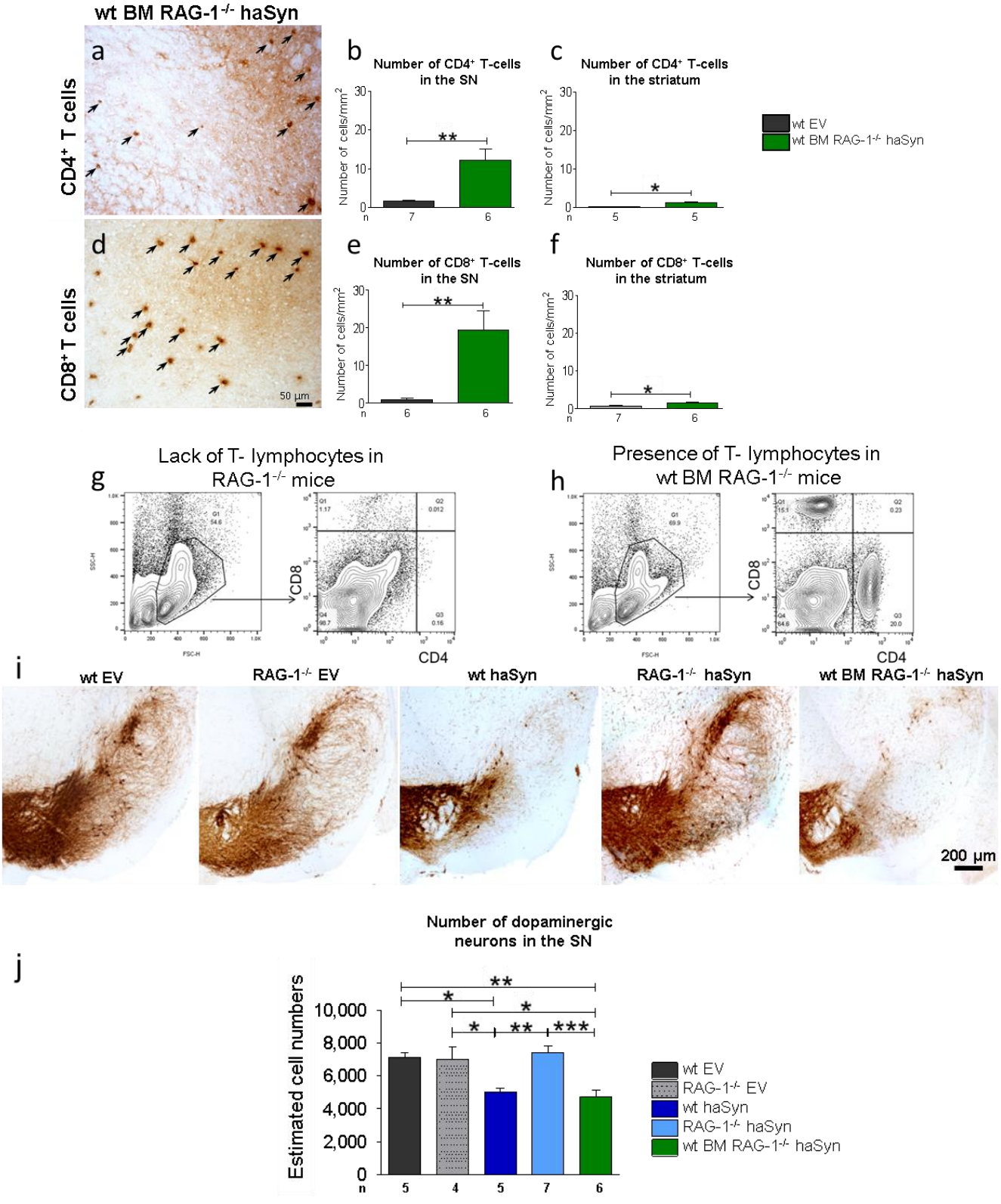

Fig. 13. RAG-1 deficient mice have rescue of dopaminergic neurons

a-h: The success of wt bone marrow transfer was proven by the presence of T cells in histological and FACS analyses. Statistical analysis of quantified infiltrated T lymphocytes was

*done with Mann-Whitney test shown as mean ± s.e.m. n = number of independent animals, * P<0.05, ** P<0.01. i-j: Enumeration of SN TH$^+$ dopaminergic neurons indicated that the lack of T cells was protective against cell body loss. Statistics performed by using one-way ANOVA followed by Tukey's multiple comparisons test. Mean ± s.e.m. n = number of independent samples, * P<0.05, ** P<0.01.*

4.1.7 RAG-1 $^{-/-}$ deficiency does not confer protection against haSyn-induced striatal DA neurochemistry deficit.

After the observation that the lack of matured T lymphocytes granted protection against TH$^+$ cells loss, TH$^+$ terminals and DA neurotransmitter with its metabolites were quantified by optical density measurements, DAT binding assay and HPLC analysis. As shown in Fig. 14a-b, TH$^+$ fiber optical density in the striatum revealed TH$^+$ terminal loss in all mice that were injected with haSyn regardless of the lack of T cells or otherwise. In addition, the DAT binding assay also confirmed the observation that the lack of T cells does not confer protection against haSyn toxicity to TH$^+$ fibers. Thus, T cell deficient RAG-1$^{-/-}$ mice had a significant reduction of DAT as was also observed in the wt and wt BM RAG-1$^{-/-}$ haSyn mice. The levels of striatal DA neurotransmitter was also decreased by haSyn injection and the lack of T lymphocytes was not protective. However, with DA turnover which is described as the ratio between DA metabolites and DA itself (e.g.HVA/DA), there was an elevation in both the wt haSyn and wt BM RAG-1$^{-/-}$ haSyn, whereas the RAG-1$^{-/-}$ haSyn mice showed a tendency of a normal DA turnover.

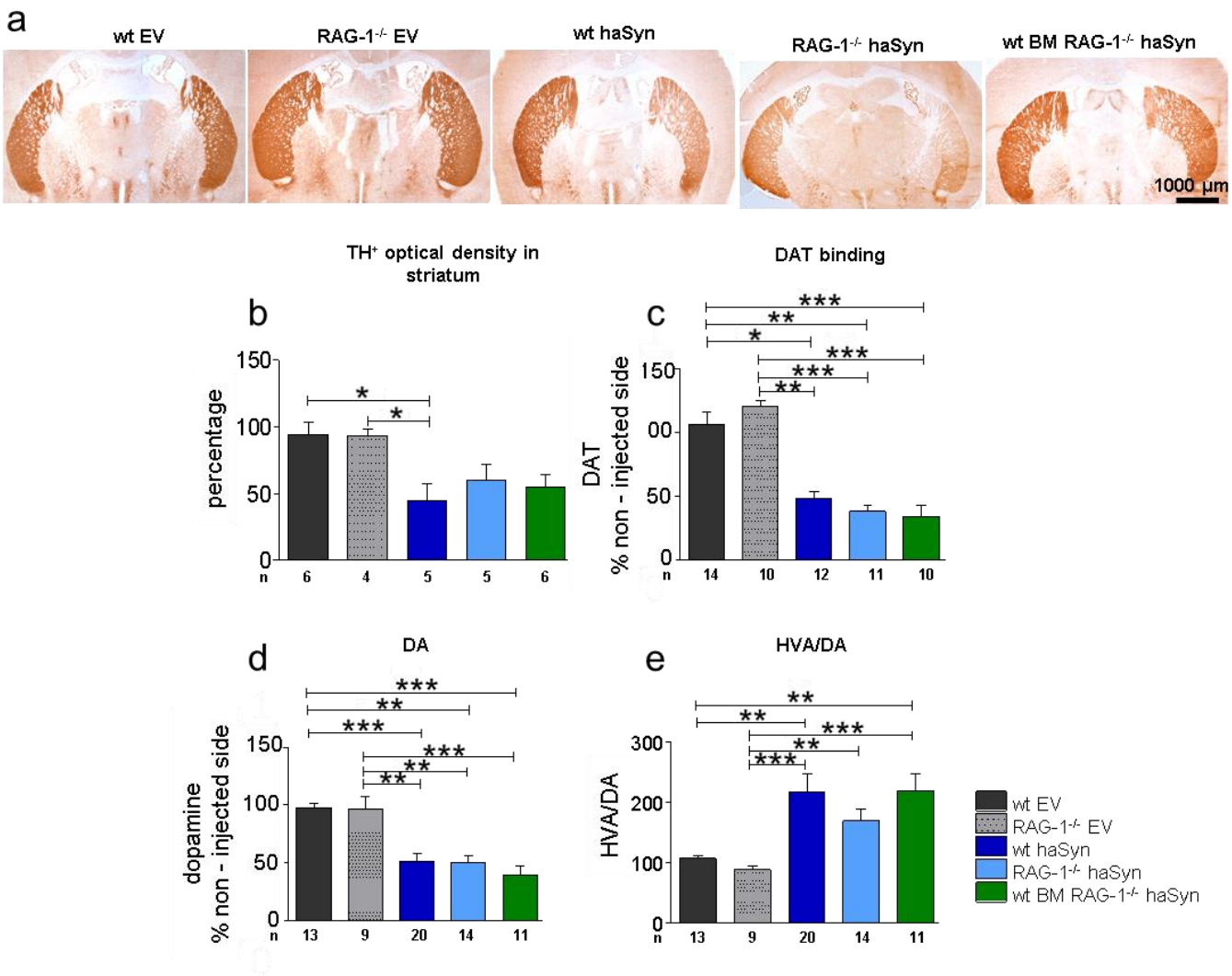

Fig. 14. Dopaminergic axonal terminals degenerate irrespective of T cell contribution.

a-c: The density of TH$^+$ fibers reduction is observed in all haSyn injected mice irrespective of immune competence as revealed by TH$^+$ optical density and DAT binding experiments.

*d-e: haSyn mice also exhibit impairment of DA neurochemistry with less DA availability and higher turnover (HVA/DA), although RAG-1$^{-/-}$haSyn mice showed a tendency of regular DA turnover. Statistical analyses for TH$^+$ optical density and DAT binding were performed using one-way ANOVA followed by Tukey's multiple comparison tests, whereas Kruskal-Wallis test followed by Dunn's multiple comparison was used to analyze DA levels and its turnover. * P<0.05, ** P<0.01, ***P<0.001. n= sample size, data is shown as mean ± s.e.m.*

4.1.8 Activated (CD11b^{+}) microglial cells are lower in RAG-1$^{-/-}$ haSyn mice.

A previous study by Sommer et al. proved that the presence of T cells in the brain of mice with α-synucleinopathy induced an activated phenotype of microglial cells (Sommer et al 2016). With the observation that the absence of T cells rescued dopaminergic cells from neurodegeneration, the numbers of CD11b^{+} microglial cells were quantified to assess the level of activation following disease induction. The results as shown in Fig. 15, revealed a decrease in activated cells in immune deficient RAG-1$^{-/-}$ haSyn mice compared to wt haSyn and wt BM RAG-1$^{-/-}$ haSyn immune competent mice.

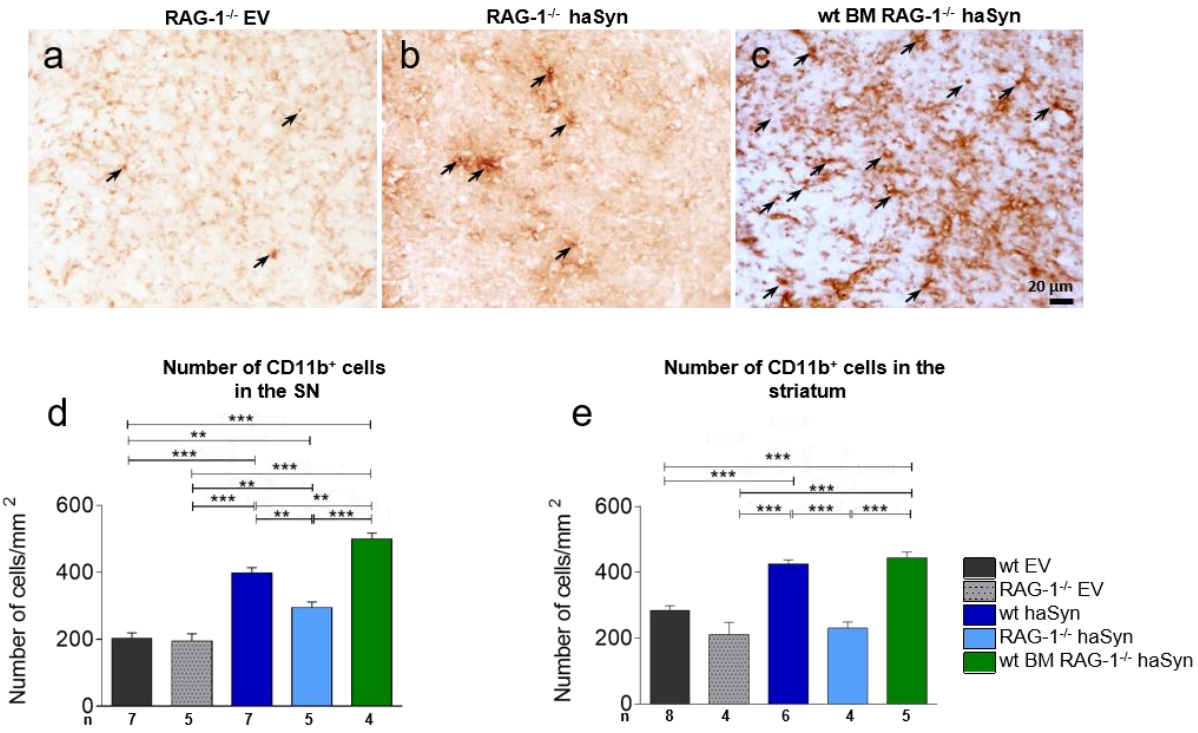

Fig. 15. RAG-1 deficient haSyn mice have less activation of microglia in the SN and striatum.

a-c: Representative histological images of CD11b^{+} microglial cells in the SN of RAG-1$^{-/-}$ EV (a), RAG-1$^{-/-}$ haSyn (b) and wt BM RAG-1$^{-/-}$ haSyn mice (c).

*d-e: Quantified cells in SN (d) and striatum (e). Statistical analysis was performed using the one-way ANOVA followed by Tukey's multiple comparison, mean ± s.e.m. n = sample size, ** P<0.01, *** P<0.001.*

4.1.9 Determination of the culprit lymphocyte population

Earlier research involving PD patients have indicated that there is an activation of the adaptive immune system with a decrease in CD4:CD8 ratio (Sommer et al 2017, Stevens et al 2012). However, the assessment of the specific lymphocyte population that greatly influences the disease progression has been controversial. To that end, we investigated the lymphocyte subpopulation that contributed to the progression of PD in this mouse model of PD. Bone marrow cells from $CD4^+/CD8^-$, $CD8^+/CD4^-$ and $CD4^+/CD8^+$ ($JHD^{-/-}$) donor mice were intravenously injected into RAG-$1^{-/-}$ recipient (BM RAG-$1^{-/-}$) mice. Following bone marrow cell transfer, RAG-$1^{-/-}$ recipient mice were injected with haSyn viral vector. Ten weeks post-injection, lymph nodes were harvested for FACS and brain collected for histological and HPLC analyses. FACS analysis of splenocytes revealed the presence of $CD4^+$ and $CD8^+$ T lymphocytes in RAG-$1^{-/-}$ which indicated the success of bone marrow cell transfer, Fig.11a-c. Representative images of the SN (Fig. 16d) showed the loss of TH^+ dopaminergic cells in the SN of $CD4^+/CD8^-$ BM RAG-$1^{-/-}$ and $CD4^+/CD8^+$ BM RAG-$1^{-/-}$ mice as compared to the EV and $CD8^+/CD4^-$ BM RAG-$1^{-/-}$ mice. Stereological quantification of the cells confirmed a significant loss of TH^+ neurons in the $CD4^+/CD8^-$ BM RAG-$1^{-/-}$ and $CD4^+/CD8^+$ BM RAG-$1^{-/-}$ mice, Fig. 16e. With regards to the $CD8^+/CD4^-$ BM RAG-$1^{-/-}$ mice, there was only a moderate reduction in cell numbers which was not significant when compared to the control EV groups.

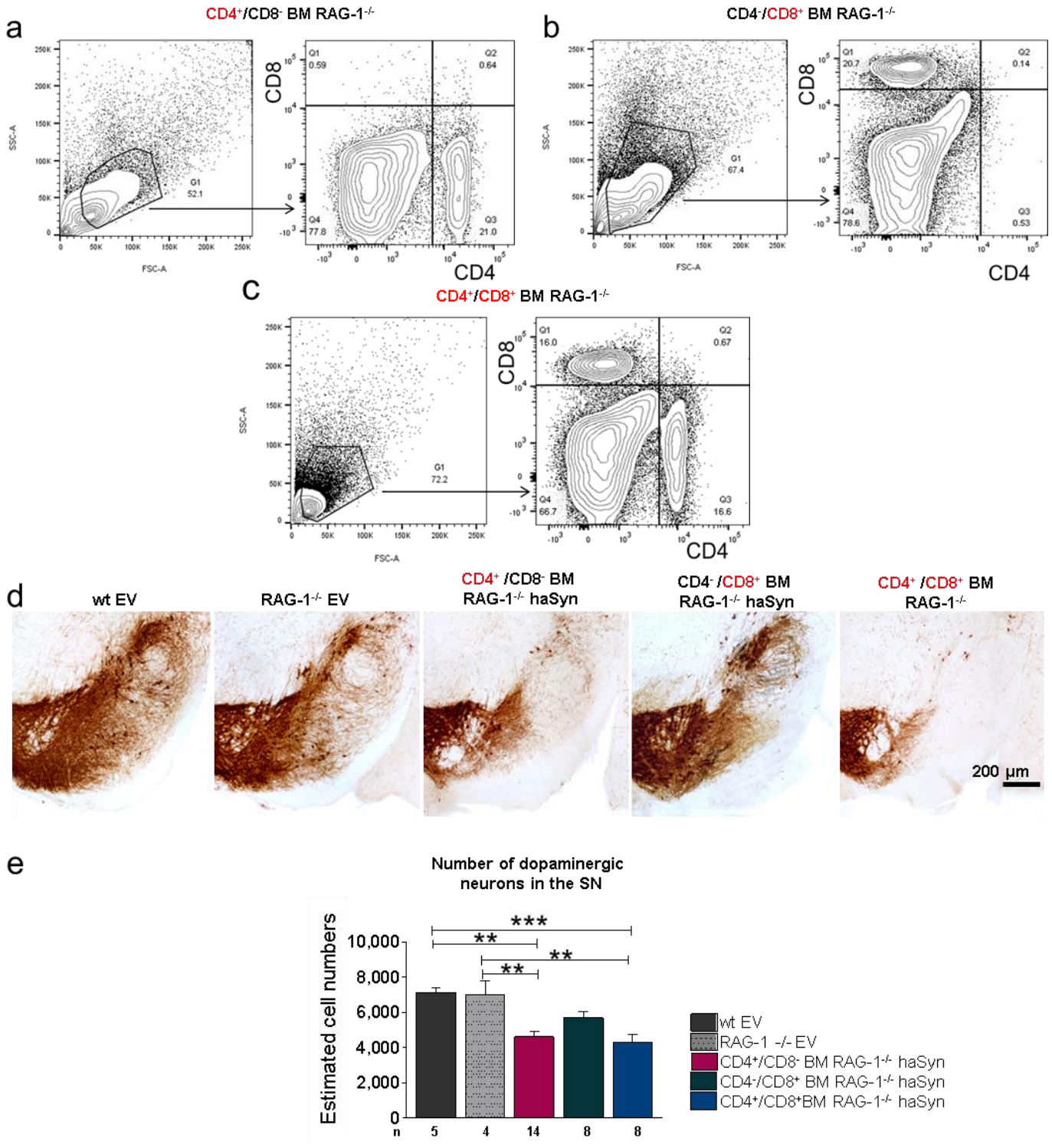

Fig. 16. SN dopaminergic cell death is principally mediated by CD4+ T cells.

a-c: FACS images from the spleen of RAG-1-/- recipient mice confirm a successful bone marrow cell transplantation with either CD4+/CD8-, CD4-/CD8+ or CD4+/CD8+ cells.

d: Histological images of SN dopaminergic neurons from EV injected controls and the 3 T cell subpopulation-reconstituted and haSyn injected mice.

*e: The estimated number of SN dopaminergic cells by stereological analyses. *P<0.05, ** P<0.01, ***P<0.001. n = sample size. Statistical analysis was performed using the one-way ANOVA followed by Tukey's multiple comparison.*

4.2.0 haSyn-induced striatal DA neurochemistry deficit is evident in all mice regardless of the lymphocyte population.

To determine whether the presence or absence of a lymphocyte subpopulation had any effect on striatal neurochemistry deficiency, levels of DA and its metabolites, as well as DAT binding assay and optical density measurements, were analyzed. Again there were lower DA levels in all groups that received haSyn injection Fig. 17a. A higher DA turnover was however observed in $CD4^+/CD8^-$ BM RAG-$1^{-/-}$ and $CD4^+/CD8^+$ BM RAG-$1^{-/-}$ as compared to $CD4^-/CD8^+$ BM RAG-$1^{-/-}$ mice Fig. 17b. TH^+ neurons terminal loss as assessed by TH^+ OD and DAT binding assay was also detected in all haSyn injected groups, reiterating earlier observation that dopaminergic fiber loss is a T cell-independent process.

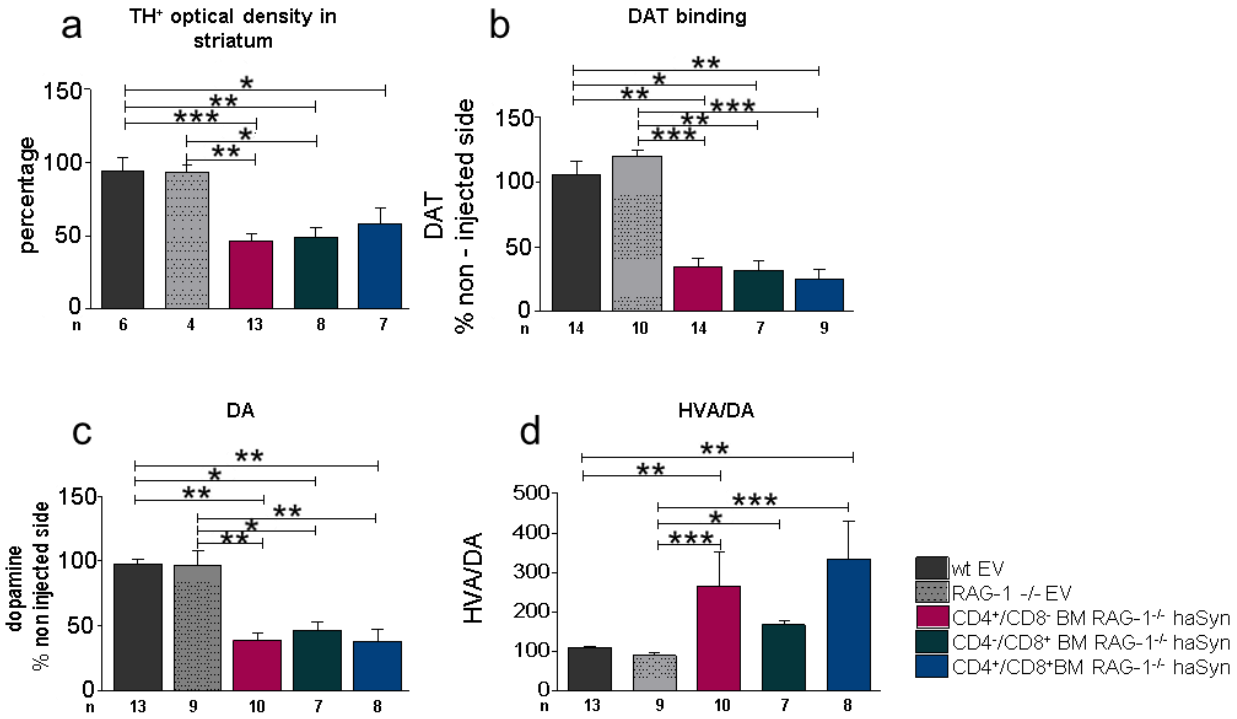

Fig. 17. TH⁺ fiber loss is a T cell-independent process.

a-b: Loss of dopaminergic terminals was evident in all haSyn injected mice. Data is represented as mean ± s.e.m. n = sample size for each group. Statistical analyses were performed using the one-way ANOVA followed by Tukey's multiple comparison test for TH⁺ OD and Kruskal-Wallis test followed by Dunn's multiple comparison test for DAT binding.

*c-d: Striatal DA levels were decreased in haSyn injected PD mice with high DA turnover except for the CD4⁻/CD8⁺ BM RAG-1 -/- haSyn mice. Statistical analyses were done by using the Kruskal-Wallis test followed by Dunn's multiple comparison test. *P<0.05, **P<0.01, ***P<0.001.*

4.2.1 T cells from haSyn mice demonstrate antigen-specific responses to haSyn-derived peptides.

It has been discovered that α-synuclein peptides can elicit responses from helper and cytotoxic T cells from PD patients (Sulzer et al 2017). So far, there hasn't been any investigations in a PD animal model that addresses the question of the involvement of α-synuclein T cells in the pathogenesis of the disease. Therefore, we sought to answer the inquiry of α-synuclein-derived specific T cells in our mouse model. To do this, we employed the ELISpot assay where BILs which include $CD4^+$ and $CD8^+$ T cells extracted from cervical lymph nodes and spleen of haSyn vector injected mice were stimulated with various haSyn peptides and examined for IFN-γ production. Different antigenic peptides from the haSyn sequence (Fig. 18a) were chosen based on their predicted affinity and probability to be presented by murine MHC I molecules $H\text{-}2K^b$ and $H\text{-}2D^b$ and MHC II molecule $I\text{-}A^b$ (Fig.18b). The peptide sequence at position 121-128 was altered (P128L) to increase its affinity to $H\text{-}2K^b$. In a total of 10 peptides that were screened, 2 peptides at positions haSyn 68-78 and haSyn 100-114 gave rise to increased IFN-γ production in the T cells in the ELISpot assays. These responses were observed in T cells extracted from cervical lymph nodes of 3 out of 5 haSyn mice (Fig. 18c) and not in control naïve animals. To rule out the possibility of hidden responses as a result of background IFN-γ production in the remaining 2 mice, splenocytes from the 2 haSyn and control mice were further expanded being exposed to all 10 peptides in addition to IL-2 for 10 days. The cells were subsequently rested and analyzed for IFN-γ production in response to the different individual peptides in ELISpot assays. There was a significant IFN-γ production detected in the 2 haSyn mice when the expanded cells were stimulated with the peptide haSyn 68-78 (Fig. 18d). On the whole, T cells from the peripheral lymphatic organs of all haSyn mice exhibited an antigen-specific response with a preference for peptide haSyn 68-78.

With regard to the brain, BILs extracted from 2 or 3 mice were pooled into 2 groups owing to the limited amount of BILs in this organ. Nonetheless, T cells from the pooled mice of haSyn injected cells responded to peptide at position haSyn 68-78, (Fig. 18e) which was observed in cervical lymph nodes and spleen. Furthermore, peptides at positions haSyn 68-76, haSyn 100-114, haSyn 121-128 and haSyn 120-134 induced activation of T cells from the brain which resulted in significant IFN-γ specific responses. In all, these data validate the presence of haSyn antigen-specific $CD4^+$ and $CD8^+$ T cells in the brain, cervical lymph nodes and in lower frequencies in the spleen of haSyn mice that could be partly responsible for the observed T cell responses *in vivo* after disease induction. We further subjected expanded $CD8^+$ T cells to FACS analyses to screen for memory T cells using the markers for L-selectin (CD62L) and the type I transmembrane glycoprotein CD44. Out of the 3 haSyn mice, T cells from one mouse with a $CD8^+$ $CD62L^-$ $CD44^+$ memory phenotype responded to peptides at positions haSyn 68-76, haSyn 68-78 and haSyn 99-107.

a

1 MDVFMKGLSK AKEGVVAAAE KTKQGVAEAA GKTKEGVLYV GSKTKEGVVH GVTTVAEKTK
61 EQVTNVGGAV VTGVTAVAQK TVEGAGSIAA ATGFVKKDQL GKNEEGAPQE GILEDMPVDP
121 DNEAYEMP(L)SE EGYQDYEPEA

b

List of peptides

haSyn68-76	GAVVTGVTA	H-2D^b	MHC I
haSyn68-78	GAVVTGVTAVA	H-2D^b	MHC I
haSyn80-94	**KTVEGAGSIAAATGF**	**I-A^b**	MHC II
haSyn92-100	TGFVKKDQL	H-2K^b	MHC I
haSyn99-107	QLGKNEEGA	H-2D^b	MHC I
haSyn100-107	LGKNEEGA	H-2K^b	MHC I
haSyn100-114	**LGKNEEGAPQEGILE**	**I-A^b**	MHC II
haSyn120-134	**PDNEAYEMPSEEGYQ**	**I-A^b**	MHC II
haSyn121-128	DNEAYEMP	H-2K^b	MHC I
haSyn121-128(P ➔L)	DNEAYEML	H-2K^b	MHC I

c

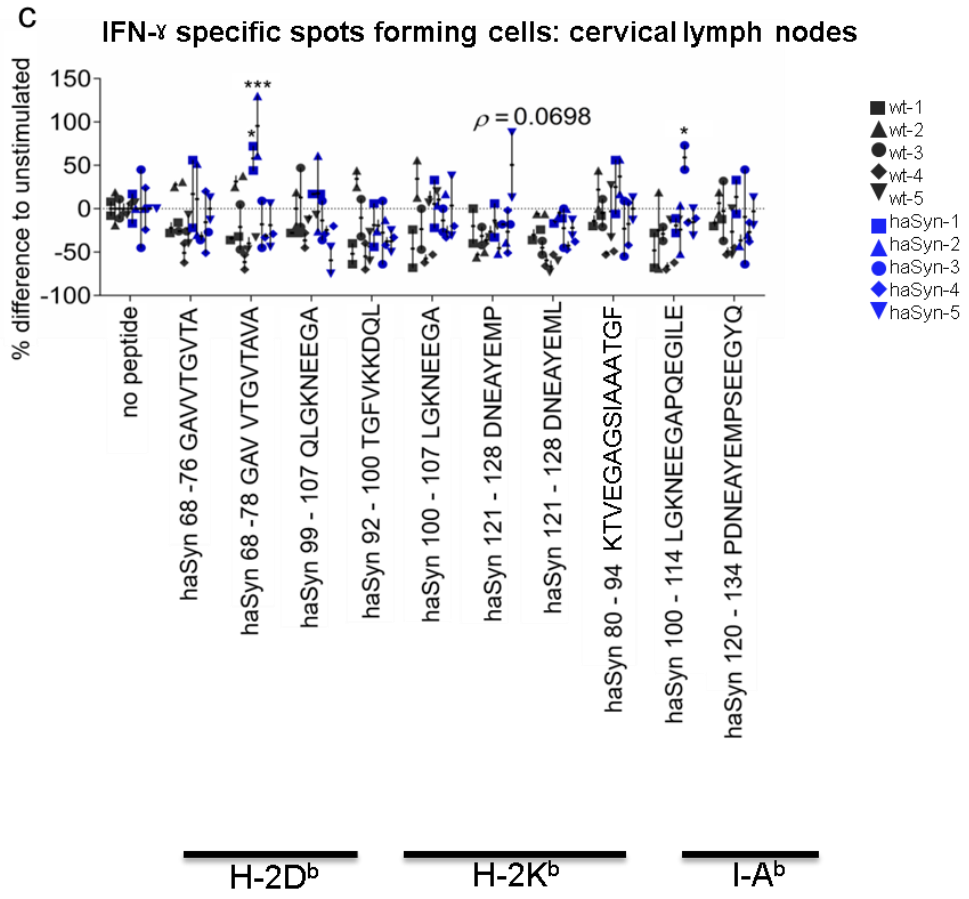

Predicted haSyn peptide sequence & the corresponding MHC molecules

d

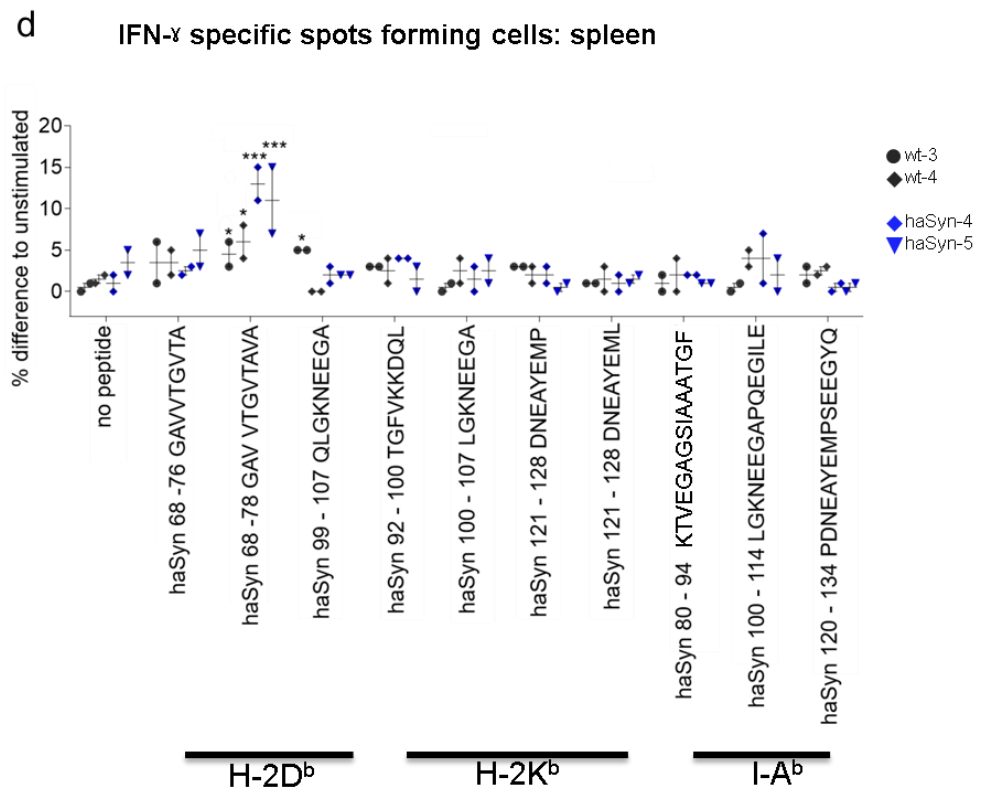

Predicted haSyn peptide sequence & the corresponding MHC molecules

e

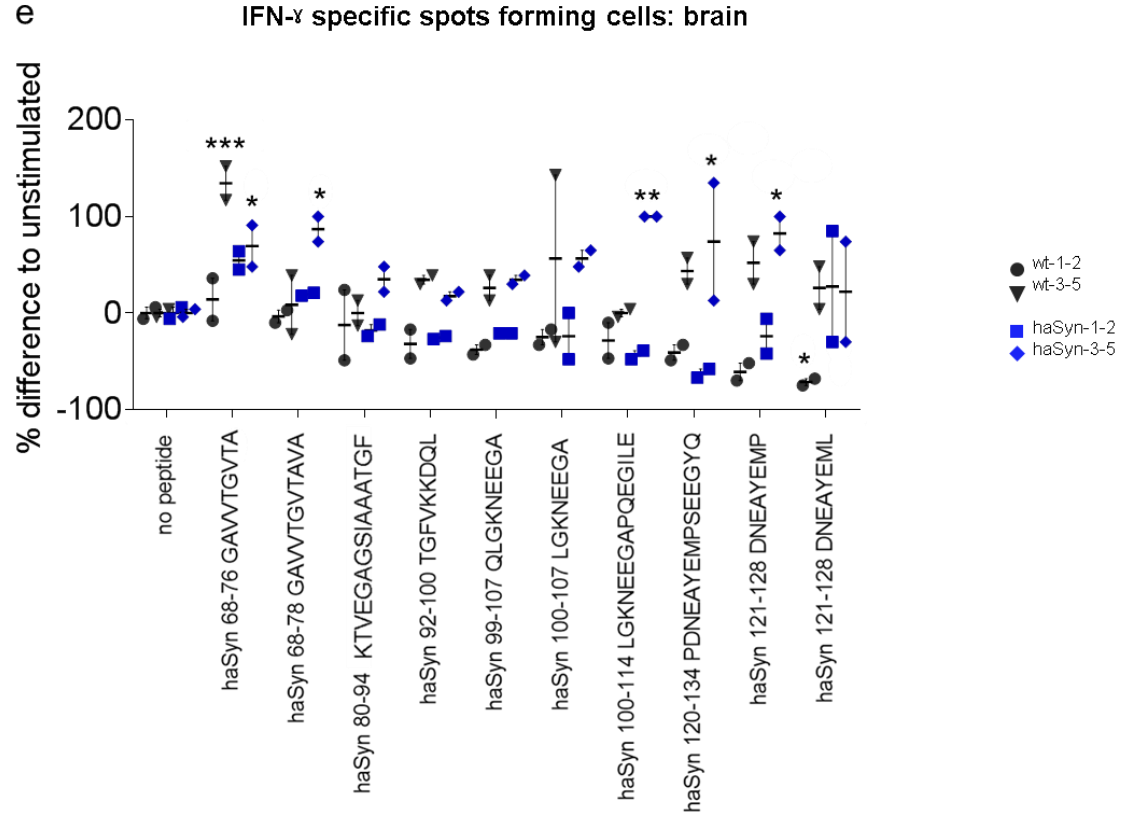

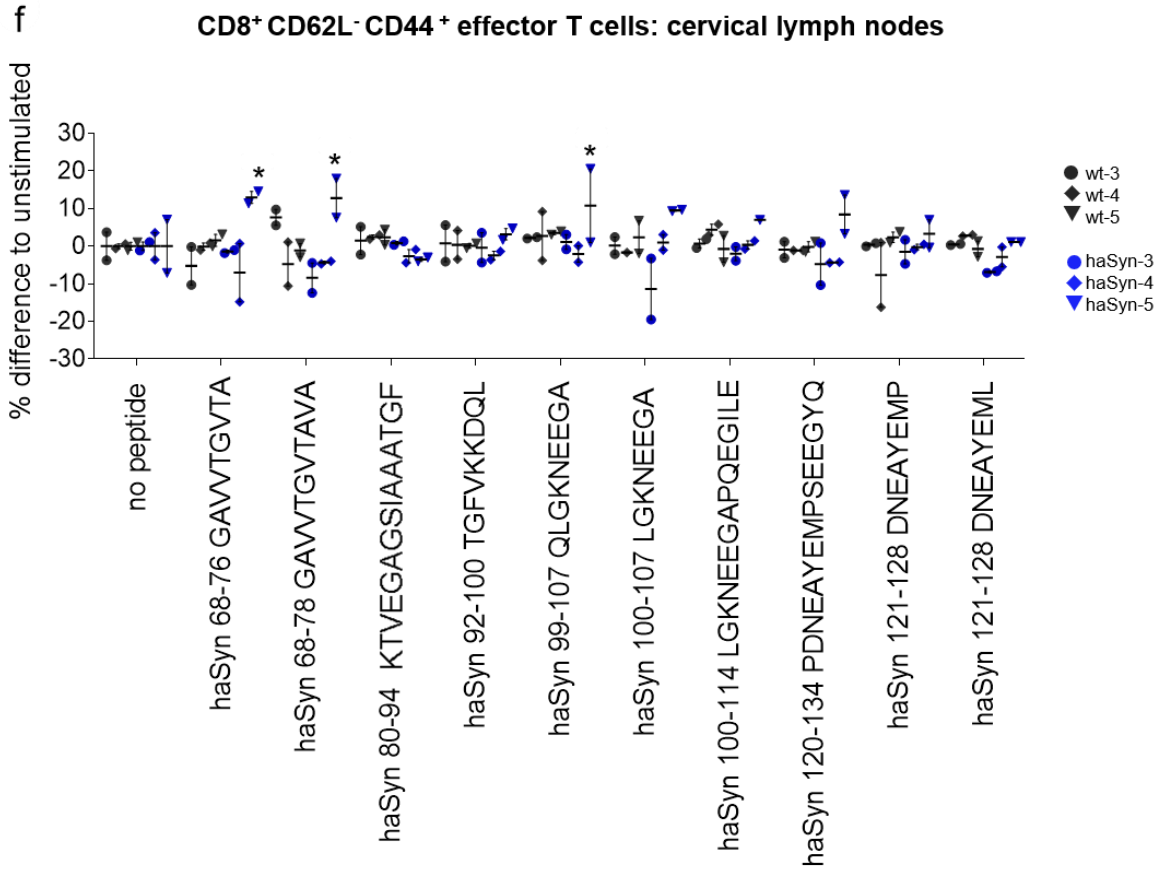

Fig. 18. T cells from haSyn injected mice respond to haSyn derived peptides.

a: Shows the amino acid sequence of haSyn, where A at position 53 is mutated to T (also displayed in red in sequence). In addition, the modification at position 128 of P to L is indicated in brackets. b: A table of the 10 peptides obtained from the haSyn sequence and predicted to bind MHC I molecules (H-2D^b and H-2K^b) and MHC II molecule I-A^b are shown with positions in the sequence. c: Outcome from IFN-γ ELISpot experiments after stimulation of leukocytes from cervical lymph nodes of haSyn (blue) and control mice (black) with predicted peptides. Data is displayed as mean ± s.e.m. n = 5 independent animals for each group. d: Demonstrate results of IFN-γ ELISpot from the exposure of leukocytes from spleens of the 2 haSyn and control mice, exposed to all 10 haSyn predicted peptides. Data is shown as mean ± s.e.m. n = 2 independent animals for each group. e: Shows the presence of haSyn specific T cells in the brain that gave rise to IFN-γ specific spots. Data shows mean ± s.e.m. n = 2 (from 2 or 3

*pooled animals for each group). f: Depicts FACs data from 3 control and haSyn mice after 10 days of expansion of T cells from cervical lymph nodes. Data shows mean ± s.e.m. n = 3 independent animals for each group. Statistical analysis was done with two-way ANOVA with pairwise Fisher's LSD test. *P<0.05, ***P<0.001.*

4.2.2 haSyn triggered toxicity is concentration dependent

In preparation of our subsequent *ex vivo* and *in vitro* experiments which involved the transduction of primary hippocampal neurons with viral vectors, a titration of haSyn vector was done to ascertain the appropriate concentration for the cells. Using the microtubule-associated protein-2 (MAP2) and mouse anti-βIII tubulin (TUJ1) for the immunolabeling of dendrites (Fig. 19a-c) and axons (Fig. 19d-f) respectively, it was detected that higher doses of haSyn were selectively injurious to cells. The toxicity of haSyn was particularly evident in the neurites (axons and dendrites), with the reduction and loss of MAP2 and TUJ1 immunoreactivity. MAP2 is a cytoskeletal crosslinking protein that increases the stability of microtubule network and is found mainly in dendrites and soma of neurons (Posmantur et al 1996, Wang & Rubel 2008). It is a key indicator of neuronal injury and cell death and reduction in MAP2 labeling occurs prior to eminent neuronal cell loss (Huh et al 2003). In addition, the destabilization and mutations of tubulin subunits can influence the stability of microtubules and axonal transport, resulting in the disintegration of axons (Dubey et al 2015, Nishio et al 2008). These observations corroborate the earlier evidence in our *in vivo* experiments that degeneration occurred earlier in neurites and was not dependent on T lymphocyte contribution.

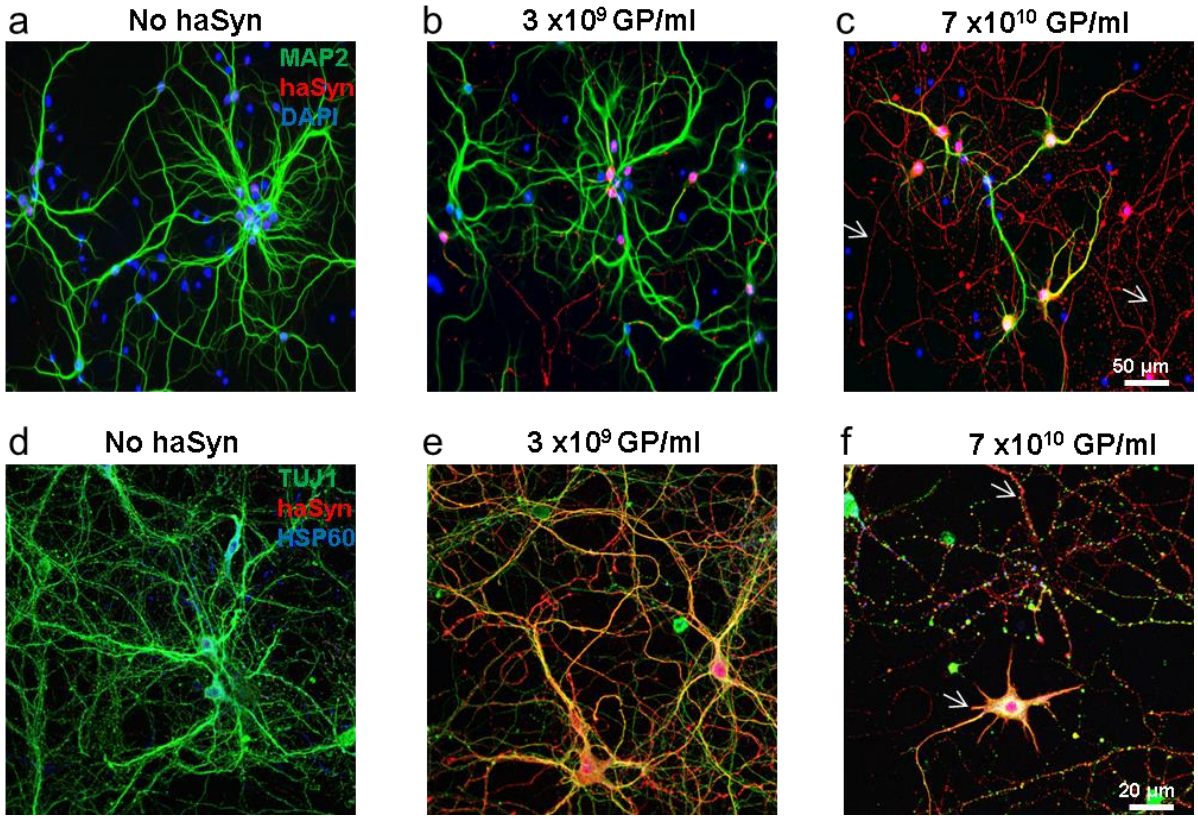

Fig. 19. Higher doses of haSyn induce a prominent neurite loss and damage.

a: Non-viral vector infected neurons showing a high MAP2 immunoreactivity

b: At a concentration of 3.096 x10^{9} GP/ml which was used in our in vitro experiments, an evident MAP2 immunoreactivity could still be observed. c: A severe loss of MAP2 staining at a concentration of 7.74 x10^{10} GP/ml. Arrows are pointing to the absence of MAP2 immunoreactivity in neurites (c). MAP2: green, haSyn: red and DAPI: blue immunofluorescence.

d-f: immunolabelling of TUJ1 in axons (green) with the same concentrations in a-c. Arrows point to prominent axonal loss noticeable by the reduction in TUJ1 and axonal stumps (f).

4.2.3 T cells from haSyn injected mice show specificity in their actions.

As data from the ELIspot assays proved the presence of antigen-specific T cells in our mouse model for PD, the inquiry of whether these T cells were capable of directly inducing neuronal cell loss was investigated. For this reason, primary hippocampal neurons were cultured in 96 well plates and cells were transduced with either haSyn or EV viral vectors for 4 days. Following cellular transduction (Fig. 20a), BILs were isolated from haSyn injected mice and cocultured with neurons overnight. Results from the *ex vivo* / *in vitro* experiments showed that haSyn transduced neurons exposed to isolated BILs were more prone to cell death than EV and uninfected control neurons. The intensity of the MAP2 neuronal marker was significantly decreased in the haSyn infected neurons (Fig. 20f, k) which were incubated with the isolated BILs when compared to EV and uninfected neurons (Fig. 20c, k). This outcome proved that the BILs were selective in causing neuronal cell death and thus demonstrating antigen specificity toward haSyn, which is a characteristic of T cells that differentiate them from other leukocytes in the BILs. On the contrary, CD3 activated T cells did not show discrimination in inducing cell death to haSyn, EV and uninfected neurons (Fig. 20d, g, j, l), buttressing the observation that the T cells from haSyn mice induced cell death in an antigen-specific manner.

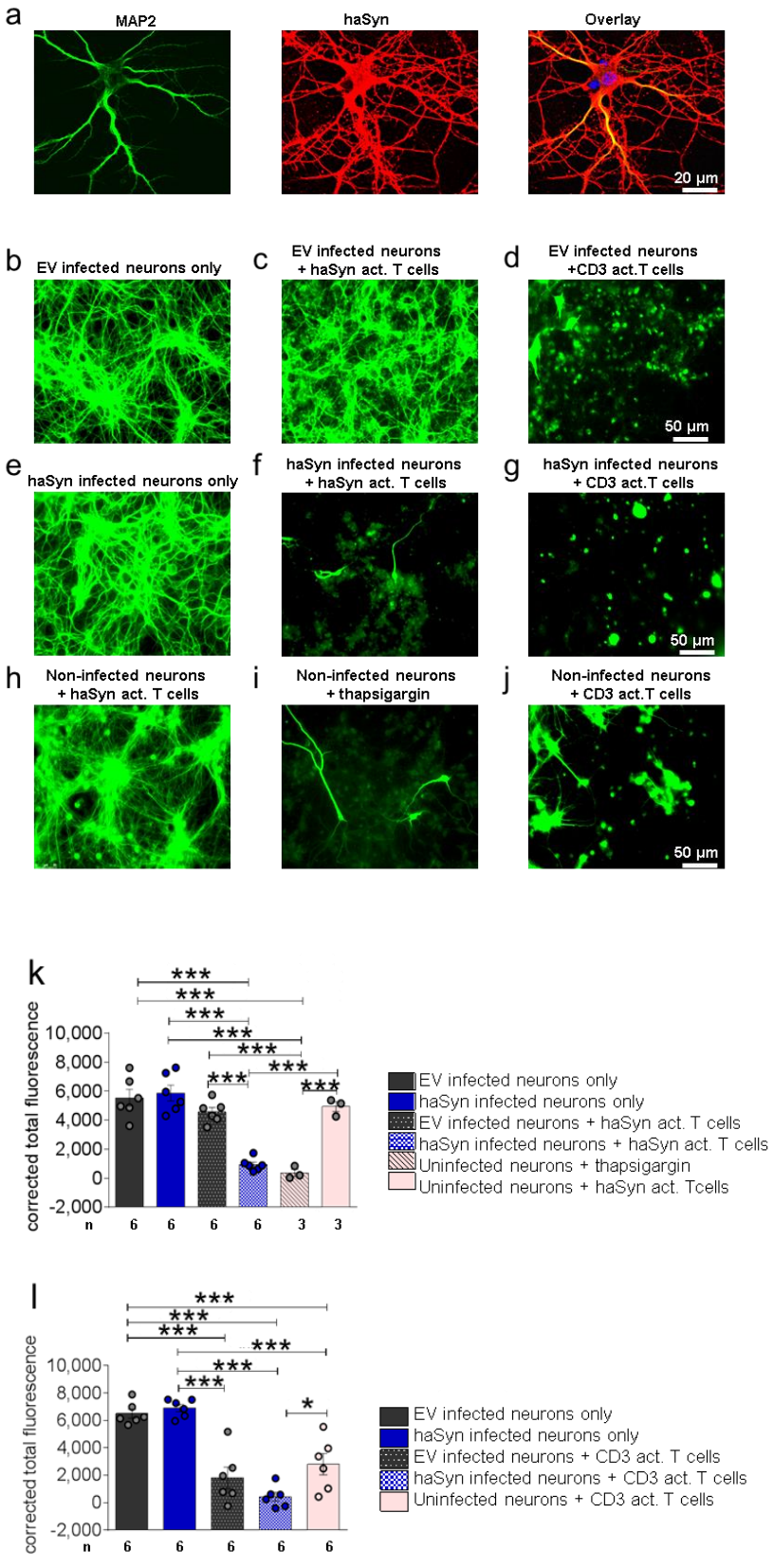

Fig. 20. Activated T cells derived from haSyn mouse brains demonstrate selective neuronal damage.

a: Hippocampal neurons (illustrated by MAP2 staining) cultured on coverslips and infected with haSyn show an expression of haSyn (haSyn, overlay).

b-j: MAP2 images of neurons cultured in 96 - well plates and transduced with haSyn, EV or uninfected for 4 days.

c-d: Depicts EV transduced neurons and cocultured with T cells from haSyn brains (c) or with CD3 activated T cells (d).

f-g: haSyn infected neurons exposed to haSyn mice derived T cells (f) or CD3 activated T cells.

h-j: Uninfected neurons cocultured with T cells from haSyn mice (h), thapsigargin (positive control, i) and CD3 activated T cells (j).

*Corrected fluorescent intensity of MAP2 staining is shown as mean ± s.e.m. n = number of independent cell cultures for each experiment. Statistical analysis was done using Kruskal-Wallis test followed by Dunn's multiple comparison test. * P<0.05, ** P<0.01, ***P<0.001.*

4.2.4 MHC I and MHC II antibodies did not abrogate T cell-mediated neurotoxicity

To determine the mechanism of T cell-induced neuronal death, neurons were treated with 20 µg of MHC I and MHC II antibodies and cultured with isolated T cells from haSyn injected mice or CD3 activated T cells. The presence of the antibodies could not inhibit cell death, as the pattern of T cell killing as seen in earlier experiments were observed in the presence of the antibodies. Again, there was a significant cell loss in haSyn transduced neurons (Fig. 21c - f) when cocultured with haSyn T cells, which was not seen in EV infected mice (Fig. 21a, b, e, f). The CD3 activated T cells were injurious to all vector infected neurons (Fig. 21g - l). These results suggest that the detected T cell-provoked toxicity does not involve MHC I and MHC II.

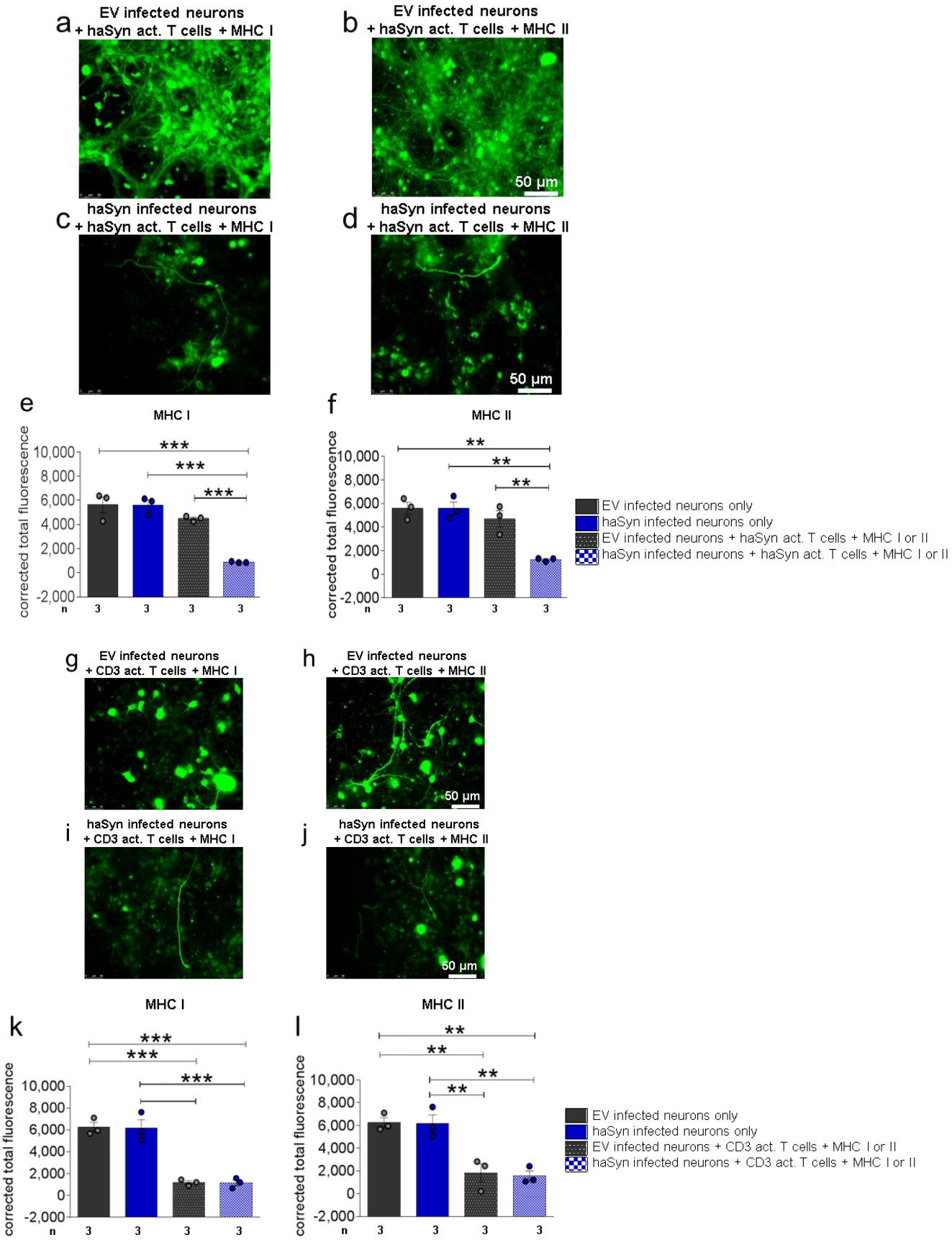

Fig. 21. T lymphocytes induced cell killing is independent of MHC I and II.

a-b: EV infected neurons cocultured with haSyn derived T cells in the presence of 20 µg MHC I (a) and II (b) antibodies.

c-d: haSyn neurons cocultured with T cells from haSyn injected mice in the presence of 20 µg MHC I (c) and II (d) antibodies.

e-d: Measured corrected total fluorescent MAP2 intensity.

*Representative images of EV (g - h), haSyn (i - j) infected neurons cultured with CD3 activated T cells and MHC I and II antibodies. Total corrected fluorescent intensity is shown in k and l. Statistical analysis was done using Kruskal-Wallis test followed by Dunn's multiple comparison test. ** P<0.01, ***P<0.001.*

4.2.5 Soluble factors are not responsible for the observed T cell toxicity

Following the failure of MHC I and MHC II to neutralize the T cell toxicity, we treated the neurons with different concentrations of IFN-γ, IL-4, and TNF-α. IFN-γ and IL-4 were chosen because higher levels of these cytokines were observed in haSyn injected mice in our *in vivo* studies. TNF-α was included because it is chiefly produced by microglial cells in the CNS (Welser-Alves & Milner 2013). Infected neurons were exposed to different concentrations of these cytokines either as a single or cocktail treatment. However, none of these conditions resulted in any evident cell death in the vector infected neurons Fig. 22.

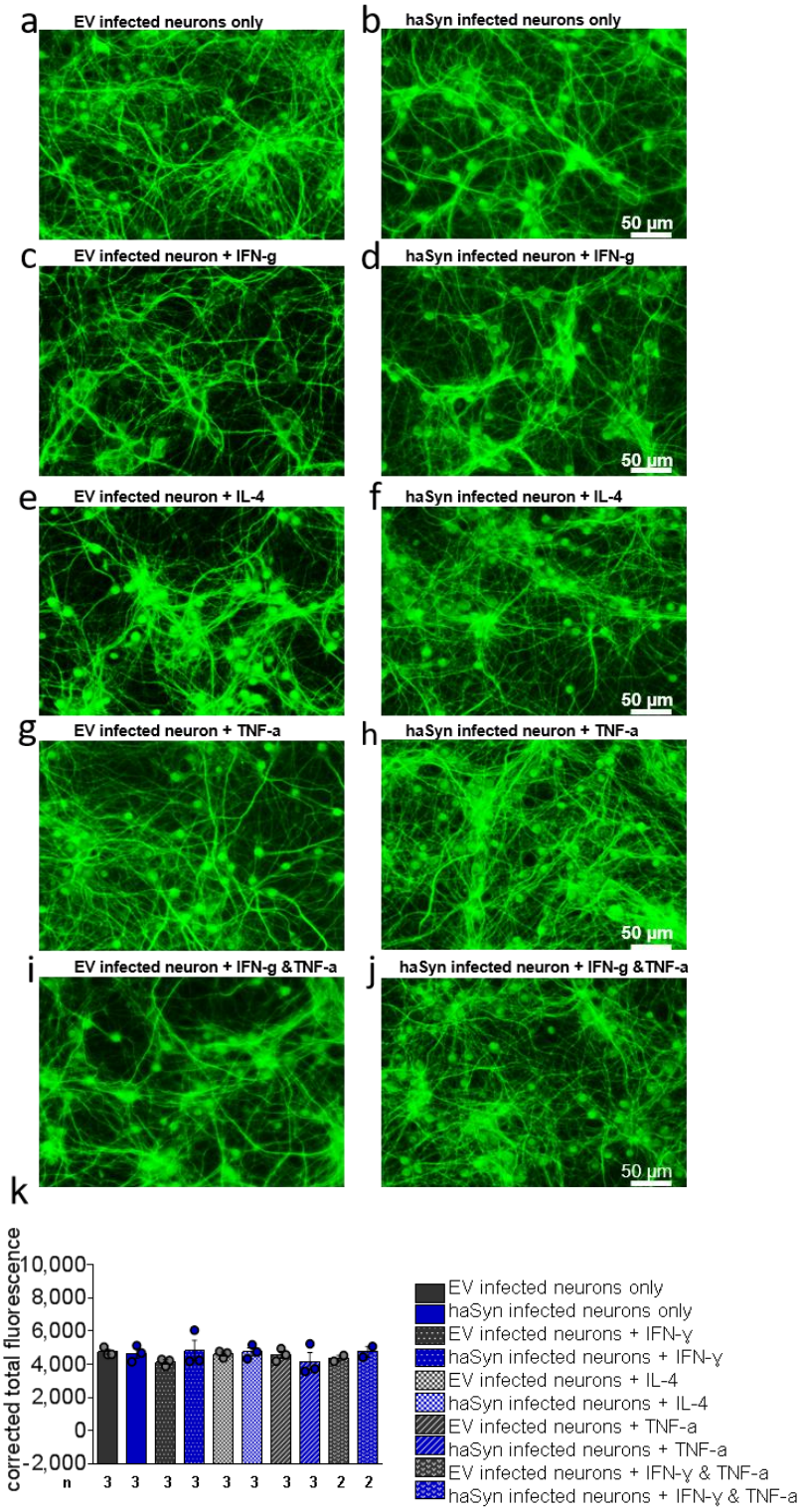

Fig. 22. Cytokines do not induce cell death in vector infected neurons.

a-j: EV and haSyn transduced neurons incubated with different combinations of cytokines.

k: Quantification of corrected total fluorescent intensity. Statistical analysis was done using Kruskal-Wallis test followed by Dunn's multiple comparison test.

Chapter FIVE

5.0 Discussion

Mounting evidence in recent years has implicated inflammation in the development and progression of PD. Though several studies have demonstrated the role of the innate system, a few have focused on the adaptive arm of the immune system. The contribution of the humoral system in PD has been a subject of controversy and its role in the disease remains obscure as stipulated earlier. Contradictory to an earlier conception that peripheral immune cells are unable to enter the CNS, it is now recognized that cells of the immune system monitor and invade the CNS enormously particularly under neuropathological instances (Cose et al 2006, Togo et al 2002a). Indeed, in this study, we provide evidence to the effect that there are not only higher levels of activated microglial cells in postmortem SN tissues from PD patients but there is also an increase in the numbers of transmigrated $CD3^+$ T cells in the brain parenchyma. Moreover, we discovered a similar trend of microglial activation and lymphocyte accumulation in haSyn lesioned mice as compared to the EV control groups. This is in agreement with reports from previous studies, which reported the activation of microglial cells as well as T lymphocyte infiltration in the CNS of PD patients and mouse models of PD (Brochard et al 2009, Reynolds et al 2008, Sommer et al 2016, Sommer et al 2018). Following the detection of lymphocytes in PD tissues and in the SN of lesioned mice, the specific phenotype of the infiltrating cells was determined by FACS analysis. Previous investigations to assess the different lymphocyte subsets in the blood of PD patients produced an uncertain outcome (Sommer et al 2018). In animal models of PD, there hasn't been any clear description of lymphocyte subsets in the pathogenesis or progression of the disease. Questions such as the time point at which lymphocytes transmigrate into the brain and whether there are corresponding peripheral indicators were all unresolved. For that reason, following haSyn and EV injection in C57BL/6 mice the brain, cervical lymph nodes and spleen were harvested for FACS analysis at 1, 5- and

10-weeks post-injection. From the FACS data as shown in Fig. 4, we see an early activation at 1week post-injection of both $CD4^+$ and $CD8^+$ T cells by using the $CD69^+$ activation marker. This activation was observed in the brain of haSyn injected mice as compared to the EV and naïve wt controls. At 5 weeks, there was no apparent difference in these lymphocyte subpopulations in all three mice groups. There was a robust activation however at 10 weeks in the brain and to some extent in cervical lymph nodes, which is indicative of the fact that inflammation had persisted. It must be stated that from the immunohistochemical examination, we detected that neurons in the SN of haSyn injected mice were transduced 1-week post-injection. With α-synuclein being predominantly a presynaptic protein (Alderson & Markley 2013) and having the ability to spread like a prion (Allen Reish & Standaert 2015), it can be speculated that the observed initial activation of T lymphocytes in the brain of haSyn injected mice was an immediate response to the dysregulation of the immune homeostasis in the microenvironment of the CNS. The presence of haSyn in the extracellular fluid could have triggered a microglial response with the release of cytokines that could serve as chemoattractants for brain circulating lymphocytes. In the brain, microglia are the main MHC II expressing cells (Hayes et al 1987) and thus, they are capable of haSyn processing and presentation to blood-derived T cells which are continuously surveilling the CNS (Ousman & Kubes 2012). A characteristic of haSyn is that it can be secreted into body fluids such as human plasma and CSF (Borghi et al 2000). In addition, fluids from the brain drain into deep cervical lymph nodes which means a transduction of neurons with haSyn in the brain can lead to drainage of the protein into lymph nodes especially through meningeal lymphatic vessels (Aspelund et al 2015, Prinz & Priller 2017). Therefore, it can be deduced that the transduction of dopaminergic neurons led to the continuous drainage of haSyn into peripheral lymphoid organs resulting in the recruitment of T cells into the brain, hence the persistent activation of T lymphocytes at 10-weeks post-injection.

Whereas there was an increase in activated T cells, the expression of $CD4^+CD25^+$ Foxp3 T and $CD8^+$ $CD122^+$ T cells which are regulatory T lymphocytes (Tregs), was low at all time points except for an elevation of $CD8^+$ $CD122^+$ T cells numbers in the cervical lymph nodes and spleen of haSyn mice at 1-week post-injection. In a study by Baba et al. they discovered a decrease in the numbers of $CD4^+CD25^+$ T cells in the peripheral blood of patients with PD (Baba et al 2005). It is also crucial to mention that a dysfunction of Tregs has been discovered in many neurodegenerative diseases, particularly at the early state but not in their chronic stages indicating a causative role of inflammation in the course of the pathogenesis of neurodegenerative diseases (He & Balling 2013). As to whether our findings imply the depletion of this cell population as a result of the increased inflammatory environment or shows a dysfunction of these Tregs, could be a subject for further research.

Central to the appropriate function of the immune system is the release of cytokines which provides the required signals for cross-talk between the innate and adaptive system. Therefore we screened for the presence of 13 cytokines in this research. Prominent among the cytokines detected included IL-2, IL-4 and IFN-γ with some amount of IL-17 production. Some of the cytokines that have been reported in PD include IL-1β, IL-2, IL-4, IL-6 and TNF-α. Although, there was no elevation of IL-6 and TNF-α and IL-1β was not detected in haSyn injected mice, elevated levels of IL-2, IL-4 and IFN-γ were observed. IL-6 and TNF-α were detected to some extent in EV control mice but this was inconsistent in the three organs and for the various time points making it difficult to draw any conclusion. The presence of IL-2, IL-4, IFN-γ and IL-17 suggest that the T cells in this model were mainly of Th1 phenotype with some contribution from Th 17 cells pointing to a pro-inflammatory state. Though IL-4 is secreted by Th2 cells and is considered an anti-inflammatory interleukin (Chatterjee et al 2014, Cuneo & Autieri 2009), under certain conditions, IL-4 is known to induce the recruitment of activated T cells to the site of injury, therefore, contributing to inflammation. IL-4 acting through the IL-4 type II receptor increases phosphorylation of the signal transducer and activator of transcription 6 (STAT6)

which induces the expression of over 900 genes involving those encoding vascular cell adhesion molecule 1 (VCAM-1), P-selectin and C-C motif ligand 26 (CCL26) (Sharma et al 2015). P-selectin and VCAM-1 are known to enhance the recruitment of lymphocytes, eosinophils and monocytes (Sharma et al 2015). Additionally, IL-4 is known to indirectly foster Th1-type inflammation in a mouse model of colitis (Fort et al 2001), therefore it is possible that IL-4 contributes to the inflammatory state in this model of PD.

Our results showed an increase in activated T cells in the brain of haSyn mice. To verify the impact of T lymphocyte infiltration, 2 groups of RAG-$1^{-/-}$ mice with or without wt bone marrow cell reconstitution were employed. We discovered that the presence of T cells aggravated the loss of TH^{+} dopaminergic neurons in the wt haSyn and wt BM RAG-$1^{-/-}$ haSyn mice. On the other hand, their absence enhanced survival of neurons in the RAG-$1^{-/-}$ haSyn mice when compared to the control groups. This finding is contrary to the observations in toxin-based PD models by Wheeler et al. and Ip et al. (Ip et al 2015, Wheeler et al 2014) and congruent with the findings of Brochard et al. (Brochard et al 2009) as there was a detrimental effect of T cells on the survival of dopaminergic neurons. We further did an analysis of microglial activation in the SN and striatum using the $CD11b^{+}$ marker and the results indicated an elevation of activated microglial cells especially in the wt haSyn and wt BM RAG-$1^{-/-}$ haSyn mice as compared to EV controls. The RAG-$1^{-/-}$ haSyn which lacked matured lymphocytes and received haSyn injection had relatively lower microglial activation. This observation reveals that the presence of T cells contributes to the activation state of microglial cells which can enhance the progression of neuroinflammation.

There have been proposed mechanisms to explain the deleterious of T cells on neurons. Brochard et al. conversely showed that T cells caused neuronal cell death via Fas/Fas ligand signaling in the MPTP model of PD (Brochard et al 2009). A recent study also proposed an enhanced T cell toxicity mediated by lymphocyte function-associated antigen 1 (LFA-1) and ICAM-1 expressed on the T cells and neurons respectively in the MPTP model (Liu et al 2017).

Given the suggested mechanisms of T toxicity, further investigations to ascertain the mechanisms of T cells induced neurotoxicity in this synucleinopathy model of PD should be carried out.

Although in the SN neurons were rescued in the absence of T cells, in the striatum we discovered that the TH^+ fibers were not spared from degeneration even with the lack of T cells. Furthermore, the level of striatal DA neurotransmitter was reduced and DA turnover was high in all haSyn injected mice except in the RAG-$1^{-/-}$ haSyn mice, where there was a trend towards lower DA turnover. A curious observation from the immunohistological analysis and quantification of activated microglia in the striatum revealed higher levels of activated cells as compared to the SN in all immune competent mice. This could possibly suggest a microglial involvement in haSyn induced axonal degeneration with further contribution from infiltrating T cells. However, further investigations to ascertain the ratio of a pro-inflammatory and anti-inflammatory microglial phenotype should be carried out to determine the dominant phenotype in this model of PD. Data from imaging analyses from postmortem neurochemical studies, genetic and neurotoxin animal models suggest that the loss of dopaminergic axons begin early in PD (Tagliaferro & Burke 2016). In postmortem studies, it was discovered that terminal loss was more pronounced with about 80% decrease of striatal dopamine without a corresponding loss of cell bodies in the SNpc and thus there are clinical manifestations of Parkinsonism when there is a high deficiency of striatal dopamine (Bernheimer et al 1973, Dauer & Przedborski 2003).

An increase in DA turnover has also been reported in animal models with a partial nigrostriatal lesion, which are all indications of a compensatory mechanism for the loss of dopaminergic terminals projecting to the striatum (Spina & Cohen 1989). Experimental evidence using a transgenic mouse model based on the expression of truncated α-synuclein (1–120), showed a significant reduction in DA and HVA levels detected from 3 months and beyond with no apparent loss of neuronal cell death (Tofaris et al 2006). In addition, these mice exhibited an

age-dependent redistribution of synaptic soluble NSF attachment protein receptor (SNARE) proteins SNAP-25, syntaxin-1 and synaptobrevin-2, in addition to a reduction in dopamine release (Garcia-Reitbock et al 2010).

Additionally, studies from the BAC human LRRK2 (R1441G) mutant transgenic mouse model of PD reveal that axons are affected the foremost in the dopaminergic system (Tagliaferro et al 2015). At 2 to 4 months of age, there was axonopathy with the presence of spheroids in the medial forebrain bundle and striatum even though there were a normal number and morphology of dopamine neuronal cell bodies (Tagliaferro et al 2015).

In the acute MPTP neurotoxin model of PD, studies in cynomolgus monkeys revealed a noticeable decrease of dopaminergic axons that preceded the loss of nigral cell bodies (Herkenham et al 1991). Likewise, chronic administration of MPTP to macaques resulted in 80% reduction in DAT and DA levels in the striatum while TH^+ cells in the SN were reduced by only 43% (Meissner et al 2003). Brochard et al. also discovered that striatal T cell infiltration was not a significant contributor to dopaminergic fiber injury in the MPTP mouse model of PD (Brochard et al 2009). Moreover, in the cell culture experiments, we detected an early loss of the somatodendritic and axonal cytoskeletal markers MAP2 and TUJ1 with increasing concentrations of haSyn.

It is has been established that the means of axonal degeneration are different from those of neuronal cell body disintegration as the processes leading to axonal destruction do not follow the orthodox pathways of programmed cell death (Tagliaferro & Burke 2016). For instance, in various models of axonal disintegration particularly in adult animals, the activation of caspase 3 does not typically happen (Finn et al 2000, Tagliaferro & Burke 2016). In the case of dopaminergic fibers, the neurotransmitter DA itself is problematic for the survival of axons due to its propensity to be easily oxidized (Hastings 2009). In addition, there are other ascertained mechanisms that make these axons particularly vulnerable. For example, it has been discovered that the size of mitochondria in dopaminergic neurons is only 40% that of other neurons and

they are also three times slower than mitochondria in non-dopaminergic axons (Burke & O'Malley 2013). Furthermore, it's been discovered that dopaminergic axonal terminal fields can be more extensive than those of other neurotransmitter types (Matsuda et al 2009). As a result, moving mitochondria to sites under stressful conditions may be more challenging for dopaminergic axons than it is for other neurons making them more susceptible to degeneration (Burke & O'Malley 2013). In this regard, it can be construed that the aggregation of haSyn in our mouse model engenders early axonal degeneration through impaired axonal transport as seen in the loss of cytoskeletal immunoreactivity in the cell culture experiments and microglial activation.

The outcomes from our experiments as well as some data from some previous studies have attested to the fact that the infiltration of T cells into the SN speed up nigrostriatal degeneration. As a result, it will be relevant for the involvement of immunological interventions in the treatment of PD. To effectively do this, the identification of the problematic T cell subpopulation is imperative. Therefore, proceeding in this study, we did bone marrow cell transfer from $CD4^+/CD8^-$, $CD4^-/CD8^+$ and $CD4^+/CD8^+$ ($JHD^{-/-}$) donor mice into $RAG\text{-}1^{-/-}$ recipient mice. From the results, it was detected that $CD4^+$ T lymphocytes were very potent in exacerbating the loss of SN dopaminergic neurons, whereas $CD8^+$ T lymphocytes contributed to a minor loss of DA neurons. When the 2 subsets were present, the loss of DA neurons was comparable to that observed in the $CD4^+/CD8^-$ T cells group, reiterating the observation that $CD8^+$ T cells contributed to a minimal cell loss in this model of PD. This data largely corroborate the findings of Brochard and colleagues where they discovered that in the MPTP model, $CD4^+$ T and not $CD8^+$ T cells participated in the loss of DA neurons. T lymphocytes generally recognize antigens when bound to MHC molecules. α-synuclein is capable of inducing MHC II expression on microglia which in turn can lead to $CD4^+$ T cell proliferation and activate cytokine release (Harms et al 2013). In the MPTP model, the investigators argued that MPTP induced a brain antigen alteration via MHC II that generated a secondary and

harmful Th response by $CD4^+$ T cells (Brochard et al 2009). Again, Sulzer and colleagues showed that the predominant T cells from the blood of patients with PD that responded to α-synuclein peptides were of $CD4^+$ phenotype (Sulzer et al 2017). Taking into account these findings in conjunction with our observations, it can be deduced that the injection of haSyn antigen provoked a Th 1 response that was aided by MHC II expression, hence the reason for the more detrimental role of $CD4^+$ T lymphocytes. Although $CD4^+$ T lymphocytes were the main culprit in our study, we also detected the contribution of $CD8^+$ T cells to neurodegeneration, nonetheless to a lesser extent. The lower contribution of $CD8^+$ T cells could be due to lower levels of MHC I in the brain. Generally, mature neurons do not express MHC molecules (Garretti et al 2019). Notwithstanding, dopaminergic neurons have been shown to express MHC I which are capable of presenting α-synuclein in the presence of the pro-inflammatory cytokines such as IFN-γ (Cebrian et al 2014, Garretti et al 2019). Thus, whereas the mere presence of α-synuclein enhances MHC II expression on microglia, MHC I expression is subjected to the levels of pro-inflammatory cytokines in the brain. Therefore, it is possible that the required conditions for an enhanced MHC I expression was not enough at the time point of the experiment to drive a significant $CD8^+$ T cell-induced toxicity. These observations show that both MHC I and II play a role in the immune response in this model of PD.

The assessment of striatal DA neurochemistry was carried out again to determine whether any of the lymphocyte subgroups enhanced the survival of dopaminergic fibers or otherwise. From the analysis, it was discovered there was a deficit in the nigrostriatal system with the loss of TH^+ terminals and lower levels of DA in all haSyn injected mice compared to the control EV mice. These observations again substantiate the assertion that the mechanism for axonal damage is void of lymphocyte contribution as was proven in the earlier experiments.

Sulzer and colleagues discovered in their studies that peptides derived from α-synuclein, represent antigenic epitopes that drive helper and cytotoxic T cell responses in patients with PD (Sulzer et al 2017). To have a mouse model that has characteristics close to the human pathology

will augment research for therapeutic interventions in PD. We have previously described how this AAV1/2 human A53T α-synuclein mouse model of PD has neurological deficits that are comparable to the human condition. Therefore, an immunological characterization, especially to demonstrate that the T cells are specific to α-synuclein peptides would aid to advance research into immunomodulatory interventions in PD. Further on this study, investigations were conducted into the specificity of the T cells to haSyn peptides as well as haSyn specific T cell-induced neurotoxicity. For this purpose, ELISpot and primary hippocampal neuronal cell cultures experiments were carried out. Results from the ELISpot analysis showed that the T cells from the cervical lymph nodes and spleen of haSyn injected mice recognized haSyn peptides at amino acid (a.a.) positions 68-78 (GAVVTGVTAVA) with predicted affinity for MHC I, a.a.100-114 (LGKNEEGAPQEGILE) predicted to bind MHC II and to some extent at positions a.a.121-128 (DNEAYEMP). The T cells from the brain were also activated in response to haSyn peptides at positions a.a. 68-78, a.a. 100-114 and a.a.121-128 additionally to haSyn peptide at a.a. 120-134 (PDNEAYEMPSEEGYQ), a predicted MHC II peptide. However, further analyses should be carried out to establish this trend of observation in the brain due to the small sample size that was used in this experiment. For their study, Sulzer et al. discovered 2 antigenic regions in α-synuclein. The first antigenic sequence was near the N terminus made up of a.a.31-46 (GKTKEGVLYVGSKTKE) referred to as the Y39 region and the second antigenic region was near the C terminus a.a. 116-140 (MPVDPDNEAYEMPSEEGYQDYEPEA) referred to as the S129 region (Sulzer et al 2017). Drawing observations from the 2 studies, it can be said that apart from position a.a. 121-128, which overlap with the antigenic region discovered in the study by Sulzer et al. the other antigenic regions do not coincide. It must, however, be noted that there are physiological differences between mice and humans (Yang et al 2013) and molecules of the immune system including MHC molecules in different species, have all evolved rapidly in different directions (Kametani et al 2018). For this reason, there will be differences in recognition of the different

antigenic epitopes of α-synuclein. With that said, an important fact is that the a.a. residues from positions 30-110 are essential for the polymerization of α-synuclein and the deletion of the a.a. residues at 71- 82 within the hydrophobic region abolishes the ability of human α-synuclein to fibrillate (Harada et al 2009, Waxman et al 2009). Therefore, it can be presupposed from this study and of Sulzer et al. (2017) that the T cells recognize segments of the human α-synuclein which have the important elements with the propensity to form fibrils. Additionally, we observed more MHC I restricted T cell responses as compared to MHC II responses whereas Sulzer et al. detected higher MHC II-restricted $CD4^+$ T cell responses as opposed to $CD8^+$ T cells which may be due to different techniques in experimental design. Howbeit, both studies have shown that MHC I and II are important in driving PD pathogenesis.

Following this outcome, we subjected the T cells to a proliferation assay to assess their memory status, though the subpopulation of $CD4^+$ T cells could not be determined because of a technical challenge. We identified some effector memory $CD8^+$ T cells in one haSyn mouse following FACS analysis of expanded of the T cells. Considering the fact that only a minute fraction of activated cells evolve into long-lived memory cells (Zhan et al 2017), it is possible that we may have lost memory T cells during the expansion process in the other haSyn mice. In this regard, further investigations should be done using different time points for expansion and markers that differentiate between the various subtypes of memory T cells in this model of PD. In spite of this, it can be concluded that the observed T cell responses in this study were mediated by memory cells which drive the chronic inflammatory processes detected at 10 weeks in addition to regular activated effector cells. In parallel to the role of memory cells in this model, it was discovered in the MPTP model of PD that the T cells were of an activated memory phenotype being LFA-1 and CD44 positive (Brochard et al 2009, Kurkowska-Jastrzebska et al 1999).

Following the determination of antigen-specificity of the T lymphocytes by the ELISpot assay, the subsequent question we addressed was whether the T cells would show selectivity in their effector function *ex vivo*. Though Sulzer and colleagues (2017) demonstrated that T cells from

PD patients recognized α-synuclein peptides, there was no proof that these cells were or would be neurotoxic particularly considering the fact that the T cells came from the blood which is peripheral to the CNS. An investigation by Sommer et al. (2018) showed that T cells from PD patients were detrimental to the survival of autologous human induced pluripotent stem cells (hiPSC) differentiated into midbrain dopaminergic neurons. In this study, however, they could only predict that there was some specificity towards TH^+ neurons compared to TH^- neurons because there was a slightly higher cell death rate in the TH^+ neurons (Sommer et al 2018). In this regard, we transduced primary hippocampal neuron cell cultures with either the haSyn or EV viral vectors. As a measure of control, some neurons were not transduced. Our experiments demonstrated that the isolated T cells from the haSyn injected mice induced severe neuronal cell death in the haSyn infected neurons as compared EV or uninfected neurons. Further investigations were subsequently conducted to determine that the observed selective T cell-induced neurotoxicity was not a common feature of activated T cells. As a result, we employed CD3 activated T cells in the consecutive control experiments. When the CD3 activated T cells were co-cultured with haSyn, EV or uninfected neurons, there was a significant cell death observed in all groups regardless of treatment. These outcomes show that the T cells isolated from the haSyn injected mice were specific in their action and the specific neurotoxicity observed was not a common characteristic of activated T cells.

In summary, whereas Sulzer and colleagues (2017) identified α-synuclein specific T cells in the periphery of PD patients, what could not be proved in their outcome was the ability of the T cells to extravasate into the CNS and cause dopaminergic cell death (Garretti et al 2019). In this study, we have proven the presence of haSyn specific T cells in peripheral lymphoid organs and the brain by ELISpot as well as demonstrated an α-synuclein dependent T cell neurotoxicity via *ex vivo*/*in vitro* experiments. This is the first data to substantiate that T cells from a mouse model of PD show specificity to α-synuclein peptides and to confirm their capability of killing α-synuclein transduced neurons. Taken together, the outcome of this research and that of Sulzer

et al. suggest that there is an autoimmune component in PD pathogenesis. Though the autoimmune response may not be the trigger for the development of the disease, it evolves in the course of PD producing a detrimental effect.

The subsequent investigations were to verify whether the T cell-mediated killing was MHC I and II-dependent. The results revealed that both MHC I and II were not required for the observed toxicity. A previous study using human fetal neuronal cell cultures showed similar results that MHC I and II were not needed for CD3 activated T cell-induced toxicity (Giuliani et al 2003), which is in agreement to our study. In summary, it can be deduced from our data and that of previous studies that MHC I and II are not indispensable in the effector function of activated memory T cells. There are reports from studies on memory T cells which suggest that this T cell population do not depend on MHC molecules for survival nor effector function (Berard & Tough 2002, Bevan & Goldrath 2000, Swain et al 1999). This could partly explain our observation in the blocking experiment although positive control experiments where there is a known MHCI and II-mediated toxicity are needed to establish the results above.

Given that T cells can mediate their effects through cytokine production, we examined the possibility of cytokine-mediated toxicity. Our data indicated that the cytokines IFN-γ, TNF-α and IL-4 were not responsible for the observed toxicity. This is contrary to the data of others that pro-inflammatory cytokines including TNF-α can kill neurons *in vitro*, though they used human fetal neurons (Downen et al 1999). It however, corroborates the data from Giuliani et al. (2003), that demonstrated neither IFN-γ nor TNF-α induced neurotoxicity whether used alone or as a combination.

We have demonstrated in this research, that some of the T cells from haSyn injected mice are of a memory phenotype. It has been proven that the survival of antigen-specific $CD4^+$ and $CD8^+$ memory T cells is independent of the presence of antigen (Berard & Tough 2002). Memory T cells are not only able to survive in the absence of the antigen but also preserve their rapid response reactions even with the lack of ligands for their T cell receptor (Bevan & Goldrath

2000). The implication of not needing the presentation of an antigen is that they would not require MHC I and II to mediate their actions. This may account for the MHC I and II independent toxicity that was seen in this study.

With regards to the role of cytokines, especially the pro-inflammatory ones and their effect on neurons, there are inconsistencies in data on whether they are neuroprotective or neurotoxic in both *in vivo* and *in vitro* experiments (Giuliani et al 2003). Deducing from our investigations and that of others, it can be predicted that these cytokines may induce indirect neurotoxicity by influencing other cells such as microglia and T cells but not directly on the neurons per se.

Chapter SIX

6.0 Conclusion

One of the main challenges of PD research has been the issue of the lack of an appropriate model to exemplify the disease in various regards such as behavior, clinical and pathological characteristic of the disease. Though there are several models of PD none has been successful in summarizing all the key features of the disease. We have previously described the neuropathological hallmarks of PD in this model which is an advantage over the more classical models of PD. With a growing interest in defining the role of the immune system in PD research currently, it was important that we carried out an immune characterization of a model that has vast similarity to that of the human situation.

In this study, we have shown that there is an increased T lymphocyte invasion coupled with higher microglial activation in the SN of PD patients and PD induced (haSyn) mice. Furthermore, we discovered that the invasion and activation of immune cells included the nigrostriatal tract as there was inflammation in the striatum as well.

Using FACs analyses, we confirmed that the infiltrated T cells were of an activated phenotype with lower and insignificant numbers of regulatory T cells, pointing to a pro-inflammatory condition. With histological and stereological analyses, we proved that the presence of T cells was not beneficial to the rescue of dopaminergic cells but contributed to their degeneration as the absence of T cells in RAG-$1^{-/-}$ led to the survival of neurons. The striatal neurochemical deficit we observed occurred earlier and was not dependent on lymphocyte contribution.

This study has also substantiated that $CD4^+$ and $CD8^+$ T cells do not contribute equally to neurodegeneration in this model of PD. Dopaminergic cells were more susceptible to cell death in the presence of $CD4^+$ than $CD8^+$ T cells indicating a more detrimental role of the former.

The data from the ELISpot and cell culture experiments showed that the T cells from the PD induced mice were haSyn antigen-specific, recognizing peptides from haSyn. In addition, they

demonstrated selectivity in engendering cell death mainly to haSyn infected neurons and not to control cells. This feature was not seen CD3 activated T cells. The mechanism of T cell-induced cell loss however, could not be elucidated in this study as the effect of T cells *in vitro* was not truncated by MHC I and II antibodies. It can, however, be predicted that the T cells being of a memory phenotype could cause injury to neurons independent of MHC molecules contribution. In accordance with other studies, we also did not observe a negative effect of cytokines on neurons.

In summary, we have shown that the peripheral adaptive immune system contributes significantly to the pathology of PD and $CD4^+$ T cells propagate a more toxic effect in the progression of PD than $CD8^+$ cells.

Secondly, a continuous inflammatory process gives rise to haSyn specific memory T lymphocytes that drive the degeneration of haSyn transduced neurons indicative of autoimmune immune disease in PD progression. Thus, this research has demonstrated for the first time that haSyn specific T cells extravasate into the brain and cause dopaminergic neuron death.

On the whole, this study has also given evidence that opportunistic or causative agents can trigger the development of PD in the local environment of the brain. With the SN having the highest number of microglial cells (McCarthy 2017), which are capable of antigen presentation and release of factors that call for lymphocyte invasion, it can be postulated that sporadic PD can arise from the presence of causative agents in the SN (Fig. 23).

Furthermore, this research also suggests that the addition of immunomodulatory molecules for therapeutic interventions in PD may provide better results in the treatment outcome.

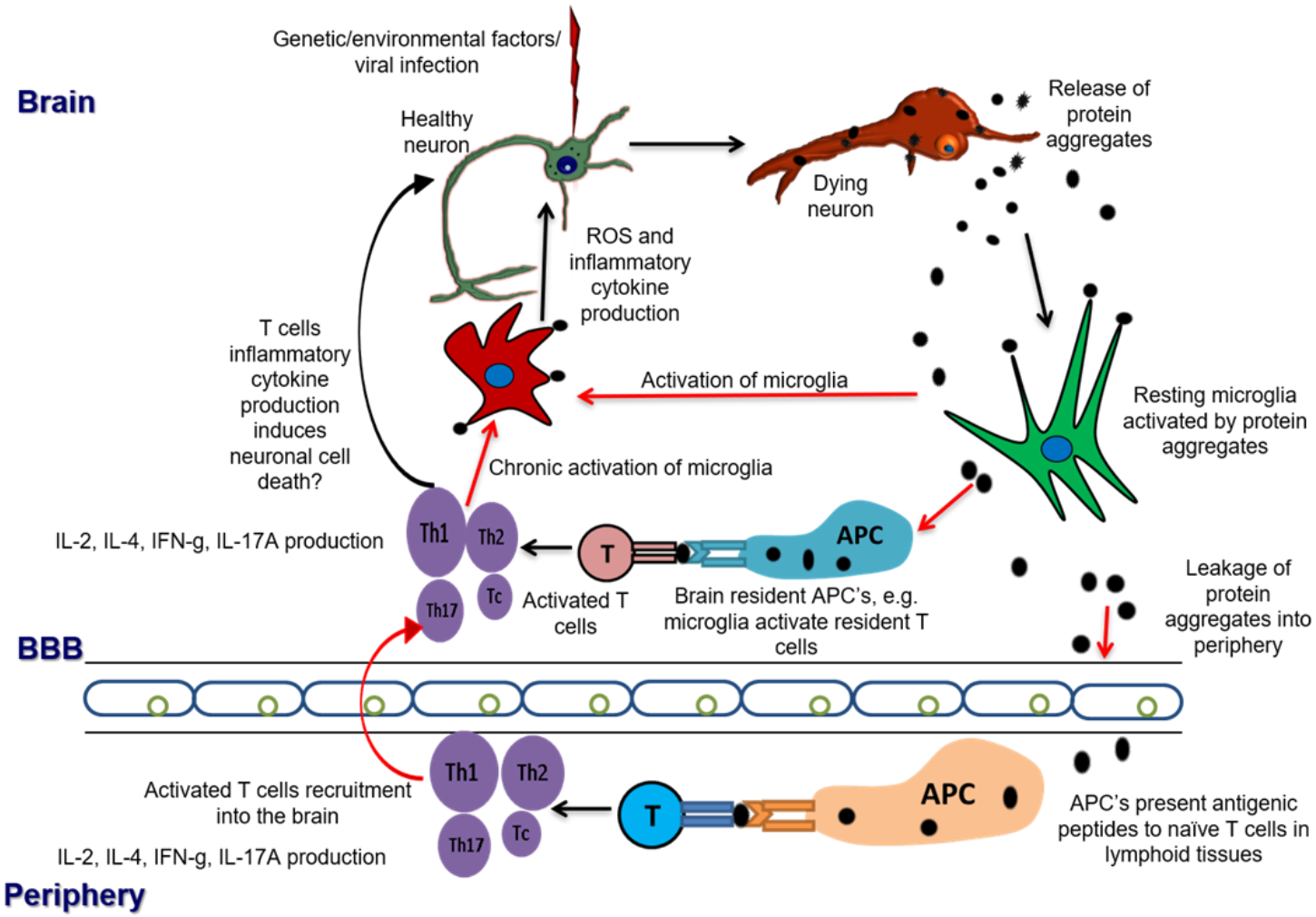

Fig. 23. Proposed mechanism of how sporadic PD can develop based on our mouse model of PD.

Exposure of dopaminergic neurons to risk factors of PD makes them susceptible to degeneration with haSyn aggregation. The release of aggregated haSyn activates leads to microglia activation and the trigger of inflammation in the microenvironment of the brain. Leakage of protein aggregates across the BBB induces a peripheral inflammatory response in lymphoid organs notably in the cervical lymph nodes and spleen, which subsequently results in the transmigration of activated T cells into the brain exacerbating the degenerative process. Red arrows indicate the major triggers of inflammation.

Th1: Type 1 T helper cells, Th2: Type 2 T helper cells, Th17: T-helper cell 17, Tc: cytotoxic T cell, APC: antigen presenting cells, T: naïve T cells, BBB: blood-brain barrier, ROS: reactive oxygen species.

6.1.0 Future perspectives

The results presented from this study has provided valuable novel insights into the adaptive immune contribution in PD pathogenesis. We have for the first time characterized T lymphocyte detrimental effect in a human mutated A53T α-synuclein mouse model of PD by;

i. showing that T cells are capable of infiltrating the brain in the course of PD
ii. demonstrating that there is an early T lymphocyte response which is most like mediated by brain circulating lymphocytes and a more robust inflammatory response orchestrated by the continuous recruitment of T cells from the peripheral lymphatic organs into the brain
iii. ascertaining that the T cells are of an activated and memory phenotype
iv. proving that $CD4^+$ lymphocytes are more injurious to dopaminergic cells than $CD8^+$ T cells although both MHC I and II predicted peptides could evoke T cell responses with increased IFN-γ production.
v. establishing that there is an autoimmune component in PD in which haSyn specific memory T cells target haSyn transduced neurons for destruction.

With all the aforementioned insights notwithstanding there are some pertinent questions which remain unanswered from this project and can be addressed in future studies. Some inquiries that should be looked at include;

i. the surprisingly lower numbers of regulatory T cells in this PD model. Were the regulatory T cells exhausted as a result of the highly inflammatory conditions or were they dysfunctional?

ii. the mechanism of T cell-induced neurotoxicity. Is the T cell toxicity as a result of contact to contact killing or due to soluble factors?

iii. which cell adhesion molecules are involved the recruitment of T cells in the brain and their expression pattern in the progression of the disease?

iv. the type of memory T cells using the various memory specific markers.

v. regarding PD treatment, a study involving an autologous regulatory T cell immunotherapy in PD patients should be considered as part of the therapeutic interventions.

References

Abeliovich A, Schmitz Y, Farinas I, Choi-Lundberg D, Ho WH, et al. 2000. Mice lacking alpha-synuclein display functional deficits in the nigrostriatal dopamine system. *Neuron* 25: 239-52

Albert K, Voutilainen MH, Domanskyi A, Airavaara M. 2017. AAV Vector-Mediated Gene Delivery to Substantia Nigra Dopamine Neurons: Implications for Gene Therapy and Disease Models. *Genes (Basel)* 8

Alderson TR, Markley JL. 2013. Biophysical characterization of α-synuclein and its controversial structure. *Intrinsically disordered proteins* 1: 18-39

Allen Reish HE, Standaert DG. 2015. Role of α-synuclein in inducing innate and adaptive immunity in Parkinson disease. *Journal of Parkinson's disease* 5: 1-19

Aloisi F. 2001. Immune function of microglia. *Glia* 36: 165-79

Anand VS, Braithwaite SP. 2009. LRRK2 in Parkinson's disease: biochemical functions. *FEBS J* 276: 6428-35

Antony PM, Diederich NJ, Balling R. 2011. Parkinson's disease mouse models in translational research. *Mamm Genome* 22: 401-19

Appel-Cresswell S, Vilarino-Guell C, Encarnacion M, Sherman H, Yu I, et al. 2013. Alpha-synuclein p.H50Q, a novel pathogenic mutation for Parkinson's disease. *Mov Disord* 28: 811-3

Aspelund A, Antila S, Proulx ST, Karlsen TV, Karaman S, et al. 2015. A dural lymphatic vascular system that drains brain interstitial fluid and macromolecules. *The Journal of Experimental Medicine* 212: 991-99

Baba Y, Kuroiwa A, Uitti RJ, Wszolek ZK, Yamada T. 2005. Alterations of T-lymphocyte populations in Parkinson disease. *Parkinsonism Relat Disord* 11: 493-8

Baquet ZC, Williams D, Brody J, Smeyne RJ. 2009. A comparison of model-based (2D) and design-based (3D) stereological methods for estimating cell number in the substantia nigra pars compacta (SNpc) of the C57BL/6J mouse. *Neuroscience* 161: 1082-90

Beal MF. 2010. Parkinson's disease: a model dilemma. *Nature* 466: S8

Berard M, Tough DF. 2002. Qualitative differences between naïve and memory T cells. *Immunology* 106: 127-38

Bernheimer H, Birkmayer W, Hornykiewicz O, Jellinger K, Seitelberger F. 1973. Brain dopamine and the syndromes of Parkinson and Huntington Clinical, morphological and neurochemical correlations. *Journal of the Neurological Sciences* 20: 415-55

Berry C, La Vecchia C, Nicotera P. 2010. Paraquat and Parkinson's disease. *Cell Death Differ* 17: 1115-25

Betarbet R, Sherer TB, MacKenzie G, Garcia-Osuna M, Panov AV, Greenamyre JT. 2000. Chronic systemic pesticide exposure reproduces features of Parkinson's disease. *Nat Neurosci* 3: 1301-6

Bevan MJ, Goldrath AW. 2000. T-cell memory: You must remember this&#x2026. *Current Biology* 10: R338-R40

Blesa J, Phani S, Jackson-Lewis V, Przedborski S. 2012. Classic and new animal models of Parkinson's disease. *J Biomed Biotechnol* 2012: 845618

Blesa J, Przedborski S. 2014. Parkinson's disease: animal models and dopaminergic cell vulnerability. *Front Neuroanat* 8: 155

Block ML, Zecca L, Hong JS. 2007. Microglia-mediated neurotoxicity: uncovering the molecular mechanisms. *Nat Rev Neurosci* 8: 57-69

Blum-Degen D, Muller T, Kuhn W, Gerlach M, Przuntek H, Riederer P. 1995. Interleukin-1 beta and interleukin-6 are elevated in the cerebrospinal fluid of Alzheimer's and de novo Parkinson's disease patients. *Neuroscience letters* 202: 17-20

Blum D, Torch S, Lambeng N, Nissou M-F, Benabid A-L, et al. 2001. Molecular pathways involved in the neurotoxicity of 6-OHDA, dopamine and MPTP: contribution to the apoptotic theory in Parkinson's disease. *Progress in Neurobiology* 65: 135-72

Bonifati V. 2012. Autosomal recessive parkinsonism. *Parkinsonism & Related Disorders* 18: S4-S6

Booth HDE, Hirst WD, Wade-Martins R. 2017. The Role of Astrocyte Dysfunction in Parkinson’s Disease Pathogenesis. *Trends in Neurosciences* 40: 358-70

Borghi R, Marchese R, Negro A, Marinelli L, Forloni G, et al. 2000. Full length alpha-synuclein is present in cerebrospinal fluid from Parkinson's disease and normal subjects. *Neuroscience letters* 287: 65-7

Braak H, Sastre M, Del Tredici K. 2007. Development of alpha-synuclein immunoreactive astrocytes in the forebrain parallels stages of intraneuronal pathology in sporadic Parkinson's disease. *Acta Neuropathol* 114: 231-41

Brahmachari S, Fung YK, Pahan K. 2006. Induction of Glial Fibrillary Acidic Protein Expression in Astrocytes by Nitric Oxide. *The Journal of neuroscience : the official journal of the Society for Neuroscience* 26: 4930-39

Branchi I, D'Andrea I, Armida M, Cassano T, Pezzola A, et al. 2008. Nonmotor symptoms in Parkinson's disease: investigating early-phase onset of behavioral dysfunction in the 6-hydroxydopamine-lesioned rat model. *J Neurosci Res* 86: 2050-61

Breydo L, Wu JW, Uversky VN. 2012. α-Synuclein misfolding and Parkinson's disease. *Biochimica et Biophysica Acta (BBA) - Molecular Basis of Disease* 1822: 261-85

Brochard V, Combadiere B, Prigent A, Laouar Y, Perrin A, et al. 2009. Infiltration of CD4+ lymphocytes into the brain contributes to neurodegeneration in a mouse model of Parkinson disease. *J Clin Invest* 119: 182-92

Burke RE, O'Malley K. 2013. Axon degeneration in Parkinson's disease. *Exp Neurol* 246: 72-83

Bussell R, Jr., Eliezer D. 2001. Residual structure and dynamics in Parkinson's disease-associated mutants of alpha-synuclein. *J Biol Chem* 276: 45996-6003

Cabin DE, Shimazu K, Murphy D, Cole NB, Gottschalk W, et al. 2002. Synaptic vesicle depletion correlates with attenuated synaptic responses to prolonged repetitive stimulation in mice lacking alpha-synuclein. *J Neurosci* 22: 8797-807

Campdelacreu J. 2014. Parkinson's disease and Alzheimer disease: environmental risk factors. *Neurología (English Edition)* 29: 541-49

Campelo C, Silva RH. 2017. Genetic Variants in SNCA and the Risk of Sporadic Parkinson's Disease and Clinical Outcomes: A Review. *Parkinsons Dis* 2017: 4318416

Cebrian C, Zucca FA, Mauri P, Steinbeck JA, Studer L, et al. 2014. MHC-I expression renders catecholaminergic neurons susceptible to T-cell-mediated degeneration. *Nat Commun* 5: 3633

Chatterjee P, Chiasson VL, Bounds KR, Mitchell BM. 2014. Regulation of the Anti-Inflammatory Cytokines Interleukin-4 and Interleukin-10 during Pregnancy. *Frontiers in immunology* 5: 253-53

Chou C, Kah-Leong L. 2013. Genetic Insights into Sporadic Parkinson's Disease Pathogenesis. *Current Genomics* 14: 486-501

Cose S, Brammer C, Khanna KM, Masopust D, Lefrancois L. 2006. Evidence that a significant number of naive T cells enter non-lymphoid organs as part of a normal migratory pathway. *Eur J Immunol* 36: 1423-33

Crabtree DM, Zhang J. 2012. Genetically engineered mouse models of Parkinson's disease. *Brain Res Bull* 88: 13-32

Croisier E, Moran LB, Dexter DT, Pearce RK, Graeber MB. 2005. Microglial inflammation in the parkinsonian substantia nigra: relationship to alpha-synuclein deposition. *J Neuroinflammation* 2: 14

Cserr HF, Knopf PM. 1992. Cervical lymphatics, the blood-brain barrier and the immunoreactivity of the brain: a new view. *Immunology today* 13: 507-12

Cuneo AA, Autieri MV. 2009. Expression and function of anti-inflammatory interleukins: the other side of the vascular response to injury. *Current vascular pharmacology* 7: 267-76

Dächsel JC, Farrer MJ. 2010. Lrrk2 and parkinson disease. *Archives of Neurology* 67: 542-47

Dauer W, Przedborski S. 2003. Parkinson's disease: mechanisms and models. *Neuron* 39: 889-909

Davalos D, Grutzendler J, Yang G, Kim JV, Zuo Y, et al. 2005. ATP mediates rapid microglial response to local brain injury in vivo. *Nat Neurosci* 8: 752-8

Dhawan V, Chaudhuri KR. 2007. Infectious basis to the pathogenesis of Parkinson's disease In *Handbook of Clinical Neurology*, ed. WC Koller, E Melamed, pp. 373-84: Elsevier

Dong Y, Benveniste EN. 2001a. Immune function of astrocytes. *Glia* 36: 180-90

Dong Y, Benveniste EN. 2001b. Immune function of astrocytes. *Glia* 36: 180-90

Downen M, Amaral TD, Hua LL, Zhao ML, Lee SC. 1999. Neuronal death in cytokine-activated primary human brain cell culture: role of tumor necrosis factor-alpha. *Glia* 28: 114-27

Dubey J, Ratnakaran N, Koushika S. 2015. Neurodegeneration and microtubule dynamics: death by a thousand cuts. *Frontiers in Cellular Neuroscience* 9: 343

Elwan MA, Richardson JR, Guillot TS, Caudle WM, Miller GW. 2006. Pyrethroid pesticide-induced alterations in dopamine transporter function. *Toxicol Appl Pharmacol* 211: 188-97

Emamzadeh FN. 2016. Alpha-synuclein structure, functions, and interactions. *Journal of research in medical sciences : the official journal of Isfahan University of Medical Sciences* 21: 29-29

Engelhardt B, Ransohoff RM. 2005. The ins and outs of T-lymphocyte trafficking to the CNS: anatomical sites and molecular mechanisms. *Trends in immunology* 26: 485-95

Eriksen JL, Dawson TM, Dickson DW, Petrucelli L. 2003. Caught in the Act: α-Synuclein Is the Culprit in Parkinson's Disease. *Neuron* 40: 453-56

Esteves AR, Arduino DM, Swerdlow RH, Oliveira CR, Cardoso SM. 2009. Oxidative stress involvement in alpha-synuclein oligomerization in Parkinson's disease cybrids. *Antioxidants & redox signaling* 11: 439-48

Fabio B, Marie-Therese A. 2012. Animal models of Parkinson’s disease. *The FEBS Journal* 279: 1156-66

Farkas E, De Jong GI, Apro E, De Vos RA, Steur EN, Luiten PG. 2000. Similar ultrastructural breakdown of cerebrocortical capillaries in Alzheimer's disease, Parkinson's disease, and experimental hypertension. What is the functional link? *Annals of the New York Academy of Sciences* 903: 72-82

Ferrante RJ, Schulz JB, Kowall NW, Beal MF. 1997. Systemic administration of rotenone produces selective damage in the striatum and globus pallidus, but not in the substantia nigra. *Brain Research* 753: 157-62

Finn JT, Weil M, Archer F, Siman R, Srinivasan A, Raff MC. 2000. Evidence that Wallerian degeneration and localized axon degeneration induced by local neurotrophin deprivation do not involve caspases. *J Neurosci* 20: 1333-41

Forno LS, DeLanney LE, Irwin I, Di Monte D, Langston JW. 1992. Astrocytes and Parkinson's disease. *Progress in brain research* 94: 429-36

Fort M, Lesley R, Davidson N, Menon S, Brombacher F, et al. 2001. IL-4 exacerbates disease in a Th1 cell transfer model of colitis. *J Immunol* 166: 2793-800

Gamber KM. 2016. Animal Models of Parkinson's Disease: New models provide greater translational and predictive value. *BioTechniques* 61

Garcia-Reitbock P, Anichtchik O, Bellucci A, Iovino M, Ballini C, et al. 2010. SNARE protein redistribution and synaptic failure in a transgenic mouse model of Parkinson's disease. *Brain* 133: 2032-44

Garretti F, Agalliu D, Lindestam Arlehamn CS, Sette A, Sulzer D. 2019. Autoimmunity in Parkinson's Disease: The Role of alpha-Synuclein-Specific T Cells. *Front Immunol* 10: 303

Gispert S, Ricciardi F, Kurz A, Azizov M, Hoepken HH, et al. 2009. Parkinson phenotype in aged PINK1-deficient mice is accompanied by progressive mitochondrial dysfunction in absence of neurodegeneration. *PLoS One* 4: e5777

Giuliani F, Goodyer CG, Antel JP, Yong VW. 2003. Vulnerability of Human Neurons to T Cell-Mediated Cytotoxicity. *The Journal of Immunology* 171: 368-79

Glass CK, Saijo K, Winner B, Marchetto MC, Gage FH. 2010. Mechanisms underlying inflammation in neurodegeneration. *Cell* 140: 918-34

Greenamyre JT, Cannon JR, Drolet R, Mastroberardino PG. 2010. Lessons from the rotenone model of Parkinson's disease. *Trends Pharmacol Sci* 31: 141-2; author reply 42-3

Greener M. 2013. *Pesticides and Parkinson's disease pathogenesis: The controversy continues*.

Guatteo E, Cucchiaroni ML, Mercuri NB. 2009. Substantia Nigra Control of Basal Ganglia Nuclei In *Birth, Life and Death of Dopaminergic Neurons in the Substantia Nigra*, pp. 91-101

Han JY, Choi TS, Kim HI. 2018. Molecular Role of Ca2+ and Hard Divalent Metal Cations on Accelerated Fibrillation and Interfibrillar Aggregation of α-Synuclein. *Scientific Reports* 8: 1895

Hansen MRH, Jors E, Lander F, Condarco G, Debes F, et al. 2017. Neurological Deficits After Long-term Pyrethroid Exposure. *Environ Health Insights* 11: 1178630217700628

Harada R, Kobayashi N, Kim J, Nakamura C, Han SW, et al. 2009. The effect of amino acid substitution in the imperfect repeat sequences of alpha-synuclein on fibrillation. *Biochim Biophys Acta* 1792: 998-1003

Harms AS, Cao S, Rowse AL, Thome AD, Li X, et al. 2013. MHCII is required for alpha-synuclein-induced activation of microglia, CD4 T cell proliferation, and dopaminergic neurodegeneration. *J Neurosci* 33: 9592-600

Hastings TG. 2009. The role of dopamine oxidation in mitochondrial dysfunction: implications for Parkinson's disease. *J Bioenerg Biomembr* 41: 469-72

Hayes GM, Woodroofe MN, Cuzner ML. 1987. Microglia are the major cell type expressing MHC class II in human white matter. *Journal of the neurological sciences* 80: 25-37

He F, Balling R. 2013. The role of regulatory T cells in neurodegenerative diseases. *Wiley interdisciplinary reviews. Systems biology and medicine* 5: 153-80

Herkenham M, Little MD, Bankiewicz K, Yang SC, Markey SP, Johannessen JN. 1991. Selective retention of MPP+ within the monoaminergic systems of the primate brain following MPTP administration: an in vivo autoradiographic study. *Neuroscience* 40: 133-58

Hickey WF. 2001. Basic principles of immunological surveillance of the normal central nervous system. *Glia* 36: 118-24

Hinkle KM, Yue M, Behrouz B, Dachsel JC, Lincoln SJ, et al. 2012. LRRK2 knockout mice have an intact dopaminergic system but display alterations in exploratory and motor co-ordination behaviors. *Mol Neurodegener* 7: 25

Hisahara S, Shimohama S. 2010. Toxin-induced and genetic animal models of Parkinson's disease. *Parkinsons Dis* 2011: 951709

Ho CSH, Ho RCM, Quek AML. 2018. Chronic Manganese Toxicity Associated with Voltage-Gated Potassium Channel Complex Antibodies in a Relapsing Neuropsychiatric Disorder. *International journal of environmental research and public health* 15: 783

Hoffman-Zacharska D, Koziorowski D, Ross OA, Milewski M, Poznański J, et al. 2013. Novel A18T and pA29S substitutions in α-synuclein may be associated with sporadic Parkinson's disease. *Parkinsonism & Related Disorders* 19: 1057-60

Huang D, Xu J, Wang J, Tong J, Bai X, et al. 2017. Dynamic Changes in the Nigrostriatal Pathway in the MPTP Mouse Model of Parkinson's Disease. *Parkinsons Dis* 2017: 9349487

Huh JW, Raghupathi R, Laurer HL, Helfaer MA, Saatman KE. 2003. Transient Loss of Microtubule-Associated Protein 2 Immunoreactivity after Moderate Brain Injury in Mice. *Journal of Neurotrauma* 20: 975-84

Ip CW, Beck SK, Volkmann J. 2015. Lymphocytes reduce nigrostriatal deficits in the 6-hydroxydopamine mouse model of Parkinson's disease. *J Neural Transm (Vienna)* 122: 1633-43

Ip CW, Klaus LC, Karikari AA, Visanji NP, Brotchie JM, et al. 2017. AAV1/2-induced overexpression of A53T-alpha-synuclein in the substantia nigra results in degeneration of the nigrostriatal system with Lewy-like pathology and motor impairment: a new mouse model for Parkinson's disease. *Acta neuropathologica communications* 5: 11

Ip CW, Kroner A, Bendszus M, Leder C, Kobsar I, et al. 2006. Immune Cells Contribute to Myelin Degeneration and Axonopathic Changes in Mice Overexpressing Proteolipid Protein in Oligodendrocytes. *The Journal of Neuroscience* 26: 8206-16

Iwasaki A, Medzhitov R. 2015. Control of adaptive immunity by the innate immune system. *Nat Immunol* 16: 343-53

Jackson-Lewis V, Blesa J, Przedborski S. 2012. Animal models of Parkinson's disease. *Parkinsonism & Related Disorders* 18: S183-S85

Jagmag SA, Tripathi N, Shukla SD, Maiti S, Khurana S. 2015. Evaluation of Models of Parkinson's Disease. *Front Neurosci* 9: 503

Janeway CA, Jr., Medzhitov R. 2002. Innate immune recognition. *Annu Rev Immunol* 20: 197-216

Jang H, Boltz D, Sturm-Ramirez K, Shepherd KR, Jiao Y, et al. 2009. Highly pathogenic H5N1 influenza virus can enter the central nervous system and induce neuroinflammation and neurodegeneration. *Proc Natl Acad Sci U S A* 106: 14063-8

Joe EH, Choi DJ, An J, Eun JH, Jou I, Park S. 2018. Astrocytes, Microglia, and Parkinson's Disease. *Exp Neurobiol* 27: 77-87

Kahle PJ, Neumann M, Ozmen L, Müller V, Jacobsen H, et al. 2002. Hyperphosphorylation and insolubility of α-synuclein in transgenic mouse oligodendrocytes. *EMBO reports* 3: 583-88

Kametani Y, Shiina T, Suzuki R, Sasaki E, Habu S. 2018. Comparative immunity of antigen recognition, differentiation, and other functional molecules: similarities and differences among common marmosets, humans, and mice. *Experimental animals* 67: 301-12

Kannarkat GT, Boss JM, Tansey MG. 2013. The role of innate and adaptive immunity in Parkinson's disease. *J Parkinsons Dis* 3: 493-514

Kiely AP, Asi YT, Kara E, Limousin P, Ling H, et al. 2013. alpha-Synucleinopathy associated with G51D SNCA mutation: a link between Parkinson's disease and multiple system atrophy? *Acta Neuropathol* 125: 753-69

Kiely AP, Ling H, Asi YT, Kara E, Proukakis C, et al. 2015. Distinct clinical and neuropathological features of G51D SNCA mutation cases compared with SNCA duplication and H50Q mutation. *Mol Neurodegener* 10: 41

Kim S, Seo J-H, Suh Y-H. 2004. α-Synuclein, Parkinson's disease, and Alzheimer's disease. *Parkinsonism & Related Disorders* 10: S9-S13

Klein C, Westenberger A. 2012. Genetics of Parkinson's disease. *Cold Spring Harb Perspect Med* 2: a008888

Koprich JB, Johnston TH, Huot P, Reyes MG, Espinosa M, Brotchie JM. 2011. Progressive Neurodegeneration or Endogenous Compensation in an Animal Model of Parkinson's Disease Produced by Decreasing Doses of Alpha-Synuclein. *PLOS ONE* 6: e17698

Koprich JB, Johnston TH, Reyes MG, Sun X, Brotchie JM. 2010. Expression of human A53T alpha-synuclein in the rat substantia nigra using a novel AAV1/2 vector produces a rapidly evolving pathology with protein aggregation, dystrophic neurite architecture and

nigrostriatal degeneration with potential to model the pathology of Parkinson's disease. *Mol Neurodegener* 5: 43

Koprich JB, Kalia LV, Brotchie JM. 2017. Animal models of alpha-synucleinopathy for Parkinson disease drug development. *Nat Rev Neurosci* 18: 515-29

Kortekaas R, Leenders KL, van Oostrom JC, Vaalburg W, Bart J, et al. 2005. Blood-brain barrier dysfunction in parkinsonian midbrain in vivo. *Ann Neurol* 57: 176-9

Kreutzberg GW. 1996. Microglia: a sensor for pathological events in the CNS. *Trends Neurosci* 19: 312-8

Krüger R, Kuhn W, Müller T, Woitalla D, Graeber M, et al. 1998. AlaSOPro mutation in the gene encoding α-synuclein in Parkinson's disease. *Nature Genetics* 18: 106

Kumar S, Jangir DK, Kumar R, Kumari M, Bhavesh NS, Maiti TK. 2018. Role of Sporadic Parkinson Disease Associated Mutations A18T and A29S in Enhanced alpha-Synuclein Fibrillation and Cytotoxicity. *ACS Chem Neurosci* 9: 230-40

Kumazawa R, Tomiyama H, Li Y, et al. 2008. Mutation analysis of the pink1 gene in 391 patients with parkinson disease. *Archives of Neurology* 65: 802-08

Kurkowska-Jastrzebska I, Wronska A, Kohutnicka M, Czlonkowski A, Czlonkowska A. 1999. The inflammatory reaction following 1-methyl-4-phenyl-1,2,3, 6-tetrahydropyridine intoxication in mouse. *Exp Neurol* 156: 50-61

Langston J, Ballard P, Tetrud J, Irwin I. 1983. Chronic Parkinsonism in humans due to a product of meperidine-analog synthesis. *Science* 219: 979-80

Langston JW. 2017. The MPTP Story. *Journal of Parkinson's disease* 7: S11-S19

Lashuel HA, Overk CR, Oueslati A, Masliah E. 2013. The many faces of alpha-synuclein: from structure and toxicity to therapeutic target. *Nat Rev Neurosci* 14: 38-48

Lawson LJ, Perry VH, Dri P, Gordon S. 1990. Heterogeneity in the distribution and morphology of microglia in the normal adult mouse brain. *Neuroscience* 39: 151-70

Lee HJ, Suk JE, Patrick C, Bae EJ, Cho JH, et al. 2010. Direct transfer of alpha-synuclein from neuron to astroglia causes inflammatory responses in synucleinopathies. *J Biol Chem* 285: 9262-72

Li J-Q, Tan L, Yu J-T. 2014. The role of the LRRK2 gene in Parkinsonism. *Molecular Neurodegeneration* 9: 47

Lim KL, Ng CH. 2009. Genetic models of Parkinson disease. *Biochim Biophys Acta* 1792: 604-15

Lin L, Doherty D, Lile J, Bektesh S, Collins F. 1993. GDNF: a glial cell line-derived neurotrophic factor for midbrain dopaminergic neurons. *Science* 260: 1130-32

Liu B, Gao HM, Hong JS. 2003. Parkinson's disease and exposure to infectious agents and pesticides and the occurrence of brain injuries: role of neuroinflammation. *Environ Health Perspect* 111: 1065-73

Liu Z, Huang Y, Cao BB, Qiu YH, Peng YP. 2017. Th17 Cells Induce Dopaminergic Neuronal Death via LFA-1/ICAM-1 Interaction in a Mouse Model of Parkinson's Disease. *Molecular neurobiology* 54: 7762-76

Longhena F, Faustini G, Missale C, Pizzi M, Spano P, Bellucci A. 2017. The Contribution of alpha-Synuclein Spreading to Parkinson's Disease Synaptopathy. *Neural Plast* 2017: 5012129

Low K, Aebischer P. 2012. Use of viral vectors to create animal models for Parkinson's disease. *Neurobiol Dis* 48: 189-201

Lu XH, Fleming SM, Meurers B, Ackerson LC, Mortazavi F, et al. 2009. Bacterial artificial chromosome transgenic mice expressing a truncated mutant parkin exhibit age-dependent hypokinetic motor deficits, dopaminergic neuron degeneration, and accumulation of proteinase K-resistant alpha-synuclein. *J Neurosci* 29: 1962-76

Lücking CB, Dürr A, Bonifati V, Vaughan J, De Michele G, et al. 2000. Association between Early-Onset Parkinson's Disease and Mutations in the Parkin Gene. *New England Journal of Medicine* 342: 1560-67

Manning-Bog AB, McCormack AL, Li J, Uversky VN, Fink AL, Di Monte DA. 2002. The herbicide paraquat causes up-regulation and aggregation of alpha-synuclein in mice: paraquat and alpha-synuclein. *J Biol Chem* 277: 1641-4

Manto M. 2014. Abnormal Copper Homeostasis: Mechanisms and Roles in Neurodegeneration. *Toxics* 2: 327-45

Masliah E, Rockenstein E, Veinbergs I, Mallory M, Hashimoto M, et al. 2000. Dopaminergic Loss and Inclusion Body Formation in α-Synuclein Mice: Implications for Neurodegenerative Disorders. *Science* 287: 1265-69

Matsuda W, Furuta T, Nakamura KC, Hioki H, Fujiyama F, et al. 2009. Single nigrostriatal dopaminergic neurons form widely spread and highly dense axonal arborizations in the neostriatum. *J Neurosci* 29: 444-53

McCarthy MM. 2017. Location, Location, Location: Microglia Are Where They Live. *Neuron* 95: 233-35

McGeer EG, McGeer PL. 2003. Inflammatory processes in Alzheimer's disease. *Progress in neuro-psychopharmacology & biological psychiatry* 27: 741-9

McGeer PL, Itagaki S, Boyes BE, McGeer EG. 1988. Reactive microglia are positive for HLA-DR in the substantia nigra of Parkinson's and Alzheimer's disease brains. *Neurology* 38: 1285-91

Medawar PB. 1948. Immunity to homologous grafted skin; the fate of skin homografts transplanted to the brain, to subcutaneous tissue, and to the anterior chamber of the eye. *British journal of experimental pathology* 29: 58-69

Meissner W, Prunier C, Guilloteau D, Chalon S, Gross CE, Bezard E. 2003. Time-course of nigrostriatal degeneration in a progressive MPTP-lesioned macaque model of Parkinson's disease. *Molecular neurobiology* 28: 209-18

Meredith GE, Rademacher DJ. 2011. MPTP mouse models of Parkinson's disease: an update. *J Parkinsons Dis* 1: 19-33

Mhyre TR, Boyd JT, Hamill RW, Maguire-Zeiss KA. 2012. Parkinson's disease. *Subcell Biochem* 65: 389-455

Mirza B, Hadberg H, Thomsen P, Moos T. 2000. The absence of reactive astrocytosis is indicative of a unique inflammatory process in Parkinson's disease. *Neuroscience* 95: 425-32

Mogi M, Harada M, Kondo T, Riederer P, Inagaki H, et al. 1994. Interleukin-1 beta, interleukin-6, epidermal growth factor and transforming growth factor-alpha are elevated in the brain from parkinsonian patients. *Neuroscience letters* 180: 147-50

Mogi M, Harada M, Kondo T, Riederer P, Nagatsu T. 1995. Brain beta 2-microglobulin levels are elevated in the striatum in Parkinson's disease. *Journal of neural transmission. Parkinson's disease and dementia section* 9: 87-92

Mori F, Tanji K, Yoshimoto M, Takahashi H, Wakabayashi K. 2002. Demonstration of alpha-synuclein immunoreactivity in neuronal and glial cytoplasm in normal human brain tissue using proteinase K and formic acid pretreatment. *Exp Neurol* 176: 98-104

Mosley RL BE, Kadiu I, Thomas M, Boska MD, Hasan K, Laurie C, and Gendelman HE. 2006. Neuroinflammation, Oxidative Stress and the Pathogenesis of

Parkinson's Disease. *Clin Neurosci Res.* 6: 261–81

Mosley RL, Hutter-Saunders JA, Stone DK, Gendelman HE. 2012. Inflammation and Adaptive Immunity in Parkinson’s Disease. *Cold Spring Harbor Perspectives in Medicine* 2: a009381

Mullin S, Schapira A. 2015. The genetics of Parkinson's disease. *Br Med Bull* 114: 39-52

Nandipati S, Litvan I. 2016. Environmental Exposures and Parkinson's Disease. *Int J Environ Res Public Health* 13

Nimmerjahn A, Kirchhoff F, Helmchen F. 2005. Resting microglial cells are highly dynamic surveillants of brain parenchyma in vivo. *Science* 308: 1314-8

Nishio T, Kawaguchi S, Fujiwara H. 2008. Emergence of highly neurofilament-immunoreactive zipper-like axon segments at the transection site in scalpel-cordotomized adult rats. *Neuroscience* 155: 90-103

Nonnekes J, Post B, Tetrud JW, Langston JW, Bloem BR. 2018. MPTP-induced parkinsonism: an historical case series. *The Lancet Neurology* 17: 300-01

Ogata A, Tashiro K, Nukuzuma S, Nagashima K, Hall WW. 1997. A rat model of Parkinson's disease induced by Japanese encephalitis virus. *J Neurovirol* 3: 141-7

Olsen ML, Higashimori H, Campbell SL, Hablitz JJ, Sontheimer H. 2006. Functional expression of Kir4.1 channels in spinal cord astrocytes. *Glia* 53: 516-28

Ousman SS, Kubes P. 2012. Immune surveillance in the central nervous system. *Nature Neuroscience* 15: 1096

Park HJ, Zhao TT, Lee MK. 2016. Animal models of Parkinson's disease and their applications. *Journal of Parkinsonism and Restless Legs Syndrome* Volume 6: 73-82

Paxinos G, Franklin, Keith B. J. Franklin, Keith B. J. 2001. *The mouse brain in stereotaxic coordinates*. San Diego :: Academic Press.

Perry VH, Nicoll JAR, Holmes C. 2010. Microglia in neurodegenerative disease. *Nature Reviews Neurology* 6: 193

Phatnani H, Maniatis T. 2015. Astrocytes in neurodegenerative disease. *Cold Spring Harb Perspect Biol* 7

Pisani V, Stefani A, Pierantozzi M, Natoli S, Stanzione P, et al. 2012. Increased blood-cerebrospinal fluid transfer of albumin in advanced Parkinson's disease. *Journal of Neuroinflammation* 9: 188

Posmantur RM, Kampfl A, Taft WC, Bhattachrjee M, Dixon CE, et al. 1996. Diminished Microtubule-Associated Protein 2 (MAP2) Immunoreactivity following Cortical Impact Brain Injury. *Journal of Neurotrauma* 13: 125-37

Prinz M, Priller J. 2017. The role of peripheral immune cells in the CNS in steady state and disease. *Nat Neurosci* 20: 136-44

Proukakis C, Dudzik CG, Brier T, MacKay DS, Cooper JM, et al. 2013. A novel α-synuclein missense mutation in Parkinson disease. *Neurology* 80: 1062-64

Przedborski S, Levivier M, Jiang H, Ferreira M, Jackson-Lewis V, et al. 1995. Dose-dependent lesions of the dopaminergic nigrostriatal pathway induced by intrastriatal injection of 6-hydroxydopamine. *Neuroscience* 67: 631-47

Przedbroski S, Leviver M, Jiang H, Ferreira M, Jackson-Lewis V, et al. 1995. Dose-dependent lesions of the dopaminergic nigrostriatal pathway induced by instrastriatal injection of 6-hydroxydopamine. *Neuroscience* 67: 631-47

Puschmann A, Ross OA, Vilariño-Güell C, Lincoln SJ, Kachergus JM, et al. 2009. A Swedish family with de novo alpha-synuclein A53T mutation: evidence for early cortical dysfunction. *Parkinsonism & related disorders* 15: 627-32

Qin L, Wu X, Block ML, Liu Y, Breese GR, et al. 2007. Systemic LPS Causes Chronic Neuroinflammation and Progressive Neurodegeneration. *Glia* 55: 453-62

Recasens A, Dehay B. 2014. Alpha-synuclein spreading in Parkinson's disease. *Front Neuroanat* 8: 159

Reeve AK, Grady JP, Cosgrave EM, Bennison E, Chen C, et al. 2018. Mitochondrial dysfunction within the synapses of substantia nigra neurons in Parkinson's disease. *NPJ Parkinsons Dis* 4: 9

Reynolds AD, Glanzer JG, Kadiu I, Ricardo-Dukelow M, Chaudhuri A, et al. 2008. Nitrated alpha-synuclein-activated microglial profiling for Parkinson's disease. *J Neurochem* 104: 1504-25

Richfield EK, Thiruchelvam MJ, Cory-Slechta DA, Wuertzer C, Gainetdinov RR, et al. 2002. Behavioral and neurochemical effects of wild-type and mutated human alpha-synuclein in transgenic mice. *Exp Neurol* 175: 35-48

Richter-Landsberg C, Gorath M, Trojanowski JQ, Lee VM. 2000. alpha-synuclein is developmentally expressed in cultured rat brain oligodendrocytes. *J Neurosci Res* 62: 9-14

Riederer P, Sofic E, Rausch WD, Schmidt B, Reynolds GP, et al. 1989. Transition Metals, Ferritin, Glutathione, and Ascorbic Acid in Parkinsonian Brains. *Journal of Neurochemistry* 52: 515-20

Rodriguez-Rocha H, Garcia-Garcia A, Pickett C, Li S, Jones J, et al. 2013. Compartmentalized oxidative stress in dopaminergic cell death induced by pesticides and complex I inhibitors: distinct roles of superoxide anion and superoxide dismutases. *Free Radic Biol Med* 61: 370-83

Roodveldt C, Christodoulou J, Dobson CM. 2008. Immunological features of alpha-synuclein in Parkinson's disease. *J Cell Mol Med* 12: 1820-9

Roodveldt C, Labrador-Garrido A, Izquierdo G, Pozo D. 2011. *Alpha-Synuclein and the Immune Response in Parkinson's Disease*.

Rothstein JD, Dykes-Hoberg M, Pardo CA, Bristol LA, Jin L, et al. 1996. Knockout of Glutamate Transporters Reveals a Major Role for Astroglial Transport in Excitotoxicity and Clearance of Glutamate. *Neuron* 16: 675-86

Scharr DG, Sieber B-A, Dreyfus CF, Black IB. 1993. Regional and Cell-Specific Expression of GDNF in Rat Brain. *Experimental Neurology* 124: 368-71

Schetters STT, Gomez-Nicola D, Garcia-Vallejo JJ, Van Kooyk Y. 2018. Neuroinflammation: Microglia and T Cells Get Ready to Tango. *Frontiers in Immunology* 8

Schmid CD, Melchior B, Masek K, Puntambekar SS, Danielson PE, et al. 2009. Differential gene expression in LPS/IFNgamma activated microglia and macrophages: in vitro versus in vivo. *J Neurochem* 109 Suppl 1: 117-25

Scudamore O, Ciossek T. 2018. Increased Oxidative Stress Exacerbates alpha-Synuclein Aggregation In Vivo. *Journal of neuropathology and experimental neurology* 77: 443-53

Sedelis M, Hofele K, Auburger GW, Morgan S, Huston JP, Schwarting RK. 2000. MPTP susceptibility in the mouse: behavioral, neurochemical, and histological analysis of gender and strain differences. *Behavior genetics* 30: 171-82

Sharma R, Colarusso P, Zhang H, Stevens KM, Patel KD. 2015. FRNK negatively regulates IL-4-mediated inflammation. *J Cell Sci* 128: 695-705

Shi Q, Hu X, Prior M, Yan R. 2009. The occurrence of aging-dependent reticulon 3 immunoreactive dystrophic neurites decreases cognitive function. *J Neurosci* 29: 5108-15

Shrestha R, Shakya Shrestha S, Millingtona O, Brewer J, Bushell T. 2014. Immune responses in neurodegenerative diseases. *Kathmandu University medical journal (KUMJ)* 12: 67-76

Shults CW. 2006. Lewy bodies. *Proc Natl Acad Sci U S A* 103: 1661-8

Simard M, Nedergaard M. 2004. The neurobiology of glia in the context of water and ion homeostasis. *Neuroscience* 129: 877-96

Sommer A, Fadler T, Dorfmeister E, Hoffmann AC, Xiang W, et al. 2016. Infiltrating T lymphocytes reduce myeloid phagocytosis activity in synucleinopathy model. *J Neuroinflammation* 13: 174

Sommer A, Maxreiter F, Krach F, Fadler T, Grosch J, et al. 2018. Th17 Lymphocytes Induce Neuronal Cell Death in a Human iPSC-Based Model of Parkinson's Disease. *Cell Stem Cell* 23: 123-31 e6

Sommer A, Winner B, Prots I. 2017. The Trojan horse - neuroinflammatory impact of T cells in neurodegenerative diseases. *Molecular Neurodegeneration* 12: 78

Spillantini MG, Crowther RA, Jakes R, Hasegawa M, Goedert M. 1998. α-Synuclein in filamentous inclusions of Lewy bodies from Parkinson’s disease and dementia with Lewy bodies. *Proceedings of the National Academy of Sciences* 95: 6469-73

Spillantini MG, Schmidt ML, Lee VM, Trojanowski JQ, Jakes R, Goedert M. 1997. Alpha-synuclein in Lewy bodies. *Nature* 388: 839-40

Spina MB, Cohen G. 1989. Dopamine turnover and glutathione oxidation: implications for Parkinson disease. *Proceedings of the National Academy of Sciences of the United States of America* 86: 1398-400

Stevens CH, Rowe D, Morel-Kopp MC, Orr C, Russell T, et al. 2012. Reduced T helper and B lymphocytes in Parkinson's disease. *J Neuroimmunol* 252: 95-9

Su X, Federoff HJ. 2014. Immune responses in Parkinson's disease: interplay between central and peripheral immune systems. *Biomed Res Int* 2014: 275178

Subramaniam SR, Federoff HJ. 2017. Targeting Microglial Activation States as a Therapeutic Avenue in Parkinson's Disease. *Front Aging Neurosci* 9: 176

Sulzer D, Alcalay RN, Garretti F, Cote L, Kanter E, et al. 2017. T cells from patients with Parkinson's disease recognize alpha-synuclein peptides. *Nature* 546: 656-61

Swain SL, Hu H, Huston G. 1999. Class II-Independent Generation of CD4 Memory T Cells from Effectors. *Science* 286: 1381-83

Tagliaferro P, Burke RE. 2016. Retrograde Axonal Degeneration in Parkinson Disease. *J Parkinsons Dis* 6: 1-15

Tagliaferro P, Kareva T, Oo TF, Yarygina O, Kholodilov N, Burke RE. 2015. An early axonopathy in a hLRRK2(R1441G) transgenic model of Parkinson disease. *Neurobiol Dis* 82: 359-71

Tani M, Glabinski AR, Tuohy VK, Stoler MH, Estes ML, Ransohoff RM. 1996. In situ hybridization analysis of glial fibrillary acidic protein mRNA reveals evidence of biphasic astrocyte activation during acute experimental autoimmune encephalomyelitis. *The American journal of pathology* 148: 889-96

Theodore S, Cao S, McLean PJ, Standaert DG. 2008. Targeted overexpression of human alpha-synuclein triggers microglial activation and an adaptive immune response in a mouse model of Parkinson disease. *J Neuropathol Exp Neurol* 67: 1149-58

Tieu K. 2011. A guide to neurotoxic animal models of Parkinson's disease. *Cold Spring Harb Perspect Med* 1: a009316

Tofaris GK, Garcia Reitbock P, Humby T, Lambourne SL, O'Connell M, et al. 2006. Pathological changes in dopaminergic nerve cells of the substantia nigra and olfactory bulb in mice transgenic for truncated human alpha-synuclein(1-120): implications for Lewy body disorders. *J Neurosci* 26: 3942-50

Togo T, Akiyama H, Iseki E, Kondo H, Ikeda K, et al. 2002a. Occurrence of T cells in the brain of Alzheimer's disease and other neurological diseases. *Journal of neuroimmunology* 124: 83-92

Togo T, Akiyama H, Iseki E, Kondo H, Ikeda K, et al. 2002b. Occurrence of T cells in the brain of Alzheimer's disease and other neurological diseases. *Journal of neuroimmunology* 124: 83-92

Tong Y, Yamaguchi H, Giaime E, Boyle S, Kopan R, et al. 2010. Loss of leucine-rich repeat kinase 2 causes impairment of protein degradation pathways, accumulation of alpha-synuclein, and apoptotic cell death in aged mice. *Proc Natl Acad Sci U S A* 107: 9879-84

Tysnes OB, Storstein A. 2017. Epidemiology of Parkinson's disease. *J Neural Transm (Vienna)* 124: 901-05

Ulusoy A, Decressac M, Kirik D, Björklund A. 2010. Viral vector-mediated overexpression of α-synuclein as a progressive model of Parkinson’s disease In *Recent Advances in Parkinson’S Disease - Translational and Clinical Research*, pp. 89-111

Ungerstedt U, Arbuthnott GW. 1970. Quantitative recording of rotational behavior in rats after 6-hydroxy-dopamine lesions of the nigrostriatal dopamine system. *Brain Research* 24: 485-93

Van der Meide PH, Schellekens H. 1996. Cytokines and the immune response. *Biotherapy (Dordrecht, Netherlands)* 8: 243-9

Van Maele-Fabry G, Hoet P, Vilain F, Lison D. 2012. Occupational exposure to pesticides and Parkinson's disease: A systematic review and meta-analysis of cohort studies. *Environment International* 46: 30-43

Wang Y, Rubel EW. 2008. Rapid regulation of microtubule-associated protein 2 in dendrites of nucleus laminaris of the chick following deprivation of afferent activity. *Neuroscience* 154: 381-89

Waxman EA, Mazzulli JR, Giasson BI. 2009. Characterization of hydrophobic residue requirements for alpha-synuclein fibrillization. *Biochemistry* 48: 9427-36

Welser-Alves JV, Milner R. 2013. Microglia are the major source of TNF-α and TGF-β1 in postnatal glial cultures; regulation by cytokines, lipopolysaccharide, and vitronectin. *Neurochemistry international* 63: 47-53

Wheeler CJ, Seksenyan A, Koronyo Y, Rentsendorj A, Sarayba D, et al. 2014. T-Lymphocyte Deficiency Exacerbates Behavioral Deficits in the 6-OHDA Unilateral Lesion Rat Model for Parkinson's Disease. *J Neurol Neurophysiol* 5

Wong D, Prameya R, Dorovini-Zis K. 1999. In vitro adhesion and migration of T lymphocytes across monolayers of human brain microvessel endothelial cells: regulation by ICAM-1, VCAM-1, E-selectin and PECAM-1. *J Neuropathol Exp Neurol* 58: 138-52

Yamada T, McGeer PL, McGeer EG. 1992. Lewy bodies in Parkinson's disease are recognized by antibodies to complement proteins. *Acta Neuropathologica* 84: 100-04

Yang HM, Moon SH, Choi YS, Park SJ, Lee YS, et al. 2013. Therapeutic efficacy of human embryonic stem cell-derived endothelial cells in humanized mouse models harboring a human immune system. *Arterioscler Thromb Vasc Biol* 33: 2839-49

Yuan YH, Yan WF, Sun JD, Huang JY, Mu Z, Chen NH. 2015. The molecular mechanism of rotenone-induced alpha-synuclein aggregation: emphasizing the role of the calcium/GSK3beta pathway. *Toxicology letters* 233: 163-71

Zarranz JJ, Alegre J, Gómez-Esteban JC, Lezcano E, Ros R, et al. 2004. The new mutation, E46K, of α-synuclein causes parkinson and Lewy body dementia. *Annals of Neurology* 55: 164-73

Zhan Y, Carrington EM, Zhang Y, Heinzel S, Lew AM. 2017. Life and Death of Activated T Cells: How Are They Different from Naïve T Cells? *Frontiers in Immunology* 8